AN ABSTRACT OF THE THESIS OF

Zhenlin Li for the degree of Doctor of Philosophy in Oceanography presented on May 31, 1990

Title: Longshore Grain Sorting and Beach-Placer Formation Adjacent to the Columbia River

Abstract Approved: Redacted for privacy

Paul D. Komar

The formation of beach placers primarily involves processes of waves and currents that selectively sort and concentrate the valuable minerals according to their densities, sizes and shapes. Black sand placers are found on the beaches adjacent to the mouth of the Columbia River. Reviews of historical shoreline changes show that jetty construction has caused rapid beach accretion immediately adjacent to the river mouth, and thus is important to the placer development. Beach-face sand samples were collected along 70 km of shoreline north and south from the river mouth, and were analyzed to determine the sorting processes responsible for the formation of this placer. It is found that heavy minerals are highly concentrated close to the Columbia River mouth, reaching 60% to 70% on the summer beach, and in excess of 90% during the winter. The concentration decreases systematically with longshore distance, being reduced to less than 2% after 20 km of longshore transport from the river mouth. The median grain sizes of principal minerals generally become finer with longshore distance, but an away-from-source coarsening is found within 5 to 8 km of the river mouth. These analyses indicate that the Columbia River is the major sediment source for these

beaches. The sand is transported alongshore north and south away from the river mouth. Though normal grain sorting and sediment transport processes are important for most parts of the beaches, selective grain sorting and transport processes are dominant immediately adjacent to the river mouth.

Calculations of hydraulic ratios for various mineral pairs show that the longshore transportability of a heavy mineral increases with its relative grain size and decreases with its density. This suggests that the heavy minerals of higher densities and finer grain sizes are less easily transported alongshore and are more concentrated close to the river mouth. Settling velocity measurements show that sorting due to contrasting settling rates could be responsible for the overall separation of the heavy minerals from the light minerals, but cannot explain the separation of individual heavy minerals. Evaluations of selective entrainment stresses and bedload transport rates, and results of the flume experiments show that minerals requiring higher selective entrainment stresses and with resulting lower bedload transport rates are those most concentrated in the placer deposits. This suggests that selective entrainment and differential transport sorting processes have been most important in the formation of the placer deposits adjacent to the Columbia River.

LONGSHORE GRAIN SORTING AND BEACH-PLACER FORMATION
ADJACENT TO THE COLUMBIA RIVER

by

Zhenlin Li

A THESIS

submitted to

Oregon State University

in partial fulfillment of
the requirements for the
degree of

Doctor of Philosophy

Completed May 31, 1990
Commencement June 1991

APPROVED:

Professor of Oceanography, in charge of major

Dean of College of Oceanography

Dean of Graduate School

Date thesis is presented_____May 31, 1990_____

Typed by Zhenlin Li for_____Zhenlin Li_____

献给：
　　我高中时的班主任贾翠英老师，她教会我怎样作人，并使我成熟。
　　也献给我在中国的导师秦蕴珊教授，他启蒙我进入海洋地质研究的大门，介绍我到美国完成我的学业。

　　I dedicate this thesis to my high school teacher Ms. Cuiying Jia, who tought me how to deal with life and made me mature, and also to Dr. Yuenshan Qin, my original advisor in China who led me into the door of marine geology research and helped me to come to U.S. to finish my education.

ACKNOWLEDGEMENTS

TABLE OF CONTENTS

LIST OF FIGURES

LIST OF TABLES

LONGSHORE GRAIN SORTING AND BEACH-PLACER FORMATION ADJACENT TO THE COLUMBIA RIVER

Chapter 1

INTRODUCTION

Placers are sediment deposits of residual or detrital mineral grains in which valuable minerals have been concentrated by natural processes (Slingerland and Smith, 1986; Komar, 1989). Modern and ancient placers have been significant sources of gold and platinum, and of minerals such as chromite, ilmenite, rutile, monazite, cassiterite, zircon and garnet. For example, Australian beach sands containing monazite were, until recently, the world's primary source of titanium, zirconium and rare-earth elements (Glasby, 1986). The Precambrian placer of Witwatersrand in South Africa has supplied more than half of all the gold ever mined (Pretorius, 1976).

The formation of a placer primarily involves processes of currents and waves that selectively sort and concentrate the valuable minerals according to their densities, sizes and shapes. Generally this is a concentration of the high-density heavy minerals and the removal of the lower-density quartz and feldspar grains. Due to their extreme densities, Figure 1, gold and platinum are sometimes referred to as "heavy-heavy minerals" (Emery and Noaks, 1968) or as "hyperdense minerals" (Komar, 1989). The other heavy minerals (magnetite, ilmenite, etc.) have lower densities than gold and platinum (Figure 1), but their densities still contrast sufficiently from those of quartz and feldspar that their sorting and concentration can occur.

The processes of grain sorting have been reviewed by Slingerland and Smith (1986) and Komar (1989), the latter focusing more specifically on placers of marine origin. The sorting processes are diagramed schematically in Figure 2 and include:

(1) Settling Velocities – Grains of differing sizes, densities and shapes fall through a fluid at different velocities, thereby becoming sorted.

(2) Selective Entrainment – Entrainment is the dislocation of grains from a granular bed and their initial movement by a superimposed fluid flow. Heavy minerals are denser and generally finer grained than the associated quartz and feldspar grains. Therefore, a current may selectively entrain and transport the light minerals from a deposit of mixed sizes and densities, leaving behind a lag of heavy minerals that are more resistant to movement due to their higher densities, lower exposures to the flow and larger pivoting angles.

(3) Differential Transport – Transport sorting occurs when a certainsize or density fraction of a mixed sediment is transported at a different rate than other fractions, and so may be deposited in a different location.

(4) Dispersive-Pressure Equivalence – When grains of mixed sizes are sheared, dispersive pressures created by grain interactions are greater on larger particles (Bagnold, 1954). Thus, coarser grains of light minerals tend to migrate upward within the shear layer, while the finer grains of heavy minerals move downward toward the bed, becoming more concentrated toward the base of the layer.

If we are to understand the origin of placers, it will be necessary to

Figure 1

Density spectrum of major minerals found in placers.

SPECTRUM OF MINERAL DENSITIES, ρ_s (g/cm³)
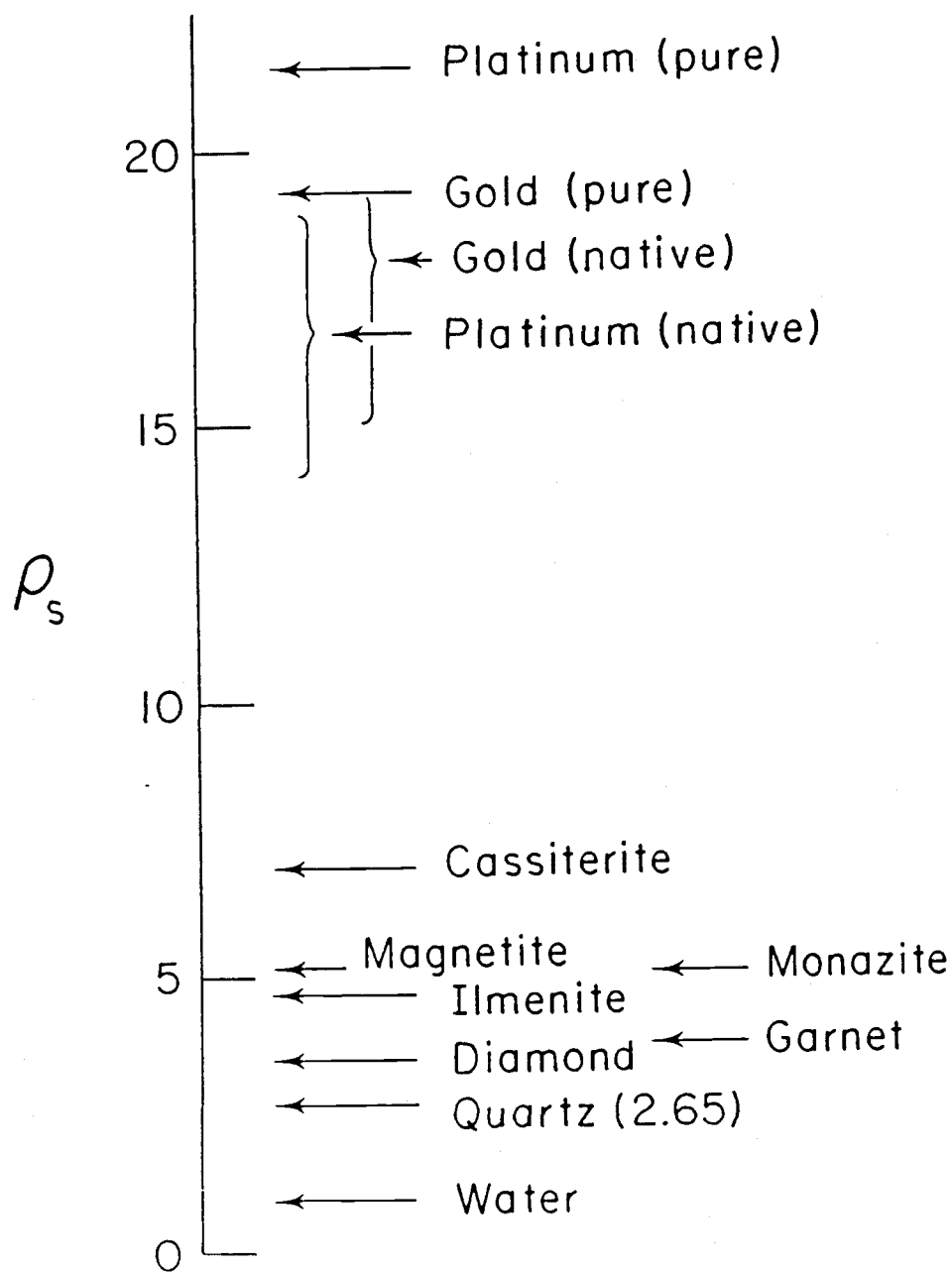
Figure 1

Figure 2

Schematic diagram of grain-sorting processes that cause the concentration of heavy minerals in placer development. Shaded grains represent heavy mineral particles.

DYNAMIC EQUIVALENCE
AND SORTING PROCESSES

A. Settling Equivalence
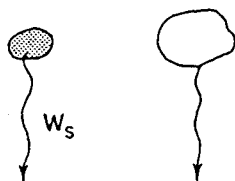
B. Entrainment Equivalence (Selective Entrainment)
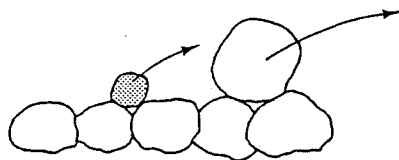
C. Transport Equivalence (Transport Sorting)

suspension

bedload
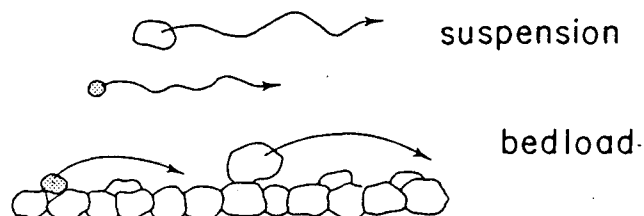
D. Dispersive – Pressure Equivalence (Shear Sorting)
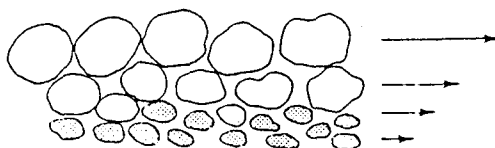
Figure 2

determine the relative roles of these sorting processes.

Placers are found in alluvial, marine, aeolian and lacustrian deposits. This thesis focuses on those of marine origin. Some of the important marine placers and their significance have been discussed by Kent (1980), Glasby (1986) and Sutherland (1987). Best known of the marine placers are those which have formed on beaches (Pardee, 1934; Twenhofel, 1943; Rao, 1957; Woolsey et al., 1975; Komar and Wang, 1984). The formation of beach placers mainly occurs in the swash zone where waves and currents selectively remove the lighter and coarser grains of quartz and feldspars, and carry them offshore or alongshore. Heavy minerals are left behind as a lag to form beach placers, apparently due to their higher densities and smaller sizes. A net long-term erosion of a shoreline and receding beach face particularly favor the formation of beach placers as these conditions permit the reworking of a large volume of sandy sediments, the long-term winnowing of the light minerals and progressive concentration of a sizeable deposit of heavy minerals. As pointed out by Komar and Wang (1984), placer formation is also enhanced in the swash zone of beaches by low flow stresses, since high-stress flows tend to actively transport both light and heavy minerals so that their separation is less efficient.

During glacial periods, sea levels have been 100 to 150 m lower than at present (Shepard, 1963; Shepard and Curray, 1967; Milliman and Emery, 1968). Lowered sea-levels permitted the transport and deposition of river sands on the exposed coastal plains, and these sediments were then reworked as beach deposits during the next sea-level rise. The high energy littoral zones migrated landward, and this tended to incorporate the heavy minerals and transport them landward, thus further concentrating them in beach sediments (Emery and Noaks, 1968). Some placers can be found on

continental shelves as part of relict beach sands. These relict placers tend to occur on high energy coasts having broad shelves and high terrigenous supplies (Kudrass, 1987). For example, placers of ilmenite and zircon have been found on the Mozambique Shelf, where they were formed along the Zambezi Delta during low sea-levels, and survived reworking of the subsequent transgression of the sea due to the large quantities of sediments (Jartiz, et al. 1977; Beiersdorf, et al. 1980). Accumulations of heavy minerals on the continental shelf off the Rogue River of Oregon have been documented by Kulm et al. (1968a) and Kulm (1988), a placer deposit that extends to mid-shelf depths but traces back to the present river mouth. It has been suggested that this deposit was concentrated in the vicinity of the river mouth, and was left behind on the shelf due to the retreat of the river mouth with the transgressing sea (Komar, 1989). In contrast, falling sea-levels and/or tectonic uplifts of coastal zones can leave beach deposits on land in which placers might be found. For example, old beach placers occur in Pleistocene terrace sands of southern Oregon, exceeding 3 m in thickness and extending 2 to 3 km alongshore (Griggs, 1945; Twenhofel, 1943; Peterson, et al. 1987).

Placers or "black sands" are found on the ocean beaches adjacent to the Columbia River, Figure 3, both to the north along the coast of Washington and southward on Oregon beaches. The overall objective of this study is to examine the long-term development and grain sorting processes involved in the formation of these black sands. The beach to the south in Oregon is part of the Clatsop Plains, which extends from the mouth of the Columbia River to Tillamook Head. To the north in Washington, the beach is primarily a part of the Long Beach Peninsula which is a 44-km long sandspit separating Willapa Bay from the Pacific Ocean. However, the

Figure 3

Location map showing the study area which extends from Tillamook Head, Oregon to Willapa Bay, Washington. The jetties are indicated by thicker black lines and headlands are shown as black areas.
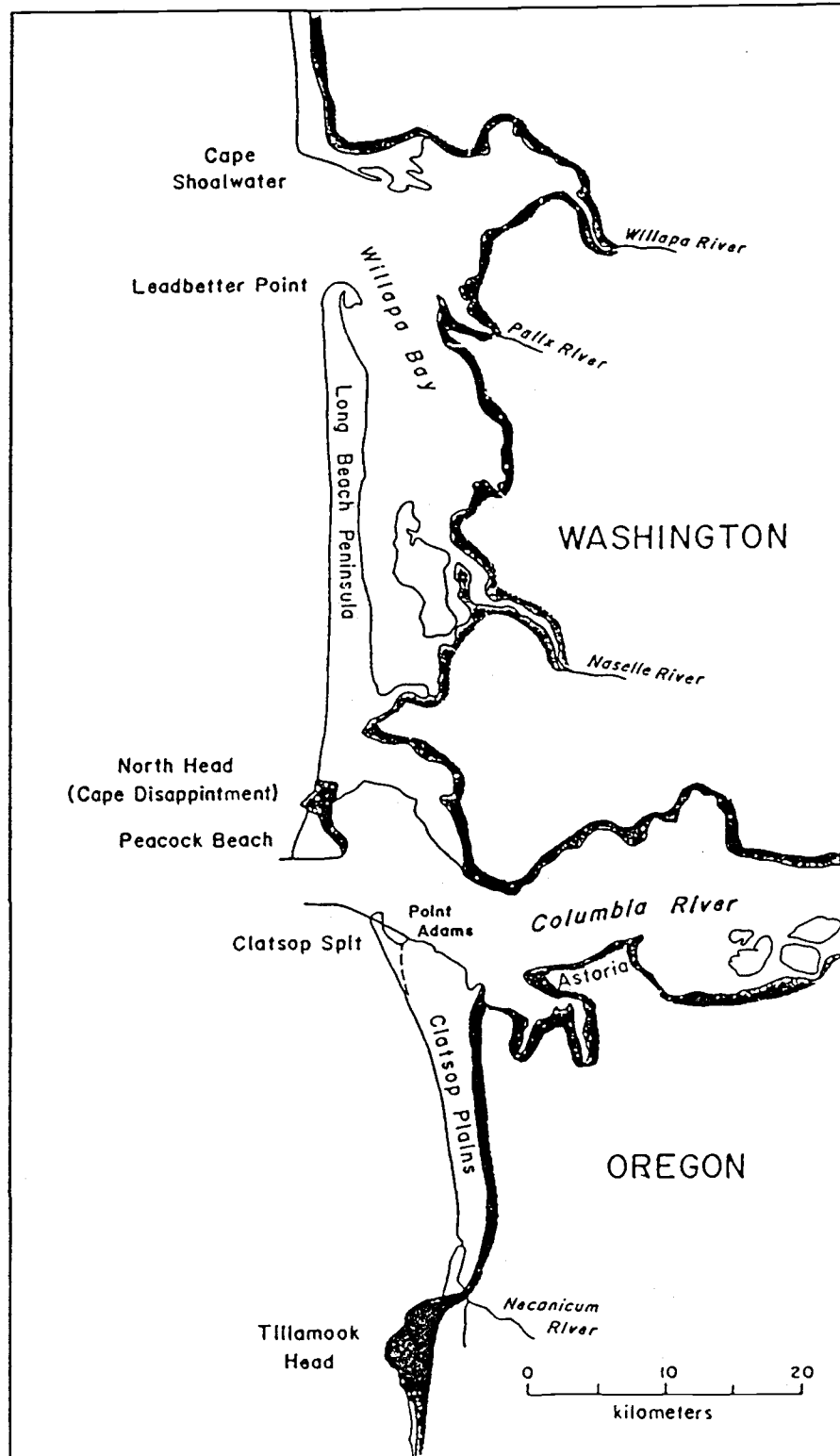
Figure 3

black sand in Washington is most highly concentrated on Peacock Beach (Figure 3), which began to accrete in 1917 after construction of the north jetty at the mouth of the Columbia River. Similarly, to the south in Oregon the most-concentrated black sand is found within Clatsop Spit (Figure 3), which attached to the south jetty after its construction. Therefore, in addition to examining the natural processes of waves and currents that formed these black sands, it will be necessary to consider the role of jetty construction.

The beach placers in the study area have attracted the attention of scientists, government agencies, and mining industries. Test drillings near Hammond, Oregon, on the Clatsop Plains were undertaken as early as the 1940's (Oregon Department of Geology and Mineral Industries, 1941; Kelly, 1947). A black sand deposit measuring approximately 500 by 800 ft, and at least 3 ft thick, was found. The concentrated heavy minerals included magnetite (40%) and ilmenite (19%). Twenhofel (1946) examined the black-sand deposits near the south jetty of the Columbia River, and on the east side of Trestle Bay, Washington, reporting that the deposits reach 74% and 91% opaque minerals, respectively; Twenhofel further concluded that rich concentrations of heavy minerals are likely present under a considerable area. In 1963, Bunker Hill Corp., Kellogg, Idaho, became interested in mining an area of approximately 3000 acres of iron-bearing sands in the Clatsop Spit (Oregon Department of Geology and Industries, 1963). Scientific studies of the deposits near the Columbia River have included that of Ballard (1964), who investigated the mineralogy of the beach sands from Tillamook Head, Oregon to Grays Harbor, Washington. He found that the concentration of heavy magnetic minerals increases significantly adjacent to the mouth of the Columbia River. Plopper (1978)

studied the textural and mineralogical characteristics of beach sands along much of the Washington coast. He also found a decrease in heavy-mineral contents northward from the Columbia River, and attempted to discern the sorting patterns by analyzing hydraulic ratios of various mineral pairs (the weight percent of a heavy mineral divided by the weight percent of a light mineral with same settling velocity). Recent surveys by Peterson and Binney (1988) have led to estimates that the black sand deposits in the study area range from 2 to 7 million cubic meters.

As stated earlier, the overall objective of this study is to examine the formation of the black sands on the beaches to the north and south of the Columbia River. Their development appears to have been associated with the construction of the jetties on the Columbia River, so part of this study will include a documentation of the shoreline changes associated with that construction. Another phase of the investigation involves an examination of the processes diagramed in Figure 2, those which are important to the formation of these black sands. It is clear that placer formation near the Columbia River is part of a pattern of longshore sorting of sand grains of contrasting densities as they are transported by the waves and currents along the ocean beaches away from the river source. This sorting is determined with beach-sand samples collected along the lengths of the beaches, analysed for their textures and mineralogies. The analysis procedures undertaken here differ from those of Ballard (1964) and Plopper (1978) in that the changing grain-size distributions of the various minerals are examined in detail. Direct measurements of the settling velocities of the grains are obtained, and the threshold flow stresses for the series of minerals are compared. Such analyses will help to determine which of the sorting and concentrating mechanisms of Figure

2 are important to the formation of the black sands. Therefore, as well as leading to a better understanding of the placers near the Columbia River and their potential exploitation, the present study will also lead to an improved general understanding of sediment transport and selective entrainment processes responsible for placer development.

This thesis is divided into eight chapters. This introductory chapter has explained the objectives and significance of the study. Chapter 2 provides a more detailed description of the study site, including a summary of the oceanographic, river, and beach conditions. The Holocene and historic changes are discussed in Chapter 3, including the analyses of shoreline changes associated with jetty construction. Chapter 4 describes the properties of these black sand deposits and reviews previous exploration and scientific studies. The sampling methods and laboratory procedures are described briefly in Chapter 5. Chapter 6 contains the results of the analyses of the overall patterns of black-sand concentrations and the longshore dispersal away from the Columbia River. The analyses of textures and heavy-mineral concentrations will be used to discuss the processes of littoral drift and the resulting formation of beach placers. In Chapter 7 the settling velocities and entrainment stresses are evaluated, and flume experiments are conducted to examine the grain-sorting processes. Finally, in Chapter 8 a summary and discussion of the overall results and their significance will be presented.

Chapter 2

THE STUDY SITE

2.1 Location and General Description

The study area is located on the Pacific coast of Oregon and Washington. Figure 3 (also Figure 11) identifies the geographic localities relevant to the study and Figure 4 shows the geomorphology and topography of the study area. The beach extends from Tillamook Head, Oregon, northward to the Willapa Bay inlet, Washington, for a total coastline distance of approximately 80 km. Central to the study area is the Columbia River, which serves as the boundary between Oregon and Washington.

2.2 Topography of the Region

The shoreline of the study area consists of broad beaches backed by coastal dunes. Dune and beach ridges are formed along the entire length and extend inland (eastward) for an average distance of 3.2 km. Usually three to five ridges are present. The orientations of these dunes and ridges are parallel or subparallel to the shoreline, and it is believed that they formed due to the stabilization of sand dunes by vegetation (Cooper, 1958). The elevations of these ridges range from 4 to 30 meters and their widths are variable. Between the beach ridges or ridge groups are linear low areas of bogs and elongated lakes, which use to be much larger water bodies but now are mostly filled with peat.

The Clatsop Plains of Oregon is bounded to the south by Tillamook Head and to the north by the Columbia River, or more specifically by the south jetty at the river mouth. The Pacific Ocean lies to the west and the low hills of the Coast Range are to the east. The area is about 28 km long

Figure 4

Portion of a Coast and Geodetic Survey chart showing the study area. The hydrographic survey dates to 1868-1877, the land topography to1868-1875, and the conditions of the Columbia River bar to surveys made in 1889-1890. The south jetty is shown which was constructed between 1885 and 1895, but its impacts on the adjacent shorelines are not included.
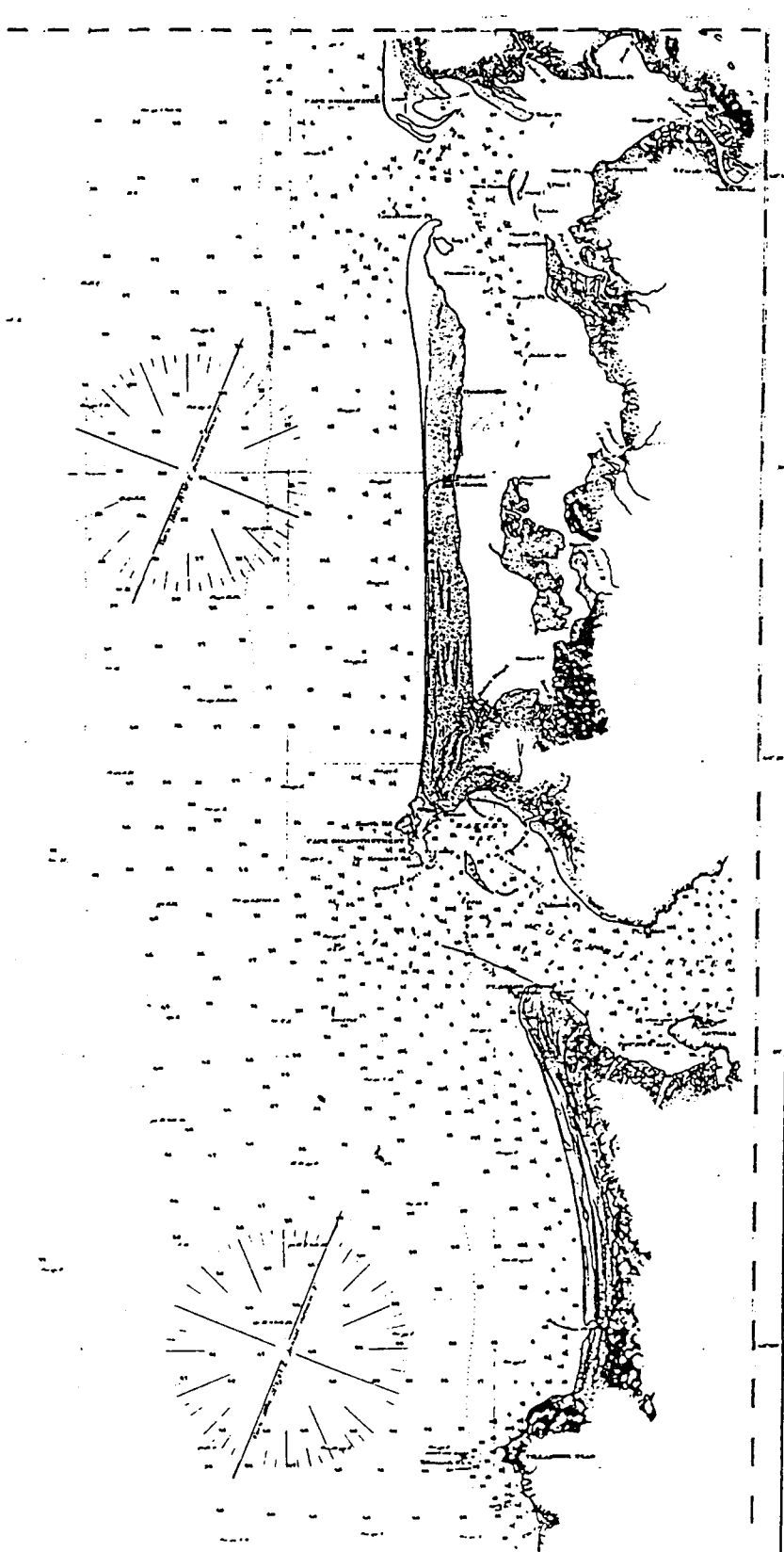
Figure 4

and its width varies from 4.5 km adjacent to the Columbia River to less than 1 km approaching Tillamook Head (Rankin, 1983). The whole beach is shaped like a gentle arc. Tillamook Head, the southern end of the Clatsop Beach, is composed of Tertiary volcanics (mostly basalt) and conglomerates. It projects about 3.5 km into the ocean and serves as a major obstacle to longshore sediment movement on the beaches (Clemens and Komar, 1988). The beach immediately north of Tillamook Head consists of boulders and cobbles, and has a steep slope (Dicken, 1961). The cobble zone fades out rapidly to the north, and is replaced by the normal sand beach. The outlet of the Necanicum River occupies a meander zone between Seaside and Gearhart. Northward from the Necanicum River is a uniform sandy beach that is nearly flat at the low-tide line, and shows a gradually-increasing slope toward the berm. The upper beach level is made up of hummocky dunes. All of these features are indicative of a progradational beach. Northward from Fort Stevens Park, an abrupt change occurs. Beach berms and foredunes show erosive characteristics, and this continues all the way to the south jetty. The color of the beach sand also becomes darker toward the south jetty due to increasing heavy mineral concentrations. The south jetty marks the northern end of the Clatsop Plains. This jetty is 10.6 km long and is aligned in a northwesterly direction with four groins along its north side. The Clatsop Spit, Figure 3, which developed at the time of construction of the south jetty, forms a hook-shaped sand body that crosses the south jetty at about its mid-length and connects to the pre-jetty shoreline further south.

The Long Beach Peninsula in Washington extends northward from the Columbia River to Willapa Bay, for a total length of 44 km (Figure 3). This peninsula mainly consists of parallel beach ridges and ridge groups. These

ridges are low (generally 6-12 m above sea-level), and their patterns are usually recognized by the trees that grow on them (Cooper, 1958). Beach ridges and ridge groups are separated by bogs and lakes which are now mostly filled with peat. The dunes in the southern half of the Long Beach Peninsula (south of Klipsan Beach) are completely stabilized. The parallel-ridge pattern extends uniformly to the shoreline. Most of the bogs and lakes also occur in this half. The northern half shows evidence of erosion, indicated by trough blow-outs and sand dunes invading the forest. A significant ridge begins at Klipsan Beach and extends northward for about 16 km to form the west boundary of the forested area. Seaward of this ridge is a strip of open sand which is narrow at the south and widens to about 800 m at its northern end. The northern-most 4 km of the peninsula is almost bare of vegetation. On the bayside of the peninsula, a low and narrow sand strip merges with the tidal flats of Willapa Bay. The north jetty on the Columbia River, which was built in 1917 with a total length of 3.9 km, defines the southern end of the peninsula. The construction of the north jetty caused rapid shoaling and beach accretion to its immediate north, so that a new land mass formed between North Head and the jetty. Similar to south of the river, dark heavy minerals are more concentrated close to the north jetty, and progressively decrease toward the north.

The nearshore zone of the study area is a complex system which extends seaward for about 1 km. The only beach profiles available that extend across the entire nearshore were obtained in the 1940's during investigations conducted by the University of California (Bascom and McAdam, 1947). These few profiles show one, two or three offshore bars separated by longshore troughs (Komar, 1977). The continental shelf of the Oregon and Washington coast is narrow and steep, with a width rarely more

than 50 km and an average gradient of 3 to 4 m/km (Byrne, 1963; McManus, 1972). The shelf south of the Columbia River is variable, the smooth inner shelf giving way seaward to a rough relict outer-shelf. To the north of the river the shelf is more uniform, and only a few shoals or depressions are found. The general depth of the shelf break is at about 180 m.

2.3 Physical Conditions of the Study Area

2.3.1 Climate

The climate of the northwest coast is typically oceanic. Winters are usually long, cool and wet, while summers are short, moderate and dry (Cooper, 1958). The coast has a humid marine climate with moderate temperatures and high annual rainfall. Thornthwaite (1948) characterizes the region as perhumid and mesothermal with little or no marked seasonal thermal concentration. Table 1 lists the average monthly and annual temperatures and precipitations at Astoria, Oregon, for the period 1950 to 1980 (based on data from National Climatic Center, Climatological Data: Oregon, 1985). It shows that for 1950 to 1980 the average annual temperature was 50.6°F with an average winter temperature of 42.8°F and that of the summer at 59.1°F. The average annual precipitation for 1950 to 1980 at Astoria is 177 cm. Most of this occurs in the winter and only 7% falls in the summer.

Due to the seasonal shifting of the Aleution Low and the North Pacific High, winds on the Oregon and Washington coasts are predominantly from north/northwest in the summer and shift to south/southwest in the winter. Cooper (1958) made a detailed study of the winds of the Oregon and Washington coast during his work on coastal dunes. He showed that onshore winds are greatly dominant in the summer. They are mostly from the

north-northwest and have the greatest average velocities. In the winter, offshore winds are more frequent but have low velocities. Onshore winter winds are mainly from south to southwest and are relatively infrequent but have by far the greatest velocities.

Table 1   The monthly and annual average temperatures T(^{0}F) and precipitations P(cm) at Astoria, Oregon, for the period 1950 to 1980 (National Climatic Center, Climatological Data: Oregon, 1985).

Month	J	F	M	A	M	J	J	A	S	O	N	D	Annual
T	41.3	43.9	44.4	47.6	52.2	56.6	60.1	60.6	58.5	52.9	46.6	43.1	50.6
P	28.7	19.8	18.5	11.7	7.1	6.1	2.5	4.1	7.9	15.7	25.1	29.5	177

2.3.2 Waves and Tides

The Oregon and Washington coast is storm-wave dominated, and is relatively more energetic than most coasts of the world. Komar et al. (1976) compiled and analyzed ocean wave data collected at Newport, Oregon, during the period 1971 to 1975. It was found that significant wave breaker heights during winter months reach an average of about 4.5 m (15 ft), with the maximum of individual storms achieving 7 m (23 ft). During the summer months, however, significant wave breaker heights averaged only about 1 m (3.3 ft).

The direction of wave approach varies with the season and coincides with the shifting of the wind direction. O'Brien (1951) analyzed waves observed at the Columbia River Light Ship for the years 1933 to 1936, and reported that the dominant wave direction is from the southwest sector (about 64%) and only 16.5% is from the northwest. National Marine Consultants (1961) studied seas and swells off the Oregon coast using

hindcast methods, and the results show that the dominant wave direction in winter is west and southwest, while in summer it shifts to northwest. In summary, locally generated waves (seas) approach mainly from SW to SSE during fall and winter, and from NW during spring and summer. Swells (uniform waves from distant storms) approach predominantly from the NW during all seasons. Waves generated by local storms are generally higher than swells. The highest waves occur predominantly during the winter months, and arrive mainly from the SW-SSE direction (Bourke, 1971).

The tides of Oregon and Washington are classified as mixed semidiurnal, that is, there are two high tides and two low tides per day, but the heights of successive tides are not equal (Komar, 1976). The average annual tides at Astoria, Oregon range from +3.0 m to -0.6 m measured in reference to the mean lower-low water level (U. S. Department of Commerce, 1981). This is classified as a mesotidal coast by Davies (1964).

2.3.3 Longshore Currents and Littoral Drift

It is known that when waves approach a coastline at an oblique angle, a longshore current will be established flowing parallel to the shoreline (Komar, 1976). This longshore current is the major mechanism of littoral sand transport, and most of this transport takes place within the nearshore between the breaker zone and shoreline.

Directions of longshore currents on the Oregon-Washington coast probably coincide with the wind and wave patterns, although no systematic long-term observations are available. Lower and longer waves generated by summer winds from the northwest transport sediment southward along the beaches, as well as tending to move sand onshore.

Winter winds approaching mostly from the south and southwest produce steeper and more erosive waves, which transport sediment northward and offshore from the beaches. Controversy initially existed over the direction of the net littoral sand transport in the study area. Twenhofel (1943) believed that since the dominant direction of the wind is from the southwest, the shore currents move northward for the most part, and therefore the net transport of sediment is in that direction. Cooper (1958) challenged this by arguing that the gentler waves generated by the prevalent northwest summer winds are more effective for littoral transport, so that the net littoral drift should be southward. By analyzing the longshore component of wave-energy flux, Ballard (1964) concluded that a net northward drift exists for most of the coast from Tillamook Head, Oregon, to Grays Harbor, Washington. Similar conflicting arguments can be found in Kidby and Oliver (1966) and Lockett (1967). Based on the shoreline geometry adjacent to the Columbia River, documented shoreline accretion rates and distributions of Columbia-derived sands on the beaches, it is clear that the formation of the Clatsop Plains must have been caused by a southward longshore drift of the river-derived sediments, while a northward sediment drift was responsible for the development of the Long Beach Peninsula. Thus the net littoral drift must be southward on the Clatsop Plains and northward along the Long Beach Peninsula. However, more sand is transported northward from the river mouth due to the dominant northward longshore currents. A smaller amount moves to the south along the shoreline of Oregon, and then only as far as Seaside where it is blocked by Tillamook Head (Clemens and Komar, 1988).

2.4 Sediment Supply From the Columbia River

It is clear that the Columbia River is the dominant sediment source for the beaches in the study area. This is confirmed by the mineralogy of the beach sands, and there are no other potentially significant sand sources (Ballard, 1964; Plopper, 1978; Luepke and Clifton, 1983). The river originates at Columbia Lake in the Rocky Mountains of British Columbia, at an elevation of about 800 m, and flows south and west for 1900 km before emptying into the Pacific Ocean. The total drainage area is approximately 667,000 km^2 (Lockett, 1967; Kulm, et al., 1968b; Whetten, et al., 1969).

The Columbia River is the third largest river in the United States, and is the largest on the west coast (Highsmith, 1962). Different estimates have been given for its mean annual discharge. The most recent estimate according to USGS Water Data Reports (1965-1976) and sumarized by Karlin (1980) is 216 km^3/yr, approximately twice the combined discharge from all other rivers in California, Oregon and Washington (Roden, 1967). The discharge from the Columbia River is distinctly seasonal; the peak flows occur in May to June due to snow melt at high elevations of the drainage area, while minimum flows are in September-October because of the dry summer. This runoff carries significant quantities of sediments. It is estimated that the annual suspended sediment discharge is about 14x10^6 tons and the bedload is about 10^6 tons (Kulm, et al., 1968b; USGS Water Data Reports, 1965-1976; Karlin, 1980). Several dams have been built on the Columbia River and its tributaries. Since dams usually act as sediment traps, there has been some concern that sediment yields from the Columbia, and hence longshore drift volumes on the beaches, might have been reduced (Lockett, 1962; Jay

and Good, 1977). However, this does not appear to have been the case. Annual sediment discharges estimated from 1914 to the 1960's have not changed significantly (van Winkles, 1914; Hidaka, 1966). Analyses by Phipps and Smith (1978) of shoreline changes along the Washington coast demonstrate a continued accretion, and therefore do not show any apparent changes that might have resulted from dam construction. It seems that the dams may interrupt sediment transport during low-stage water discharges, but most sediments will be suspended and transported during the maximum water discharges. Thus, dam construction may have amplified the seasonality of sediment discharge, but not necessarily reduced the magnitudes (Whetten, et al. 1969; Karlin, 1980). However, further study is required for a better understanding of the effects of dam construction on sediment supply to the coast.

The bulk mineral compositions of the Columbia River sediments have been studied in different investigations and are listed in Table 2. It shows that the Columbia River sediments are dominated by high percentages of lithic fragments (about 50%). The second and third most abundant components are respectively feldspars and quartz. The large differences among these investigations are probably due to differing classifications and sampling locations. Venkataratham and McManus (1972) have studied the sediment sources and dispersal on the continental shelf off Washington. They estimated that the total heavy mineral concentration of the Columbia River sediments is 14.4%, of which 4.8% are opaques. The high abundance of lithic fragments, angularity of all minerals, and the clearness or freshness of most minerals suggest that the sediments are transported rapidly down the river with minimal weathering and abrasion (Hodge, 1934). The heavy minerals of the Columbia River have been studied

by Kulm, et al. (1968b), Scheidegger, et al. (1971), and recently by Clemens (1987). Their results are listed in Table 3, which show that orthopyroxene (mainly hypersthene) is by far the most abundant component, and is followed by clinopyroxene (augite) and hornblende. Other accessory constituents include garnet, olivine, epidote and zircon. Hypersthene and augite are mainly derived from the basic igneous rocks in the drainage basin, while the rest of the heavy minerals are probably contributed by high-rank metamorphic rocks.

Table 2   Bulk mineral compositions (%) of the Columbia River
            sediments cited from various investigations.

constituent	Hodge (1934)	Whetten, et al. (1969)	White, S.M. (1970)
Quartz	23.3	13	16
Plagioclase	12.0	20	16
K-Feldspar	1.5	7	6
Lithic Fragments	39.0	55	46
Opaques	12.0	1	*
Mafics	13.0	4	16

* no opaque percentage was given by White.

Table 3   Heavy mineral compositions (in %) of Columbia River
            sediments according to different studies.

Constituent	Kulm, et al. (1968b)	Scheidegger et al. (1971)	Clemens (1987)	Average
Orthopyroxene	37	36	48.6	40.4
Clinopyroxene	32	28	20.1	26.7
Hornblende	22	28	25.4	25.1
Epidote	1	1	0	0.7
Garnet	2	1	1.6	1.5
Zircon	0	0	2.2	0.7
Olivine	1	2	0	1
Others	5	5	1.6	3.9

Chapter 3

HOLOCENE EVOLUTION AND HISTORIC CHANGES

3.1 Cycles of Sea Level

The estimated sea level curve for the Quaternary (approximately the last 2 million years) is quasi-periodic with oscillations having amplitudes of about 100 m. The general trend of sea level changes over the last 40,000 years is shown in Figure 5. The last high stand of sea level was around 30,000 years B.P. Sea level then dropped rapidly and reached a low stand at 18,000 to 20,000 years B.P., about 100 to 125 m lower than at present. The sea then rose rapidly (8 mm/yr) until about 6,000 to 7,000 years B.P., and then slowed down (1.4 mm/yr) in its rise to the present level.

Conflicting evidence exists concerning sea level changes during the past 7,000 years, shown by the curves presented in Figure 6. These differences are mainly due to regional tectonic and isostatic effects. Cooper (1958) suggests that the latest sea-level rise for the Pacific Northwest is relatively more gentle because of the uplift of its continental margin. Carbon-14 dates from the Pacific Northwest (Bloom, 1977) and from the Clatsop Plains (Rankin, 1983) are plotted in Figure 6. Rankin's data were obtained from dating interdunal peats collected across the Clatsop Plains. Since peat surface levels are higher than the mean sea level, the height of the modern peat surface above the mean sea level has been used to estimate the mean sea-levels obtained from the dated samples. Therefore, caution must be used in interpreting these data. Nevertheless, the measurements show a more gentle slope than the curve based on similar data from other locations (Figure 6). C14 dates of wood
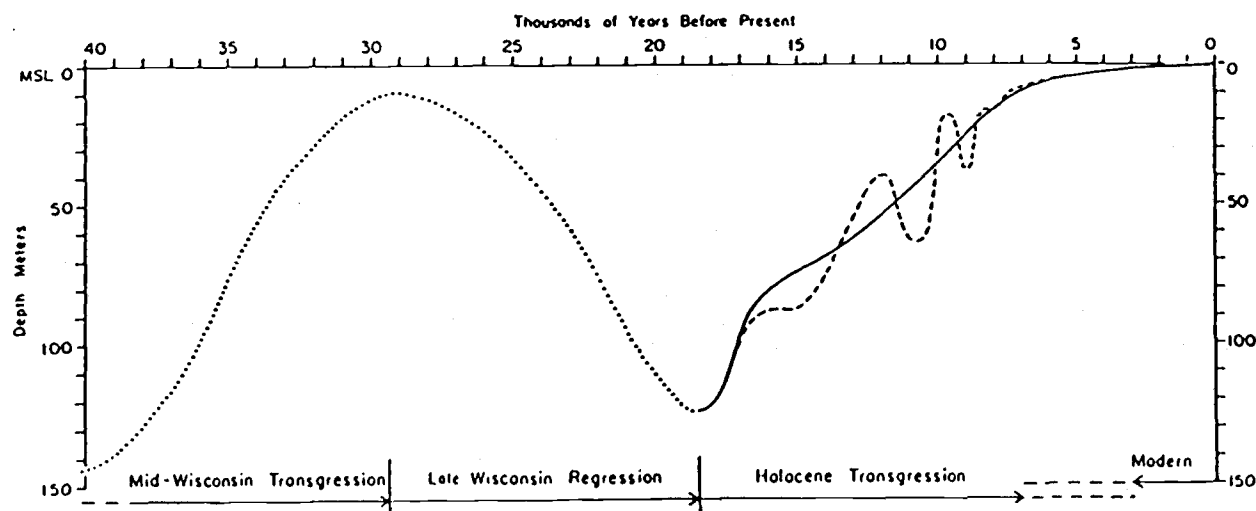
Figure 5
Sea-level changes during the last 40,000 years based on
carbon-14 dates compiled by Curray (1965) (from Komar, 1976).

29

Figure 6

Sea-level curves based on data from the Pacific Northwest for the past 7,000 years. A curve from other locations is included for comparison (modified from Rankin, 1983).
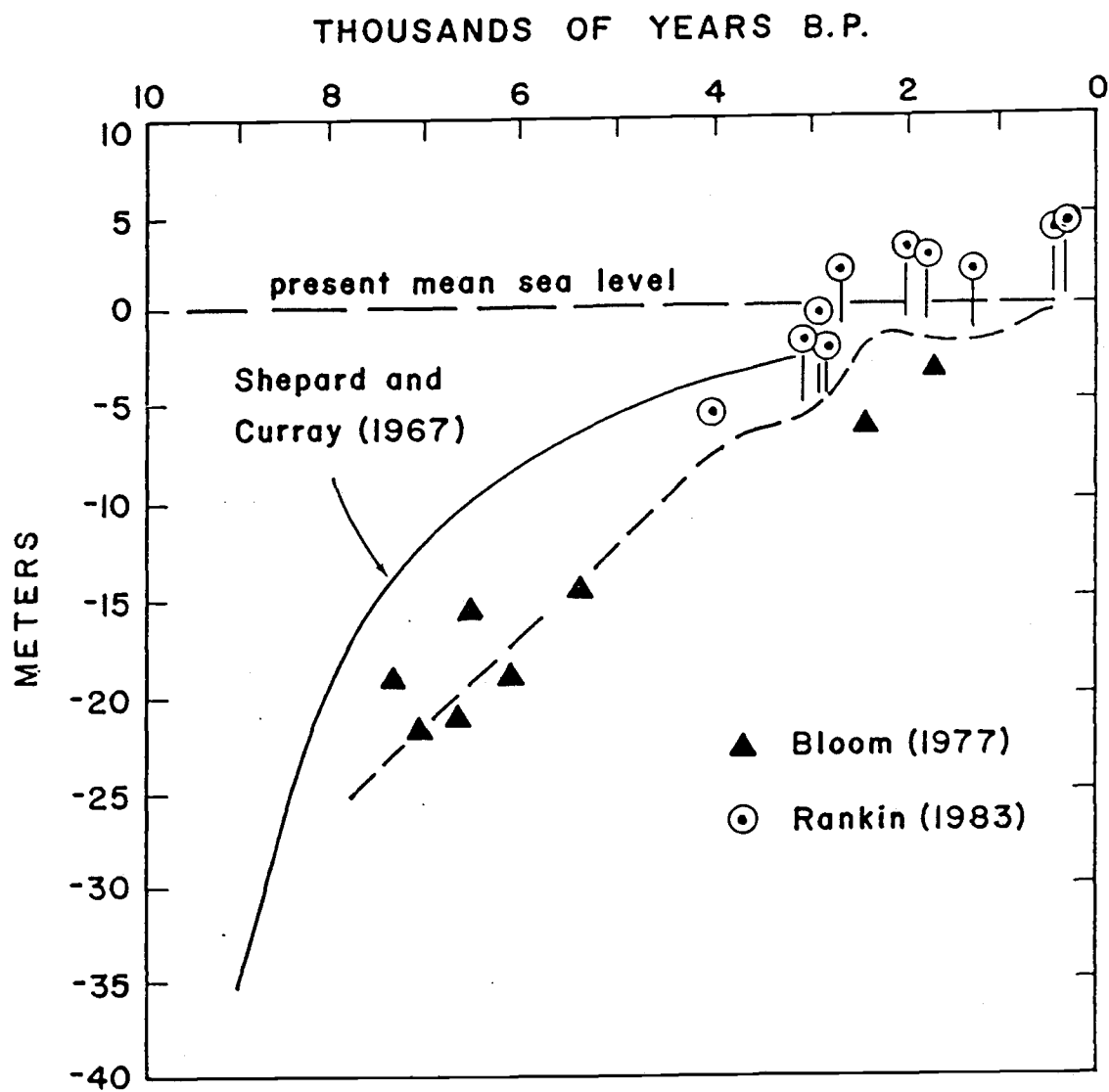
Figure 6

fragments from Alsea Bay, Oregon by Peterson et al. (1984) show a similar curve but shifted to greater depths. According to the data presented in Figure 6, the Holocene rise of the sea-level on the Northwest coast occurred from 10,000 to 4,000 years B.P. After a level-off during a period from 4,000 to 3,000 years B.P., sea level rose sharply and reached a peak at 2,200 years B.P., which was then followed by a gradual drop. It reached a low at 1400 years B.P., and then slowly rose to the present level.

Long-term tide gauge records indicate that recent globel sea-level changes correlate well with climatic changes (Marmer, 1952; Fairbridge, 1960). The sea-level rose at 1.2 mm/year between 1725 and 1770, and fell between 1800 and 1850 due to a period of cold winters. With the present warming spell, the rise of sea level resumed its 1.2 mm/year rate since 1850. This is further supported by the more recent study of Gornitz et al. (1982) which shows that the mean sea-level rose about 12 cm from 1880 to 1980. Despite this general trend of rising sea-level, relative sea-level (RSL) is presently falling along the Pacific Northwest coast due to the tectonic uplift of the area. Tide-gauge measurements collected since 1925 at Astoria, Oregon, and Neah Bay, Washington, show that sea-level is falling about 0.1 mm/year at those locations (Hicks, 1972; Barnett, 1984).

3.2 Development of the Clatsop Plains

As noted in the previous section, during the last major glacial advance in the late Pleistocene, sea level was about 100 m lower than at present and the shoreline was at least 30 km to the west of its present position. The emergent land area formed a coastal plain across which the Columbia and other rivers flowed. As sea-level rose and the shoreline

migrated landward, beach sand reworked from the coastal-plain sediments was probably also carried landward. When the advancing shore reached rock obstacles such as Tillamook Head, the formerly continuous beach was segmented. Continued landward migration progressively isolated the beaches north and south of Tillamook Head, preventing sand bypassing (Clemens and Komar, 1988). The transgression of the rising sea to the south of Tillamook Head was slowed by the erosion of moderately resistant cliff materials. In contrast, the transgression progressed much further landward north of Tillamook Head, reaching about 3 km inland of the present shoreline. A degraded bluff forms the landward extent of the Clatsop Plains, Figure 7, and records the maximum transgressive shoreline, which Carbon-14 dating by Rankin (1983) places at somewhat older than 3200 years B.P.

The subsequent building of the Clatsop Plains between Tillamook Head and the Columbia River is complicated, but well studied. In his investigations of the morphology and formation of coastal dunes in Oregon and Washington, Cooper (1958) recognized nine ridge groups on the Clatsop Plains (Figure 7) and described the development pattern of the area in great detail. Rankin (1983) distinguished eight ridge groups. Progradational time lines have been estimated on the basis of geomorphic characteristics, carbon dating of peat, and archeological dates of Indian occupation. Discontinuities between groups can be formed in three ways, a lull in progradation, coastline erosion, and selective accretion.

The growth of the Clatsop Plains can be divided into three stages. During stage one (ridge groups 0-3 of Figure 7), progradation began with beach deposition (ridge group 0) in front of Cullaby Lake and the eroded bluff, dated at 3200 years B.P. Ridge groups 1 to 3 developed from 3200 to
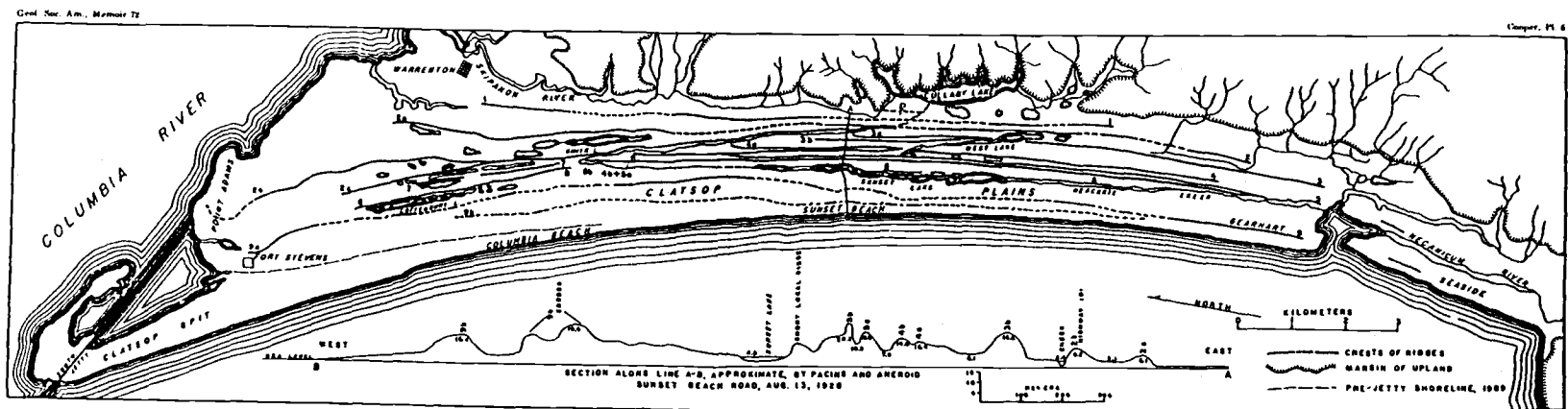
Figure 7
Beach/dune ridge groups on the Clatsop Plains (from Cooper, 1958).

1000 years B.P. As outward flow of the Columbia River spread its bedload fanwise, pronounced shoaling occurred at the southern side of the river mouth and a northward-projecting spit developed, accompanied by continued seaward progradation. Ridge after ridge appeared. Where a ridge has a wide strip of bog or lake behind it, origin as an offshore bar and a seaward jump in shoreline position are indicated. As new ridges formed, they extended themselves progressively northward. The initial spit was gradually transformed into a broad peninsula and a final limit of growth was reached at Point Adams, the northern tip of the spit prior to construction of the south jetty (Figure 7). At that stage there was a balance between coastal and fluvial forces, preventing further northward growth of the spit (Cooper, 1958). Ridges in this stage show a divergence characterized by branching, sinuous and hummocky ridge crests (Rankin, 1983). This divergence extends southward only to a common area around Cullaby Lake (Figure 7). The massive divergence at the north is due to the frequent interruptions in the progradation, and the combined attack of surf and wind on established ridges, while convergence and decreasing mass of the ridges to the south were caused by the increased distance from the Columbia River sediment source.

Stage two includes ridge groups 4, 5 and 6, which were formed 1000 to 400 years B.P. They are marked by a striking regularity and continuity of their ridge crests. The ridges are subparallel, relatively continuous, straight, and with smooth crests. With the cessation of northward extension at Point Adams, seaward progradation on the peninsula was reduced. At about the same time, renewal of progradation occurred at the south part of the beach. The growth of stage two ridges first occurred in the central and south areas. This probably suggests that the sand

contribution from the Columbia River was decreasing. Progradation was steady and uninterrupted. The remainder of the ridge groups (groups 7 to 9) can all be included in stage three and were likely formed in the last 400 years. A southward littoral sand transport of Columbia River sand was still the dominant agent, but the sand supply was greatly reduced. Thus, progradation was similar to that in stage two, producing subparallel and more continuous crests. At the north, however, outward-flowing currents of the Columbia River again became important and sand supply was abundant. This produced more massive and discontinuous ridges.

Progradation rates and sea-level fluctuation data can be combined with the above analysis. This combination suggests a cyclic succession of accretion, erosion and stabilization, followed by renewed progradation. Following initial stabilization of ridge group 0 at Cullaby Lake, there was a period of massive accretion (group 1 at a rate of 1.1 m/yr) with significant modification by waves during the sea level rise from 3000 to 2200 years B.P. During the peak and subsequent fall of sea level between 2200 to 1400 years B.P., groups 2 and 3 developed large massive dunes at a faster rate of 1.5 to 2.0 m/yr. After the sea-level reversal at 1400 years B.P., a major reorientation of the strand line occurred with accretion of groups 4, 5 and 6 at very low rates of about 0.50 m/yr. The accretionary form changed from a thick fan shape in the north to a thicker progradational wedge in the south and central Clatsop Plains. The ridge divergence pattern also shifted. High accretion rates (1.7 to 4.1 m/yr) and irregular ridges developed in the last 400 years (groups 7 to 9), likely marking a return to more massive and discontinueous progradation.

3.3 Growth of the Long Beach Peninsula

The evolution of the coast north of the Columbia River has not been studied in as great a detail as to the south. Carbon-14 dating of marsh peats has not been obtained, so the timing of shoreline changes is speculative.

With the Holocene rise in sea level, the onset of the general submergence drowned many of the river valleys that crossed the coastal plain, producing the numerous bays and estuaries found along the Northwest coast. Spits formed across submerged areas, probably by landward migrating beaches rather than by longshore beach extension. At least initially, the Long Beach Peninsula likely formed in this way, for the irregular shoreline of the landward edge of Willapa Bay offers no evidence that erosive ocean waves ever reached that shore. As sea level continued to rise during the last several thousand years, there must have been a proto-spit that sheltered the slowly-submerging Willapa Bay.

Inland migration of the beach initially formed a sand spit several thousand years ago and this was followed by seaward progradation. The Columbia River is the major sediment source for this accretion, with most of its sand moving northward. The growth pattern of the Long Beach Peninsula is relatively simple, shown by its ridge group distribution in Figure 8 based on the work of Cooper (1958). The accretion started at the outer-margin of the spit shoreline formed during the maximum inland advance of sea-level. The development of successive beach and dune ridges has subsequently converted the narrow barrrier into a wide peninsula that is stabilized and forested. Ridge building has gone on without significant interruption in the southern half of the peninsula. In the northern half, however, evidence indicates that beach erosion occurred
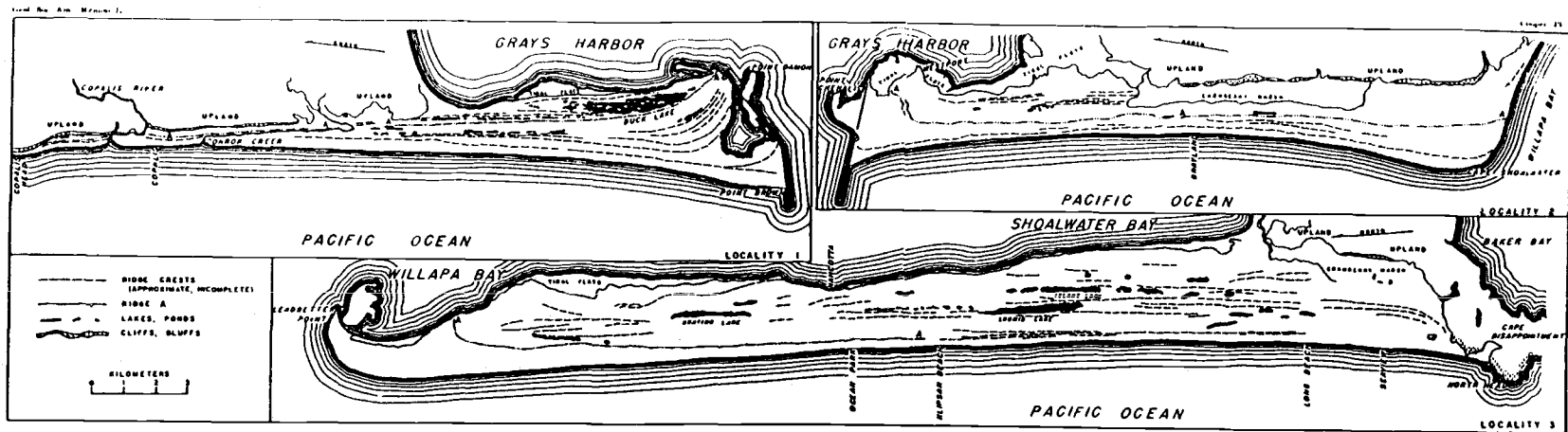
Figure 8
Beach/dune ridge groups on the Long Beach Peninsula (from
Cooper, 1958).

around 3,000 years B.P. and pushed the shore back a short distance (Cooper, 1958). This period of erosion was then replaced by another stage of progradation. The progradation of the Long Beach Peninsula has continued into modern times. Phipps and Smith (1978) analyzed maps and photographic data that cover a period 1871 to 1978. The shoreline accretion pattern is plotted in Figure 9, which shows that the progradation is regular and has continued at a high rate in the south, while the shoreline positions become confused and criss-cross one another to the north. The over-all rate of shoreline advance has been about 6 m/year.

Although the northward longshore transport of sand derived from the Columbia River has in general caused progradation of the Washington beaches, there are noteworthy exceptions. This is especially the case at Cape Shoalwater on the north shore of the entrance to Willapa Bay (Figure 3). There is no other place on the Pacific Northwest coast that has had more rapid erosion and a longer erosion history (Terich and Levenseller, 1986). Charts and field surveys by the U.S. Army Corps of Engineers have shown that the average erosion rate was 38 m/yr from 1890 to 1965, and slowed to 30 m/yr for the period 1975 to 1984. It is believed that northward accretion of the Long Beach Peninsula and migration of the entrance channel into Willapa Bay have caused the erosion of Cape Shoalwater. During the past century the inlet has been migrating toward the north, causing the erosion of the Cape. However, it appears that still earlier the migration was to the south, permitting the southward growth of small spits at Cape Shoalwater. Accretion has at times occurred simultaneously on both the Long Beach Peninsula and Cape Shoalwater, causing a narrowing of the bay entrance. This narrowing was then followed by erosion as the inlet began to migrate. These two spits

Figure 9

Shoreline accretion patterns along the Long Beach Peninsula

(Phipps and Smith, 1978).
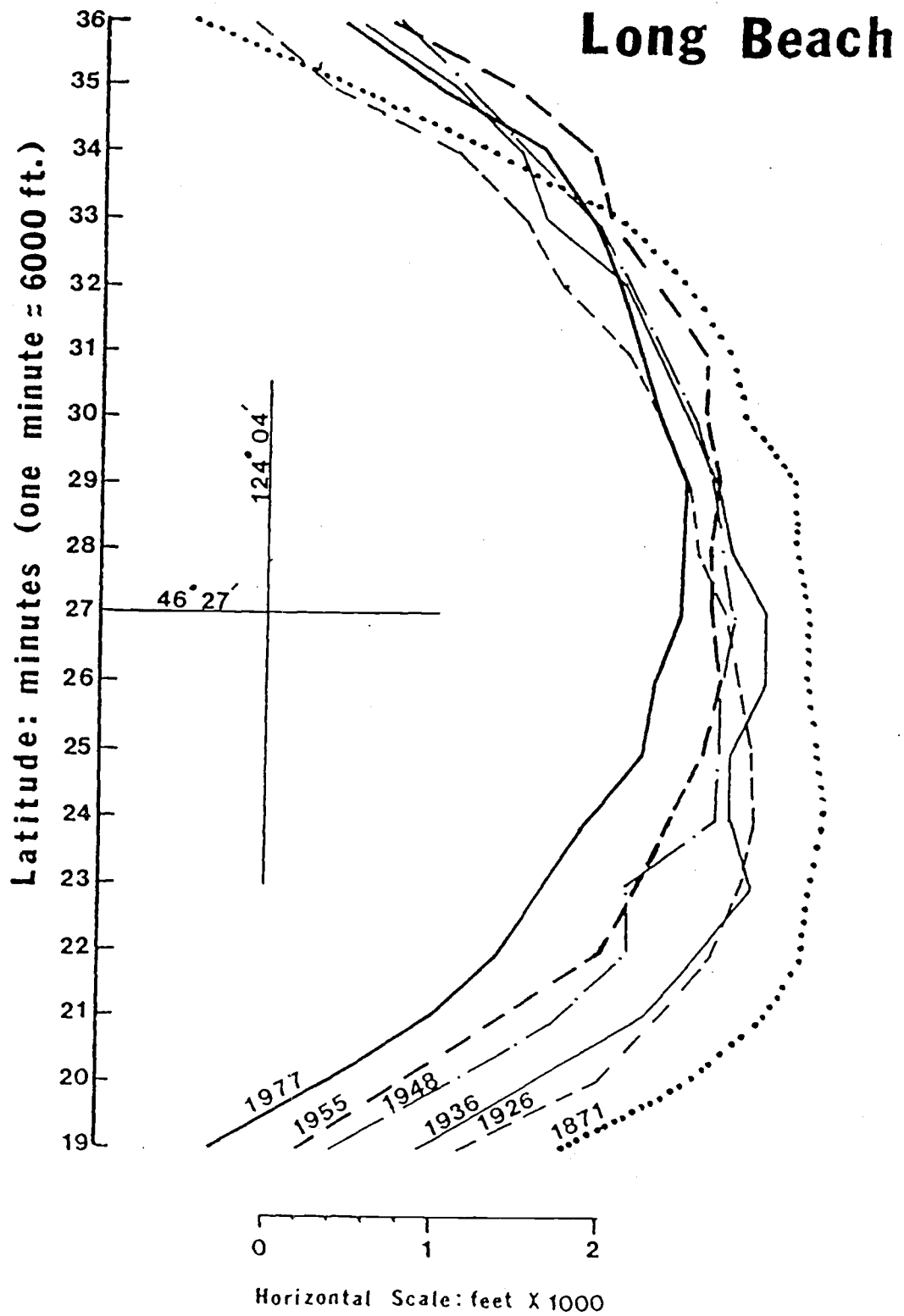
Figure 9

probably have experienced several cycles of advance and retreat. The last maximum narrowing was at the turn of the century. Between 1852 and 1887, Leadbetter Point at the tip of the Long Beach Peninsula migrated northward about 2.1 km, while Cape Shoalwater accreted 760 m southward. The bay mouth was then only 4.8 km wide (Phipps and Smith, 1978). Sometime between 1890 and 1911 this situation reversed and both spits began to erode. The erosion at Cape Shoalwater has been continuous. The erosion at Leadbetter Point has been interrupted by periods of accretion, and its average position has not changed significantly since 1887 (Phipps and Smith, 1978).

3.4 Shoreline Changes due to Jetty Construction

A map prepared by Lewis and Clark in 1806 shows the Columbia River mouth and surrounding area. It includes the dune ridges of the Clatsop Plains, and Tillamook Head is labeled as "Point of Clark" (Thwaites, 1905). Although no information is given as to water depths at the river mouth, it is of special interest that the entrance extended from Point Adams to the rocks of Cape Disappointment.

The earliest chart of the river's entrance was made by Admiral Vancouver in 1792 (Lockett, 1959, 1962). It indicated that the mouth of the Columbia had only one channel, but up river from Point Adams there were two channels separated by a shoal. By 1839, Sir Edward Belcher found that this two-channel system had moved downstream to the entrance area and a large shoal, called the Middle Sands, had developed which divided the river mouth into separate north and south channels. A portion of the Middle Sands formed an island inside the entrance, which later separated from the main shoal and migrated northward by 1879 to

form Sand Island. An 1885 chart of the river mouth is reproduced in Figure 10a, which shows Sand Island to the north of the main channel. The northern portion of Middle Sands had joined with Peacock Spit adjacent to Cape Disappointment, and the southern portion with Clatsop Spit. Peacock Spit appears to have been a submerged shoal, the minimum soundings on the chart being -1 ft MLLW. Lockett (1959, 1962) and Kidby and Oliver (1966) provide more detailed summaries of the natural changes in the Columbia River mouth prior to jetty construction.

Continued shifting of channels and shoaling at the mouth of the Columbia caused navigation problems, and it was decided that jetty protection was needed. The construction of the south jetty began in April 1885 and was completed together with four groins along its north side in October 1895. At this stage the jetty length was 7.2 km (4.5 miles), and lay in a northwesterly direction from its base at Point Adams (Lockett, 1959, 1962). A general improvement in bar crossing was achieved, and by 1895 depths of 9 m were available over the bar on an alignment which had migrated about 5 km northward apparently due to the influence of the south jetty. However, these favorable conditions were only temporary. During the construction of the south jetty, shoals had already begun to form along both sides of the jetty. Continued northward migration of the channel caused closure of the 9-meter depth contour and three separate channels developed. Shoaling continued near the south jetty within the entrance, and this shoaling appeared to be a continuation of the Clatsop Spit which had accreted to form a hook-shaped island through the south jetty, mid-way along its length, as seen in the 1902 chart of Figure 10b.

Due to the renewed shoaling problems in the entrance, it was recommended that the south jetty be extended and a north jetty be

Figure 10

Charts of the Columbia River mouth for (a)1885, (b)1902, and (c)1957 based on Coast and Geodetic Survey Charts compiled by Lockett (1963).

(a) 1885

PACIFIC OCEAN

Cape Disappointment

Baker Bay

Sand Island

Peacock Shoal

bar

COLUMBIA RIVER

Clatsop Shoal

Point Adams

0   km   5
Depths in feet below MLLW

(b) 1902

Clatsop Spit

(c) 1957

North Head

Peacock Beach

Clatsop Spit

Point Adams
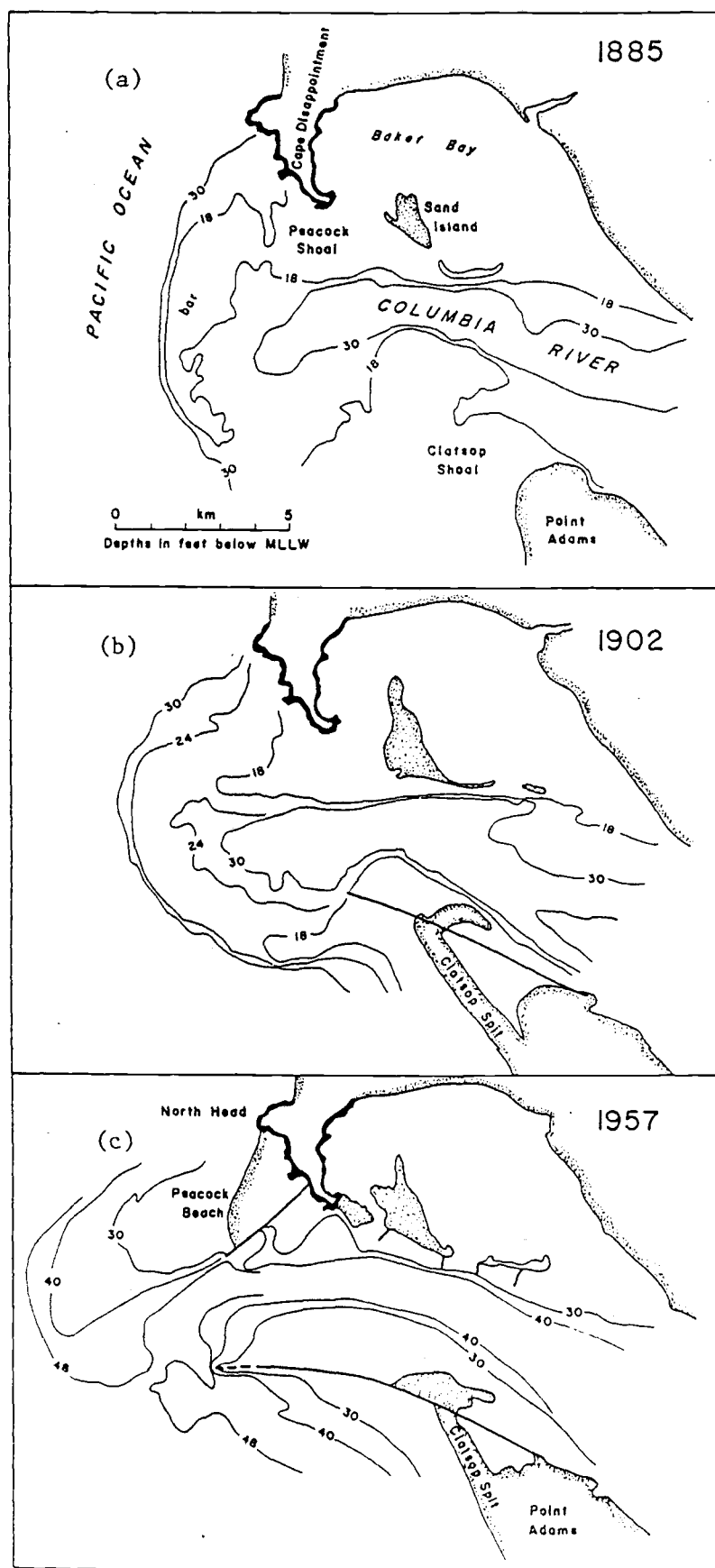
Figure 10

constructed. The extention and rehabilitation of the south jetty were carried out between 1903 and 1913, giving it a total length of 10.6 km. Construction of the north jetty began in 1913 and was completed in 1917 with a total length of 3.9 km. The completion of the north jetty and extension of the south jetty were accompanied by increased entrance depths through a narrow bar channel. In an effort to prevent the continued northward migration of the channel, four dikes were built in 1938 along the south shore of Sand Island, and Jetty A was constructed in 1939 which extends from Cape Disappointment southward to a point beyond the southern limits of Sand Island. These efforts increased channel depths and caused the channel to shift to a more east-west orientation. Since the completion of this three-jetty system, the mouth of the Columbia River has generally been stable (Kidby and Oliver, 1966). The present-day configuration of the river mouth is shown in Figure 10c, with the major north and south jetties and series of small training jetties within the channel itself.

Of interest to the context of the present study are the shoreline changes that have occurred to the north and south of the jetties, apparent in a comparison between the series of charts in Figure 10. Peacock Beach accreted to the north of the north jetty. Sand accumulation was rapid, with the seaward shift of the shoreline nearly keeping pace with the extension of the north jetty during its construction. The shoreline is presently only some 200 meters from the westward end of the jetty. However, the sand accumulation apparent in the exposed beach also continued offshore with the formation of Peacock Shoals, apparent in Figure 10c. The accreted land covers about 3.2 km^2 area, with a shoreline length of 3.7 km between the north jetty and North Head. This headland is

the small portion of Cape Disappointment that still has ocean frontage. It might appear in Figure 10c that the accreted shore is a pocket beach between the jetty and North Head, but this headland is relatively minor and it is clear that it does not offer a significant obstacle to longshore sand movements.

Accretion to the south of the south jetty took the form of Clatsop Spit, Figure 10c, which connects the pre-jetty shoreline of Point Adams to the jetty mid-way along its length. It formed at the time of the initial construction of the south jetty (1885-1889), and continued to accrete during the early 1900's before extension of the south jetty (1903-1913). The shape of Clatsop Spit gives the appearance that it developed by the northward drift of sand in the lee of the new jetty, but according to O'Brien (1936) and Lockett (1959, 1962), it first appeared as a shoal that crossed the newly-constructed jetty, and then either grew southward toward Point Adams or appeared as a bar along its full length. Formation of the spit was accompanied by significant increases in water depths immediately offshore and to the south of the jetty, so it is possible that onshore movement of sand produced the accretion.

This period of accretion of Clatsop Spit was replaced by intense erosion when the south jetty was extended and rehabilitated. The Corps of Engineers monitored this erosion with a series of profile lines and analyses of aerial photographs (Kidby and Oliver, 1966). They found that the erosion was limited to the beach extending from the south jetty to a nodal point 5 km to the south, beyond which a small amount of accretion occurred. Maximum recession rates close to the jetty amounted to 12 m/year. Offshore surveys showed that there was continued deepening of the water to the south of the jetty. The erosion of Clatsop Spit has

progressively declined through the years, and is negligible today. No consensus of opinion has emerged as to its cause. Lockett (1959, 1967) interpreted its erosion together with accretion of Peacock Beach north of the jetties as evidence for a net southward longshore transport, but such a conclusion is certainly incorrect. O'Brien (1936) concluded that the erosion of Clatsop Spit was principally due to winds blowing the sand inland to form dunes, but this explanation is also questionable. The erosion is probably a combination of several factors. All investigators agree that the seaward extension of the south jetty may have blocked the southward movement of Columbia River sediments. Thus the sediment-deficient summer littoral currents will erode the area immediately south of the south jetty, and induce erosion along the Clatsop Spit. It is also possible that waves arriving from southwest storms reflected from the extended jetty, these reflected waves then breaking at large oblique angles to the shoreline of Clatsop Spit to produce the erosion. Similar erosion due to wave reflection occurred with the construction of a breakwater in Halfmoon Bay, California (P. Komar, pers. com.).

It is seen from this history of jetty construction and accompanying shoreline changes, that the beach areas of maximum placer development, Clatsop Spit and Peacock Beach, both owe their existence to the jetties. Neither beach existed prior to jetty construction.

Chapter 4
THE BLACK-SAND DEPOSITS

4.1 Extent of Black Sand Deposits

It is seen from the history of jetty construction and accompanying shoreline changes presented in the previous chapter, that the maximum beach-placer development is found on Clatsop Spit and Peacock Beach, neither of which existed prior to jetty construction. The sands on these beaches close to the jetties are almost totally black, indicating high concentrations of heavy minerals. Away from the jetties, the beach sands become visually lighter in color, indicating a progressive decrease in heavy-mineral contents, replaced by normal tan-colored quartz and feldspar sand.

Ballard (1964) has shown that heavy mineral concentrations in the 3.0-3.5ϕ sieving fraction of summer beach-sand samples can reach 26% and 81% immediately south and north of the jetties. Ten to fifteen kilometers away from the jetties, the heavy mineral concentrations dropped to below 5% and 10% to the south and north respectively. The placer deposits exposed on the beaches are also found to be more concentrated during the winter when the beach face is cut back by erosion. Peterson and Binney (1988) collected samples in the winter of 1984, right after the strong storms and erosion associated with the 1982-83 El Niño. They found that heavy mineral abundances reached 95% and 96% immediately south and north of the Columbia River jetties. The rich concentrations of heavy minerals are known to be present under a considerable area and to some depth within these beaches. Surveys by Peterson and Binney found placer-level concentrations extending at least

100 m in the cross-shore direction, 500 m alongshore, and 2 m thick. With these dimensions and known mineral concentrations, they estimated the volume of the placer deposits to range from 2 to 7 million cubic meters, with an average of 4.5 million cubic meters.

It is apparent that Columbia River sand served as the raw material from which the black-sand heavy minerals were concentrated. In Chapter 2 it was noted that the annual bedload sediment discharge of the Columbia River is estimated to be about one million tons, and that this bedload contains about 14.4% heavy minerals, of which 4.8% are opaques. If we accept that the volume of the placer deposit is approximately 4.5×10^6 m^3, and the average volume percentage of heavy minerals in this deposit is 60% (Peterson and Binney, 1988), the number of years required to accumulate this placer deposit can be calculated as follows:

volume of heavies: 60% of 4.5×10^6 m^3 = 2.7×10^6 m^3

weight of heavies: density 3.5 times 2.7×10^6 m^3 = 9.45×10^6 tons

annual river supply: 14.4% of 1×10^6 tons = 0.144×10^6 tons

years needed: 9.45×10^6 tons/ 0.144×10^6 tons = 66 years

The average density of the heavy minerals has been taken as 3.5 tons/m^3 in the above calculation. If the same analysis is carried out using only the opaque minerals, the resulting estimate is that it would take 60 years to form this placer deposit. These calculations suggest that the placers in the study area started to accumulate early in this century, agreeing with their known development associated with construction of the north and south jetties.

4.2 Commercial Explorations

Commercial interests in black-sand deposits near the mouth of the

Columbia River pre-date jetty construction and therefore the formation of the placers on Peacock Beach and Clatsop Spit. As part of a general investigation of black sand deposits along the coast, Day and Richards (1906) collected samples from selected sites along the Columbia River as well as from nearby beaches. Analyses revealed relatively large amounts of titaniferous magnetite. As part of the War Minerals Investigation Program in the 1940's, the U.S. Bureau of Mines further investigated the magnetite resources (Glover, 1942; Kelly, 1947; Zapfee, 1949). Most of this early interest focused on deposits near Hammond, Oregon, at the tip of Point Adams, the sand spit which pre-dated the shoreline modifications due to jetty construction. At that time, 113 holes with a combined length of 440 m were drilled near Hammond, revealing a black sand deposit measuring 150 m wide, 240 m long and at least 1 m deep (Oregon Department of Geology and Mineral Industries, 1941). Another mineral deposit of early interest is located immediately across the river in the McGowan area of Pacific County, Washington; 48 holes were drilled in the McGowan deposit. Microscopic analyses of drill samples from these sites showed that the black sands consist principally of magnetite (53%) with appreciable amounts of ilmenite (18%), garnet (13%) and zircon (1%) (Kelly, 1947).

Interest in the magnetite-ilmenite resources of the area continued after World War II. During the late 1940's and early 1950's, the U.S. Bureau of Mines sampled sands dredged from the shipping channel by the U.S. Army Corps of Engineers (Norberg, 1980). However, the mineral contents were low, and it was concluded that the submerged bars at the river's mouth are not subject to processes which concentrate the heavy minerals to produce black sands, nor are there any major concentrations of

black sands in the main channel between Portland and the river's mouth.

Commercial interest then shifted to the black sands on Clatsop Spit and Peacock Beach, the deposits on the modern beaches which formed due to jetty construction. In 1963 the Bunker Hill Company of Idaho undertook exploratory drilling along Clatsop Spit, covering a six-mile-long by one-half-mile-wide area (Bunker Hill, unpublished report to the Department of Oregon Geology and Mineral Industries, 1963). The 34 holes drilled ranged in depth from 12 to 26 m, and had a combined length of 650 m. The first 3 meters of sand contained the highest concentrations of iron (about 10 kg per ton of sand), but the extent of the deposit fell well short of that necessary for commercial development. It is of interest that this bore-hole exploration showed that the placer is largely limited to the modern beach along Clastop Spit, that it has minimal landward extent and is limited to the near surface of the beach. This geometry of the deposit further establishes that the placer formed in the sand body which accumulated during construction of the south jetty, and that the heavy-mineral concentration probably took place during the later stage of erosion of Clastsop Spit.

The more extensive and concentrated deposits on Peacock Beach north of the jetties have attracted considerable commercial interest. Space Metals Inc. of Salt Lake City, Utah, reported in 1968 on the mineral contents found in drill samples that reached depths of 6 to 15 m, collected along the length of the beach at its landward limit, and from 91 m inland from the beach but still within the sands that accumulated between the north jetty and North Head. The highest reported concentration found was 31.37% magnetite which came from a 6 m long core from the modern beach. Other drillings yielded concentrations ranging 1.12 to 10.44% magnetite.

The authors of the report concluded: "There is no question that the Benson Beach [Peacock Beach] deposit is one of the most high grade heavy mineral deposits in the world. Just how rich it actually is, and how fully it can be developed, cannot be determined without further testing. However, without reservation, I can state that it is the richest deposit in heavy minerals that I have ever seen or heard of." In spite of this assessment, it is apparent from the drilling data that the principal area of black sand concentration is on the modern Peacock Beach, and that the sands quickly decrease in heavy-mineral content landward away from the beach. Furthermore, the black sand on the beach is limited mainly to the near surface, and may extend down to only some 2 to 3 meters, just as found by Bunker Hill Inc. south of the south jetty.

The most recent commercial interests have been in the potential black-sand deposits offshore from Peacock Beach. An aerial-magnetic survey conducted in 1973 identified three magnetic anomalies centered at about 2 km seaward from North Head. Limited sampling in the area during January 1975 for Beach Mining, Inc. found sands containing 5 to 10% recoverable magnetite.

4.3 Scientific Investigations in the Study Area

Nearshore sands and their longshore dispersal patterns in the study area have been studied by several investigators. The first research of note was that by Hodge (1934) who examined the mineral compositions of the beaches adjacent to the Columbia River and compared them with the river sands. He correctly concluded that the beach sands are derived from the Columbia, and also noted that the mineral grains are fresh and angular, suggesting that the sands are rapidly transported down the river and

delivered to the beaches. Hodge also speculated on the nature of the sand movements at the mouth of the river and how those transport patterns might have been affected by jetty construction.

Twenhofel (1946) undertook textural and mineralogical analyses of beach sands along the entire coast, and discussed factors that control their dispersal and deposition. He also indicated that the Columbia River is a major source of sediments, and has supplied the black heavy minerals to the beaches near the river mouth. Twenhofel noted the existence of the black sands north and south of the jetties, and also reported the existence of a deposit on Sand Island, a deposit that has not been found by subsequent investigations.

The earlier studies most closely related to the present thesis research are those of Ballard (1964) and Plopper (1978). Ballard undertook textural and heavy mineral analyses on 125 samples from the beaches and shallow offshore along the coast from Tillamook Head, Oregon, to Grays Harbor, Washington. He concluded that the Columbia River is the major contributor of sediments to this area, a sand supply that accounts for the progradation of the beaches along this coastline. Potential sand sources such as drainage systems entering Willapa Bay were found to be insignificant, a conclusion that was later supported by Luepke and Clifton (1983). Based on his textural and mineralogical data, as well as on estimates of the longshore component of wave energy flux, Ballard concluded that the dominant longshore sediment transport is to the north. He documented the high concentrations of heavy minerals immediately north and south of the Columbia River jetties, and their progressively decreasing concentrations with distance from the jetties. Ballard examined longshore variations of mineral ratios such as

hypersthene/hornblende in an attempt to document grain sorting processes.

Plopper (1978) studied the texture and mineralogy of beach sands along most of the length of the Washington coast. He again found that heavy mineral concentrations decrease northward from the Columbia River. Plopper's main objective was to examine the sorting patterns of the different minerals as they are transported northward along this coast. His approach was to examine "settling equivalent" grains, physically extracted as they descended in a laboratory settling tube. The extraction was designed to remove grains that are equal in settling rates to quartz spheres of 2.50ϕ diameter. The analysis approach was the same as that used by Trask and Hand (1985) to investigate the differential transport rates of heavy minerals along Lake Ontario beaches. Plopper found on the Washington beaches that within the extracted settling-equivalent fractions, there is a hydraulic lag wherein the higher the density ratio between two minerals, the more rapid their concentration difference increases with distance northward from the Columbia River.

Chapter 5

SAMPLE COLLECTION AND LABORATORY ANALYSES

5.1 Sample Collection

The primary objective of this study is to understand the sediment sorting processes important to the development of the black-sand deposits. This has involved an examination of longshore variations of grain sizes and mineralogies of the beach sands north and south of the Columbia River. Totally ninty beach samples were collected in the study area during February and October 1987, months which respectively represent winter and late-summer beach conditions. The locations of these samples are identified in Figure 11, and extend from Tillamook Head at the south to the end of the Long Beach Peninsula, covering a total shoreline distance of about 70 km. The samples were coded as sn, ss, wn and ws (representing summer north, summer south, winter north and winter south respectively). They were also numbered starting from the Columbia River mouth northward from 1 to 11 and southward from 1 to 7. The samples were obtained at mid-beach positions exposed during low tides. On some profiles a series of samples were obtained from the low-tide shoreline, the mid-beach level, the top of the beach, and from any adjacent sand dunes, so as to examine cross-shore sorting patterns. Thirty six mid-beach samples were selected for the longshore sorting analysis. Only the upper 1-2 cm of sand was collected so that the samples represent a contemporaneous sedimentation layer. Each sample included a cross-shore rectangular area so as to obtain a representative sand volume that eliminates local sorting such as might be produced by backwash ripples

Figure 11

A map of the study area showing the sample locations.

Figure 11

58
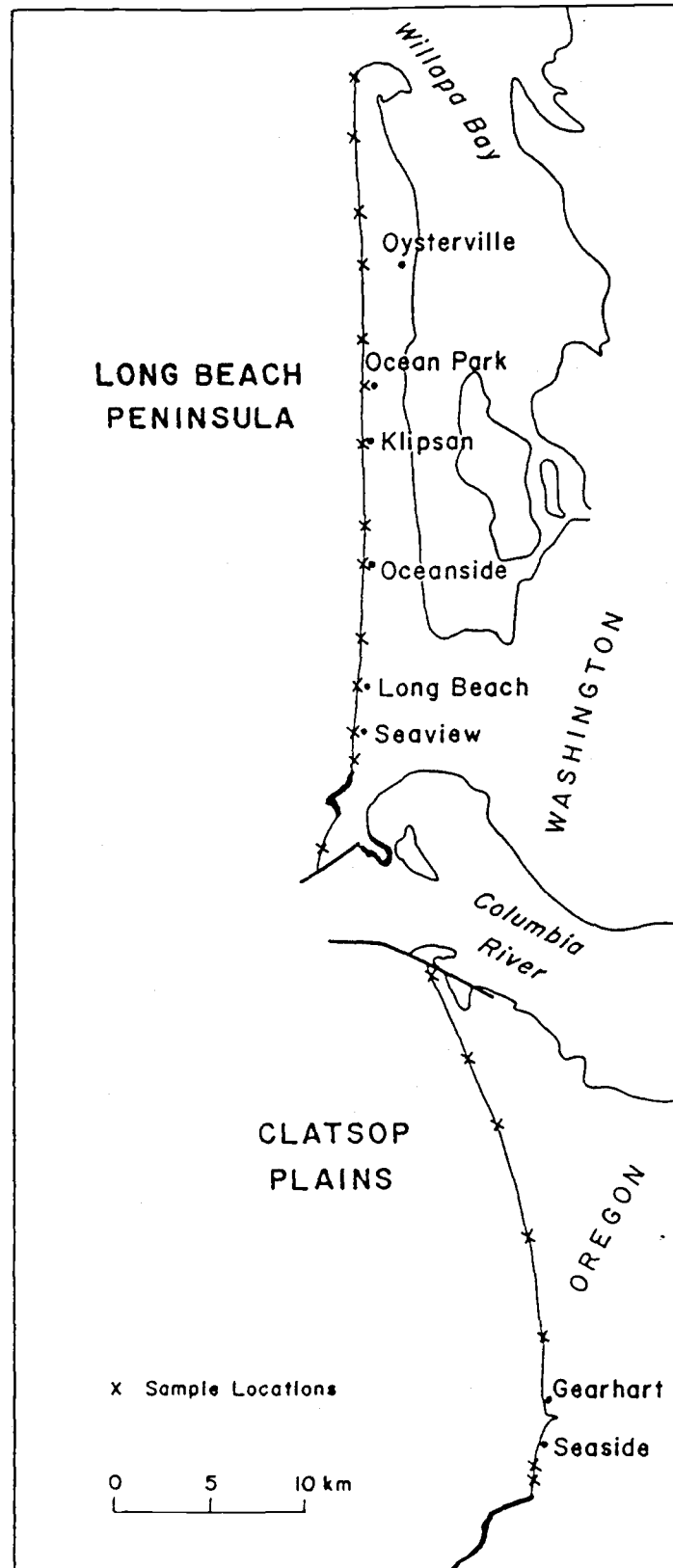
(Komar et al., 1989). The normal weight of a sample was about 400-500 grams, and each was placed in a heavy-duty plastic bag for transfer to the laboratory.

5.2 Laboratory Analyses

All sand samples were thoroughly washed with tap water to remove the salt and organic material. They were then oven dried at 88°c for 2 to 3 days, depending on the size of the sample. Two subsamples were obtained from each sample using a mechanical splitter. Sieving analysis was undertaken on one of the subsamples to determine the textural characteristics of the total sample (light and heavy minerals together). The second subsample was used in the heavy mineral separation in order to isolate the heavy mineral concentration for each sample. The details of this separation procedure are described in Appendix I. Sieving analyses were then performed on the separated heavy and light minerals.

Two types of sieves were used in the analyses. The total samples and the light fractions obtained from the heavy mineral separations were sieved using standard 20-cm diameter sieves with 1/4φ intervals. The samples were sieved for 15 minutes on a Ro-Tap machine in the Department of Geology. Due to the small sizes of the heavy-mineral fractions, their sieving was carried out using 8-cm diameter sieves on a vibrator. Because of the smaller diameter of these sieves, the vibration time was set for 20 minutes instead of 15. The detailed procedures of the sieving analyses followed those suggested by sedimentology textbooks such as that of Lewis (1984).

A small subsample of heavy minerals split from each sieving

fraction was mounted on a microscope slide in Canada Balsam. Heavy minerals were identified and counted under a petrographic microscope following standard techniques (Kerr, 1959; Phillips and Griffen, 1981). Two hundred grains were identified and counted for each slide, and the heavy minerals were classified into the following species: hornblende, augite, hypersthene, opaques (magnetite + ilmenite) and others, which include actinolite, olivine, diopside, enstatite, clinozoisite, staurolite, garnet, zircon and other altered unknowns. The identification criteria for the major heavy minerals are described in Appendix II. The number percentage obtained by point counting was then converted to weight percentage according to Rubey (1933) and Young (1966), so that the mineralogy of the heavy minerals and their grain size distributions were obtained for each sample.

5.3 Sieving and Grain-Settling Distributions

Standard sieving analyses yield distributions of sediment sizes in terms of the sieve openings. In order to understand the grain-sorting processes, it is necessary to convert these sieve sizes into actual particle diameters which can in turn be related to the settling velocities of the grains (Komar and Cui, 1984).

With that objective, five grains each of the major minerals quartz(Qtz), hornblende(Horn), augite(Aug), hypersthene(Hyp) and opaque(Opq, ilmenite and magnetite) were randomly selected from the series of sieve fractions of a typical sample (sn2). Each grain was first viewed under a binocular microscope to make sure it rested on the plane containing the longest and intermediate axial diameters, denoted

respectively by D_a and D_b, which were then measured using a micrometer.

These measured D_a and D_b diameters are listed in Appendix III, while Table

4 summarizes the mean D_b diameters based on the five selected grains.

Each grain was stored in a marked vial for the settling velocity

measurements described below.

Table 4   Sieve sizes (D_{sv}, mm) and mean intermediate diameters (D_b, mm)
for major minerals of sample sn2.

Dsv	Db-Qtz	Db-Horn	Db-Aug	Db-Hyp	Db-Mag
0.30	0.37				
0.25	0.35	0.37	0.31	0.34	0.31
0.21	0.27	0.30	0.29	0.31	0.30
0.18	0.25	0.26	0.26	0.27	0.24
0.15	0.22	0.20	0.20	0.19	0.19
0.13	0.17	0.17	0.16	0.16	0.17
0.11	0.15	0.15	0.16	0.14	0.15
0.09	0.12	0.13	0.13	0.14	0.13

The passage of a grain through sieves is governed mainly by its

intermediate axial diameter, D_b , which orients across the diagonal of the

sieve opening. Following the approach of Komar and Cui (1984), the

measured D_b diameters for grains from individual sieves were compared to

the dimensions of the square sieve openings, which would be the diameter

D_{sv} of spherical particles that could pass through the sieve. The average

intermediate diameters of the major minerals listed in Table 4 are plotted

in Figure 12 versus the sieve size, D_{sv}, upon which the fraction is retained.

Linear regression was performed and the following D_b versus D_{sv}

Figure 12

Relationship of average intermediate diameters D_b (mm) of major minerals versus their sieve median grain sizes D_{sv} (mm) for sample sn2. The linear regression equation is also shown for each mineral.
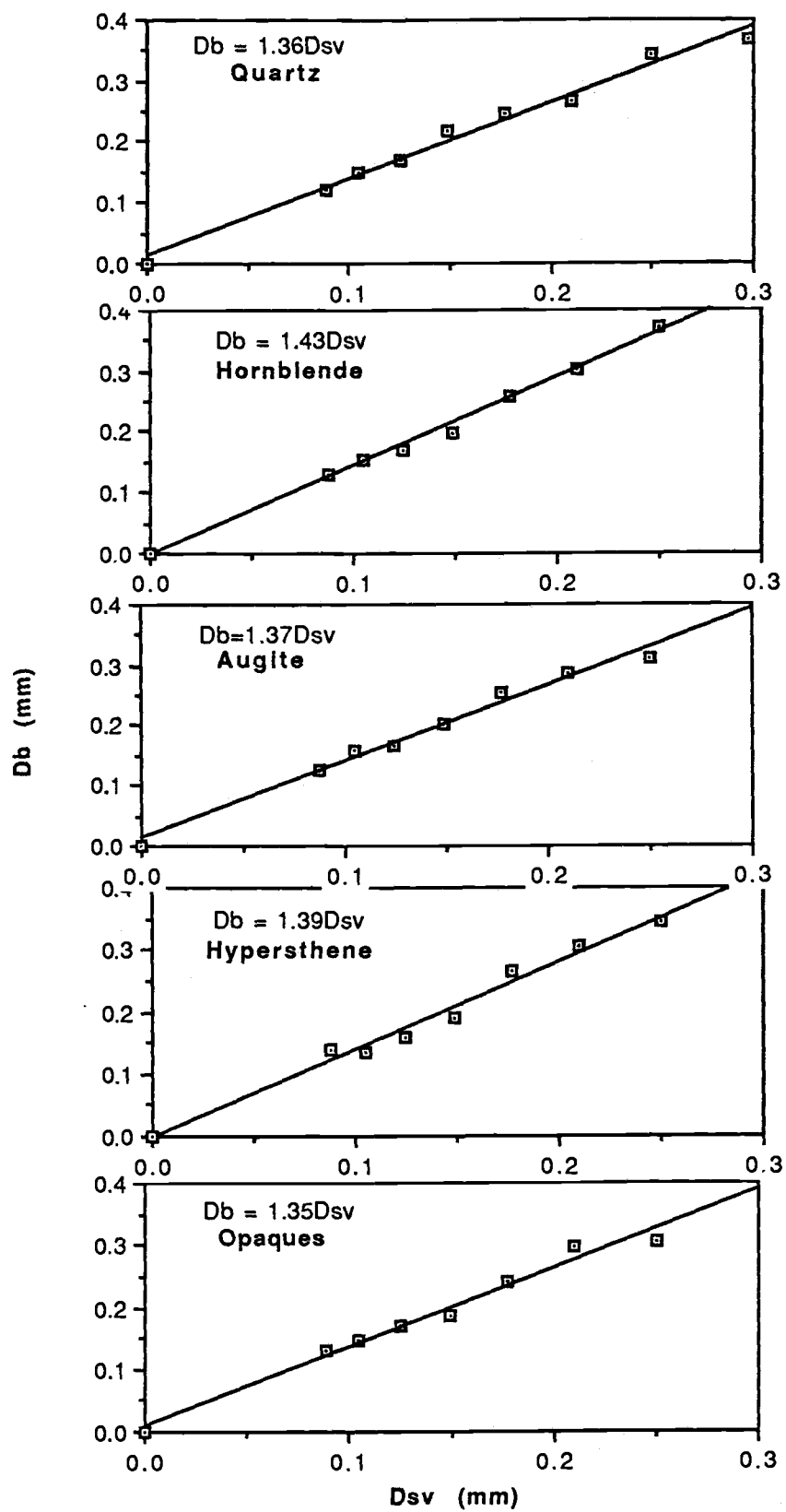
Figure 12

relationships obtained:

Quartz	$D_b = 1.36 \, D_{sv}$	(1a)
Hornblende	$D_b = 1.43 \, D_{sv}$	(1b)
Augite	$D_b = 1.37 \, D_{sv}$	(1c)
hypersthene	$D_b = 1.39 \, D_{sv}$	(1d)
Opaques	$D_b = 1.35 \, D_{sv}$	(1e)

Using the same method, Komar and Cui (1984) found a similar relationship for quartz grains: $D_b = 1.32 \, D_{sv}$. Wang and Komar (1985) concluded that this 1.32 proportionality coefficient for quartz grains can generally be used for heavy minerals, though it was noted that the increased flatness of heavy mineral grains can cause larger proportionality coefficients. Since the analyses of this study yield a large range of proportionality coefficients (1.35-1.43), the individual D_b versus D_{sv} relationships given by equation (1) will be used for the major minerals in subsequent analyses to convert their sieving sizes into intermediate axial diameters.

Evaluation of the role of grain settling in the development of placers requires predictions and comparisons of the settling velocities of various light and heavy minerals. The approach taken here is to convert the sieving distributions of the minerals into grain-settling distributions. This conversion requires relationships between D_b and the settling velocity W_m for the major light and heavy minerals found in the samples.

The mineral grains used for the D_b versus D_{sv} analyses were again utilized in direct measurements of their settling velocities. The

measurements were made in a transparent plastic settling tube which is 2 m long and has a 20 cm diameter (Figure 13). Each grain was released at the surface and allowed to settle for 30 cm before timing began, so that it could reach its terminal settling rate. Grains smaller than 0.125 mm settle slowly, and were timed over a length of 40 cm. Grains larger than 0.125 mm have higher settling velocities, and thus were timed over a 90 cm tube length. A stop-watch was used to measure the time to 0.01 second. Extra lighting from the top and changeable black and white background papers were used so that the settling of light-colored versus dark minerals could be better observed. Another difficulty encountered in the settling rate measurements is that surface tension tends to trap the mineral grains at the surface of the water column, making it difficult to provide a smooth release. This was overcome by using a vial cap to assist in the release. The convex surface of the cap was first moistened with a damp paper tissue, and the grain was then gently placed on the surface. The wetted surface held the grain secure until the moment when it was placed in contact with the water surface. Despite all of these procedures, a few grains were still lost. Tumbling and spiral motions were observed during settling for about a dozen grains, and these were also excluded from the data. A total of 160 measurements were obtained for the seven sieve fractions of sample sn2; their W_m measured settling values are given in Appendix IV together with their D_b intermediate diameters.

The measured settling velocities of the grains were compared with the settling rates of spherical particles having the same density and diameter D_b. The terminal settling velocity W_s for a sphere of diameter D

Figure 13

Schematic diagram of the settling tube used for settling velocity measurements. The interchangeable background of white or black paper and the extra lighting were helpful for locating the finer light-mineral grains.

lighting

30 cm
start line

40 cm
line

90 cm
line

2 m

interchangeable
white or black
background
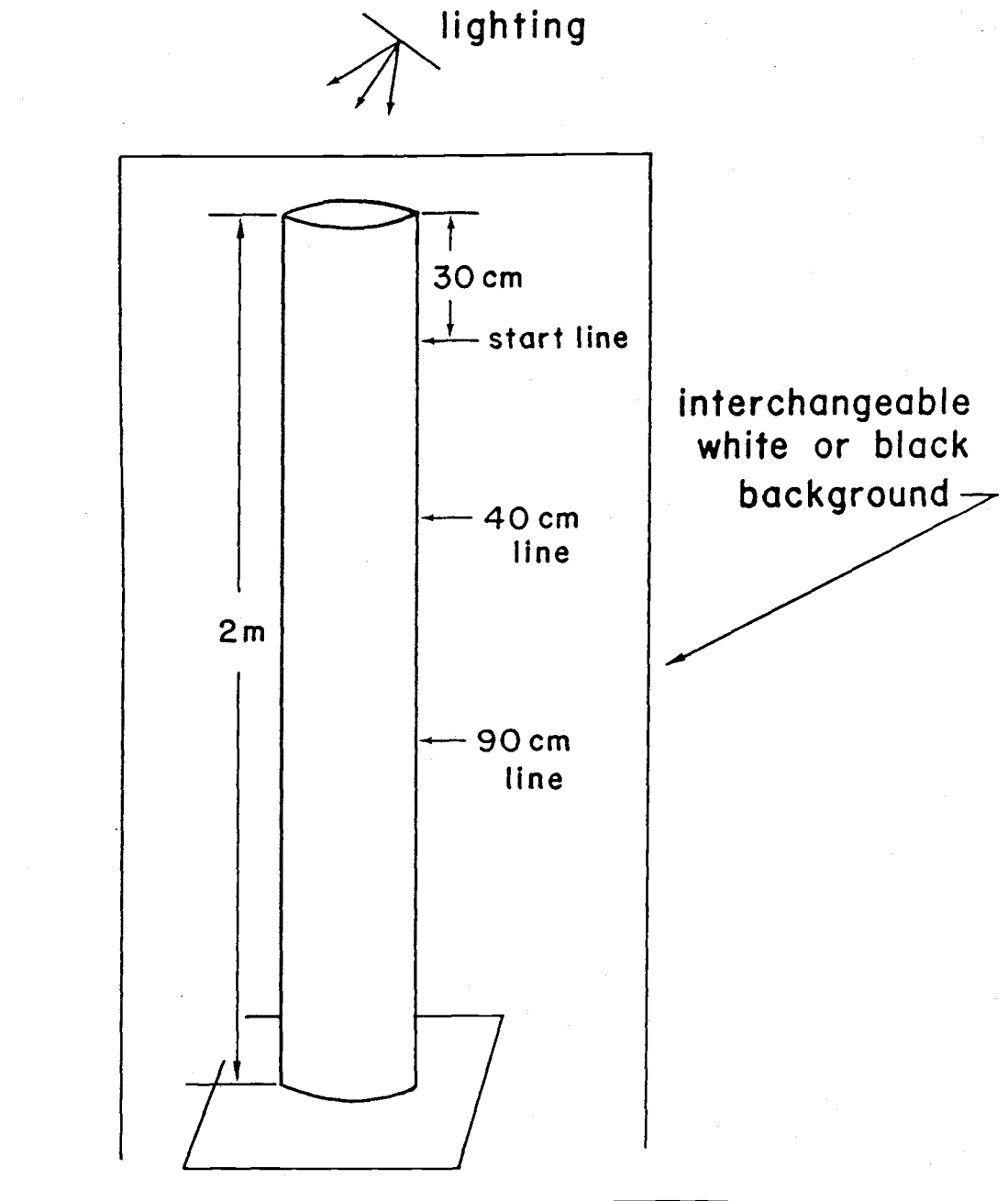
Figure 13

and density ρ_s is given by:

$$W_s = [(4/3)(\rho_s-\rho)gD/\rho C_d]^{1/2} \qquad (2)$$

Where ρ is the fluid density, g is the acceleration of gravity and C_d is the frictional drag coefficient. For small grains settling in the Stokes range (D < 0.1 mm for quartz spheres in sea water), $C_d = 24/R_e$ where $R_e = \rho W_s D/\mu$ is the Reynolds Number defined as the ratio of the inertial force to the viscous force. For Stokes settling, equation (2) can thus be simplified to

$$W_s = (1/18\mu)(\rho_s-\rho)gD^2 \qquad (3)$$

where μ is the fluid viscosity. However, for coarser grains having high Reynolds numbers, equation (2) must be used where an evaluation of the C_d drag coefficient is difficult. The theoretical settling velocities W_s of equivalent spheres for the coarser grains were calculated according to the power series of Davies (1945) as described by Warg (1973). Equation (2) can be rearranged and combined with $R_e = \rho W_s D_b/\mu$ to give

$$C_d R_e^2 = (4/3)(\rho_s - \rho)\rho g D_b^3/\mu^2 \qquad (4)$$

Davies (1945) performed least-square curve fitting for $C_d R_e^2$ versus R_e for data collected on the settling velocities of spherical particles. He obtained two polynomials:

For $C_d R_e^2 \leq 125$;

$$R_e = C_d R_e^2/24 - 2.3363\times10^{-4}(C_d R_e^2)^2$$
$$+ 2.0154\times10^{-6}(C_d R_e^2)^3 - 6.9105\times10^{-9}(C_d R_e^2)^4 \qquad (5a)$$

For $C_d R_e^2 > 125$;

$$\log R_e = -1.29536 + 0.986(\log C_d R_e{}^2)$$

$$-0.046677(\log C_d R_e{}^2)^2 + 0.0011235(\log C_d R_e{}^2)^3 \qquad (5b)$$

Thus, for a given ρ_s and D_b for the particular mineral grain, $C_d R_e{}^2$ can be calculated using equation (4). Depending on that value of $C_d R_e{}^2$, equations (5a) or (5b) are then used to obtain the Reynolds number $R_e = \rho W_s D_b / \mu$, which is then used to calculate the theoretical settling velocity W_s for a sphere that has the diameter D_b. The equivalent spherical settling velocities calculated this way for the mineral grains analyzed are listed in Appendix IV.

The measured settling velocities W_m can now be compared with the theoretically equivalent rates W_s if the particles were spheres. All of the measurements are combined in Figure 14, while individual minerals are analyzed separately in Figure 15. Power regression for all of the measurements yields the relationship,

combined	$W_m = 1.16\, W_s{}^{0.64}$	$(R^2=0.81)$	(6)

while regressions of the individual minerals yield,

quartz	$W_m = 1.07\, W_s{}^{0.68}$	$(R^2=0.84)$	(7a)
hornblende	$W_m = 1.19 W_s{}^{0.59}$	$(R^2=0.81)$	(7b)
augite	$W_m = 1.12\, W_s{}^{0.73}$	$(R^2=0.86)$	(7c)
hypersthene	$W_m = 1.07\, W_s{}^{0.65}$	$(R^2=0.84)$	(7d)
opaques	$W_m = 1.06\, W_s{}^{0.64}$	$(R^2=0.81)$	(7e)

Paired-t tests have been carried out to compare the combined equation (6)
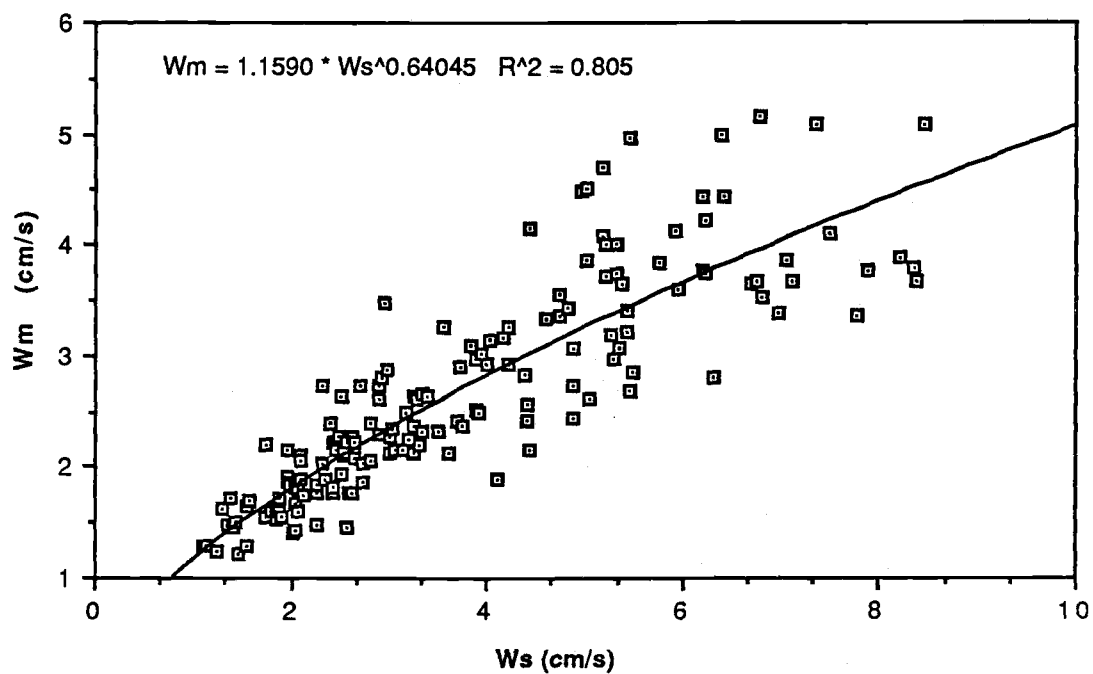
Figure 14
Overall relationship between the measured settling velocity W_m
(cm/s) and the spherical settling velocity W_s (cm/s) calclulated
according to Davies (1945) and Warg (1973). The grains were
chosen from sample sn2 and total of 160 measurements were
obtained.

Figure 15

Relationship between the measured and predicted settling velocities (W_m and W_s, cm/s) for each major mineral, with mineral grains obtained from sample sn2. The best-fit power regression line is also included in each diagram.
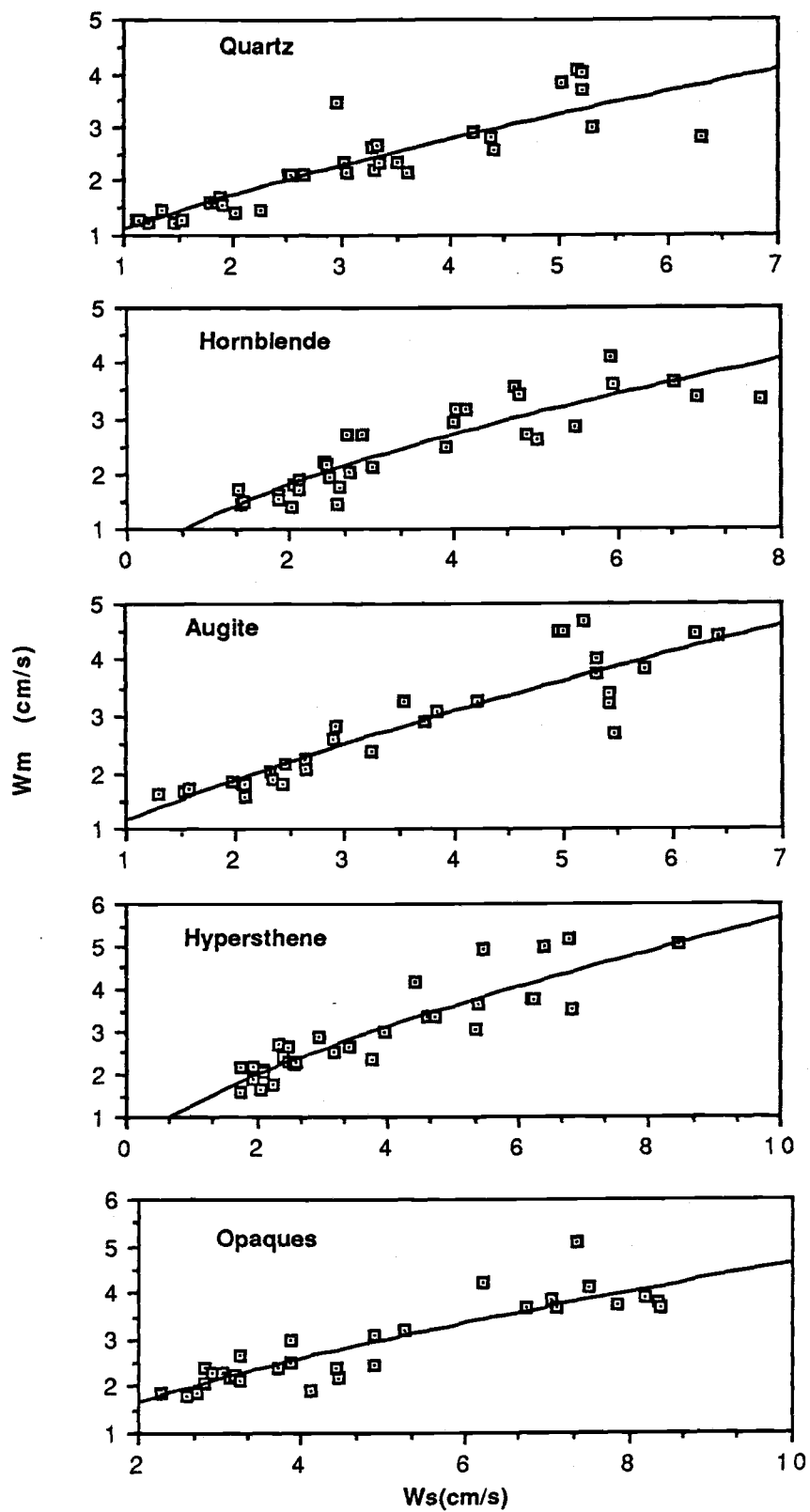
Figure 15

with the individual equations (7). It was found that at the 95% significance level, all the individual equations except that for hornblende are statistically different from equation (6). The differences in the coefficients for the series of minerals presumably reflect their contrasting shapes, that is, their sphericity and angularity (roundness). The individual equations (7) will be used in subsequent analyses so that mineral shape effects can be accounted for and that settling velocities will be best predicted for individual minerals.

The relationships of equation (1) now permit the conversion of D_{sv} sieve sizes into mean D_b axial diameters for the principal minerals in the study area, and equations (4) through (7) in turn permit the conversion to W_m settling velocities. By this approach, the sieving distributions for the minerals can be converted to W_m distributions. This is illustrated for sample sn2 in Figure 16, in which the intermediate axial diameters D_b (mm) and settling velocities W_m (cm/s) are plotted on log-normal probablility paper against their cumulative weight percents. The cumulative curves are reasonably straight, signifying that the grain sizes and settling velocities of the major minerals are normally distributed.

Figure 16

Cumulative frequency curves of intermediate diameter D_b (mm) and settling velocity W_m (cm/s) for major minerals of sample sn2. The distributions are generally normal.
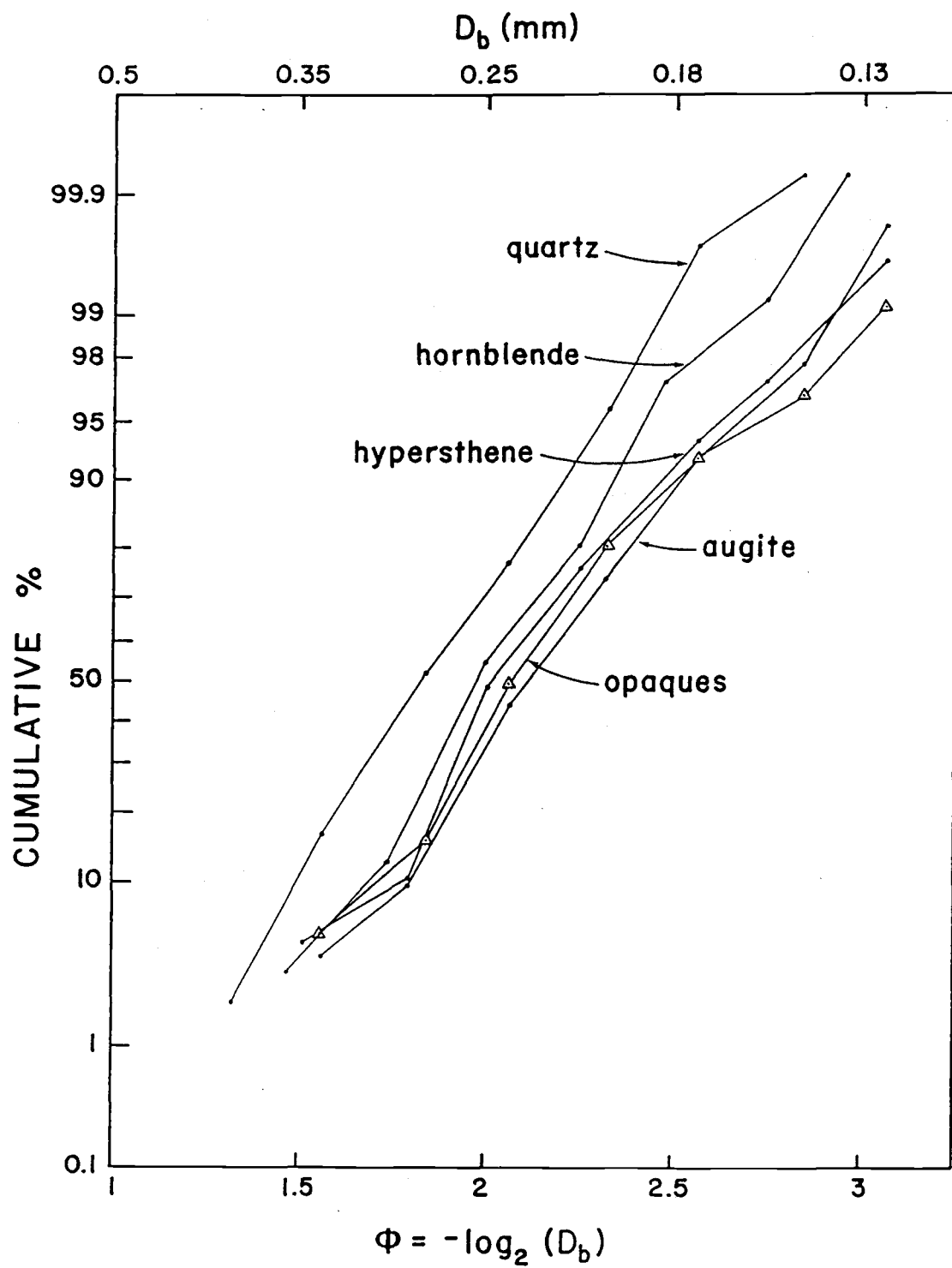
Figure 16
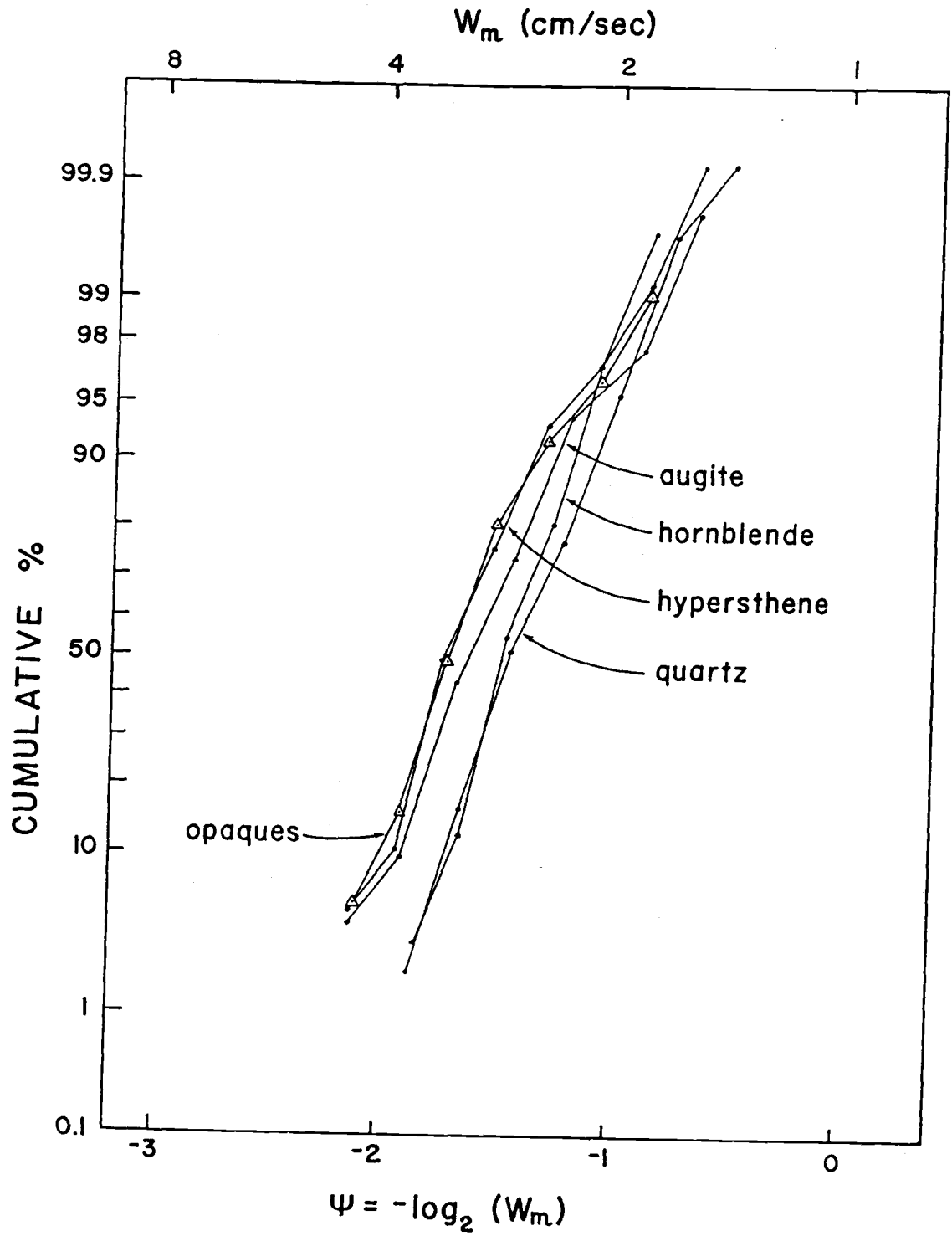
Figure 16 (continued)

Chapter 6

RESULTS OF TEXTURAL AND MINERALOGICAL ANALYSES

6.1 Textural Analyses

6.1.1 Textures of the Total Samples

Sieving analyses were first performed on subsamples of unseparated light and heavy minerals to obtain the textural characteristics of the total samples. The sieving results were plotted on probability paper as cumulative weight percent versus the grain size in phi units. The median grain size Md (the phi value at 50% weight) was obtained directly from the cumulative frequency curve. Other textural statistics, including mean grain size Mn, sorting coefficient So and skewness Sk, were calculated according to Folk and Ward (1957) and are presented in Tables 5 and 6. The median grain size, sorting coefficient and skewness of sediment samples are plotted versus the longshore distance from the Columbia River mouth in Figures 17, 18 and 19. Duplicate analyses resulted in a precision of 0.05-0.07 phi units for the sieving of the total samples and the light fractions.

6.1.2 Median Grain Size

Mean and median grain sizes represent nearly the same textural measure. The median grain size has been chosen over the mean in this study due to the fact that Md is straightforward to obtain and its use also makes the present study consistent with previous investigations [for instance, Komar and Wang (1984)]. The range of the median grain sizes is from 2.15ϕ (0.23 mm) to 3.21ϕ (0.11 mm), the average being 2.46ϕ (0.19

Table 5 Textures of the total samples from the Clatsop Plains.

Sample Number	Distance (km)	Md (ϕ)	Mn (ϕ)	Sorting Coef.	Skewness Coef.
Summer Samples					
ss1	0.6	2.76	2.82	0.35	0.17
ss2	5.1	2.63	2.64	0.25	0.05
ss3	8.6	2.56	2.54	0.35	-0.05
ss4	15.0	2.51	2.48	0.32	-0.12
ss5	20.4	2.58	2.50	0.31	-0.32
ss6	25.7	2.55	2.52	0.27	-0.13
ss7	27.5	2.60	2.59	0.29	-0.10
Winter Samples					
ws1	0.6	3.21	3.11	0.44	-0.38
ws2	5.1	2.87	2.90	0.40	0.03
ws3	8.6	2.33	2.35	0.30	0.09
ws4	15.0	2.43	2.42	0.30	-0.01
ws5	20.4	2.21	2.22	0.35	0.04
ws6	25.7	2.43	2.39	0.30	-0.17
ws7	28.2	2.50	2.45	0.32	-0.27

Table 6 Textures of the total samples from the Long Beach Peninsula.

Sample Number	Distance (km)	Md (ϕ)	Mn (ϕ)	Sorting Coef.	Skewness Coef.
Summer Samples					
sn1	1.2	2.65	2.62	0.33	-0.10
sn2	5.7	2.28	2.32	0.30	0.18
sn3	7.2	2.15	2.20	0.30	0.24
sn4	9.4	2.25	2.29	0.29	0.22
sn5	17.9	2.18	2.22	0.29	0.22
sn6	22.2	2.18	2.23	0.28	0.29
sn7	27.6	2.55	2.53	0.26	-0.12
sn8	31.6	2.55	2.52	0.29	-0.14
sn9	34.2	2.58	2.56	0.26	-0.13
sn10	38.0	2.67	2.67	0.21	-0.02
sn11	41.3	2.55	2.51	0.26	-0.19
Winter Samples					
wn1	1.2	2.68	2.66	0.41	-0.07
wn2	5.7	2.30	2.33	0.32	0.15
wn3	7.2	2.33	2.35	0.29	0.11
wn4	9.4	2.22	2.26	0.25	0.22
wn5	12.0	2.28	2.31	0.28	0.15
wn6	15.9	2.20	2.24	0.28	0.20
wn7	17.9	2.20	2.24	0.28	0.19
wn8	22.2	2.37	2.37	0.29	0.04
wn9	25.3	2.34	2.35	0.30	0.06
wn10	31.6	2.34	2.35	0.29	0.06
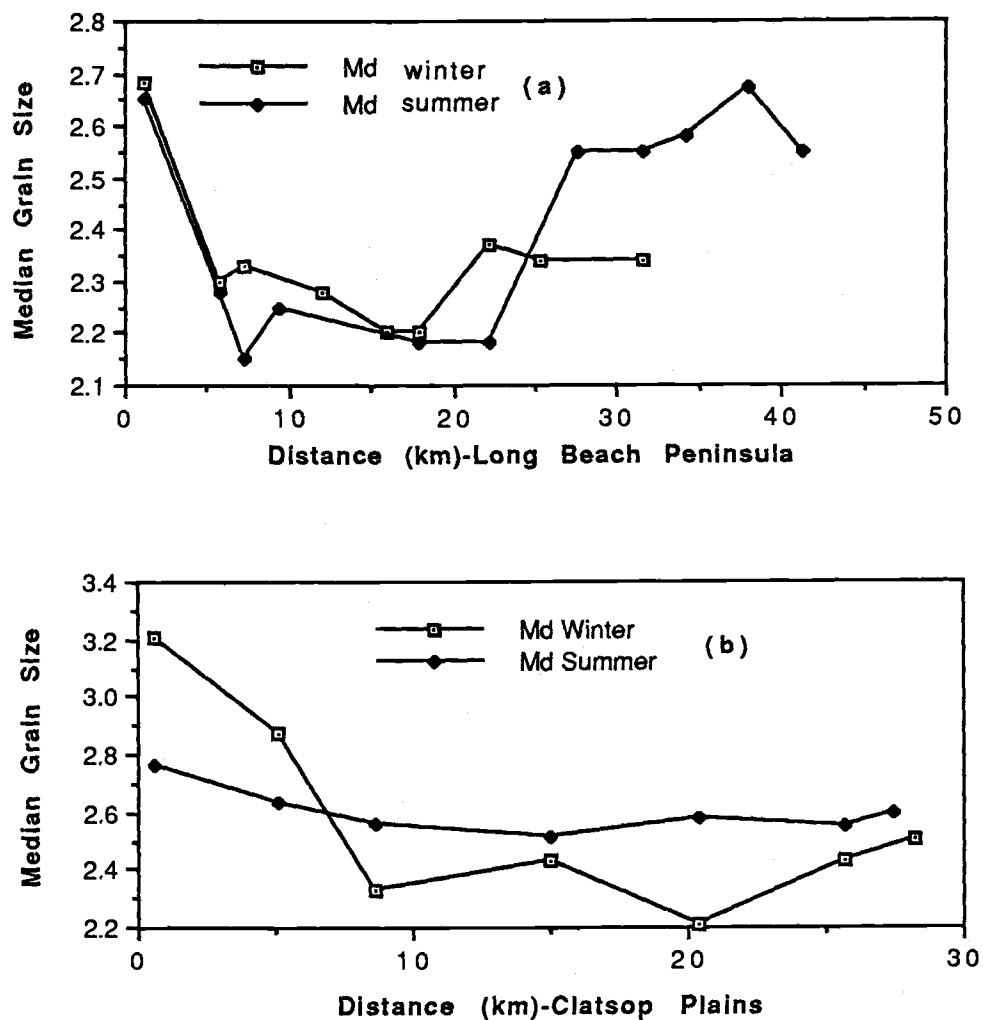
Figure 17
Variation of median grain size (in φ units) with longshore
distance (km) away from the Columbia River mouth on Long Beach
Peninsula (a) and Clatsop Plains (b). Summer and winter
samples show similar trends.
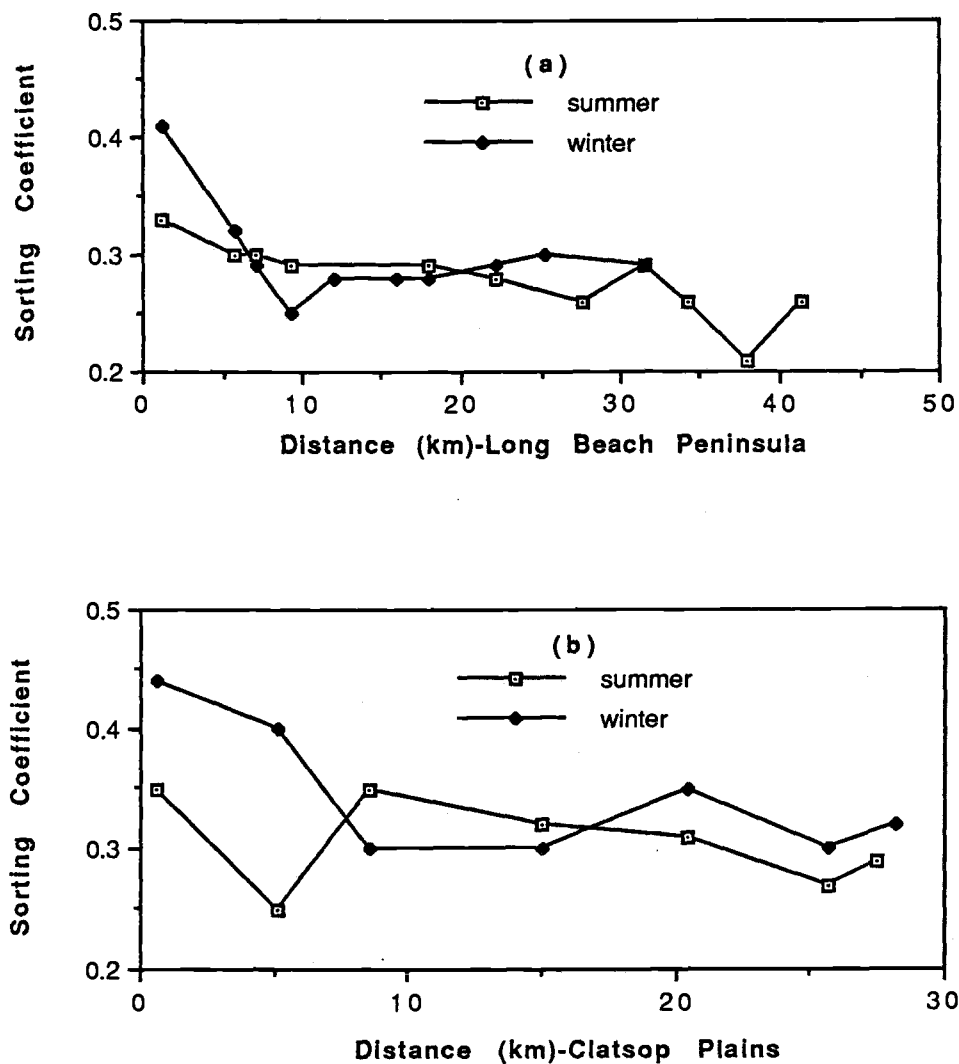
Figure 18
Variation of sorting coefficients with longshore distance
(km) away from the Columbia River mouth on Long Beach Peninsula
(a) and Clatsop Plains (b). Sands are slightly poorer sorted close to
the river mouth and become systematically better sorted at greater
distance.
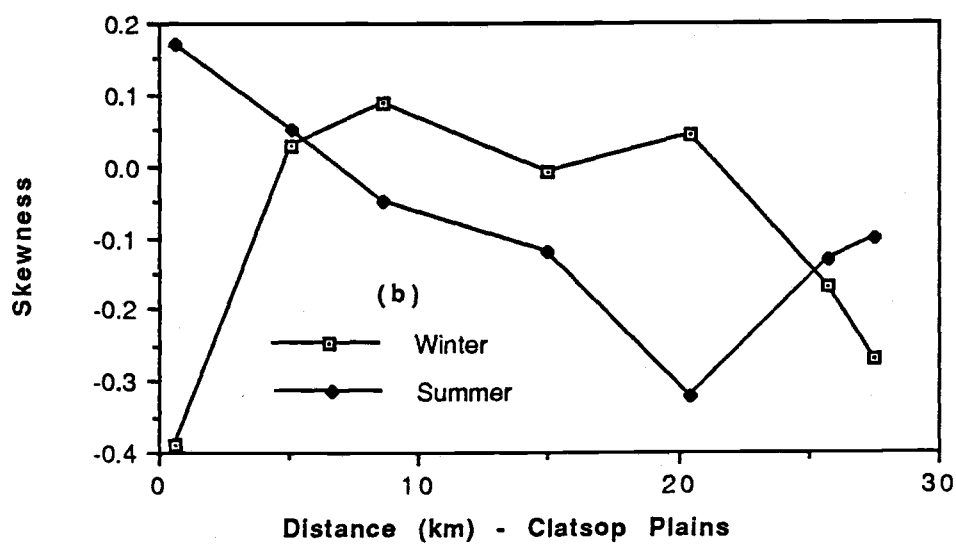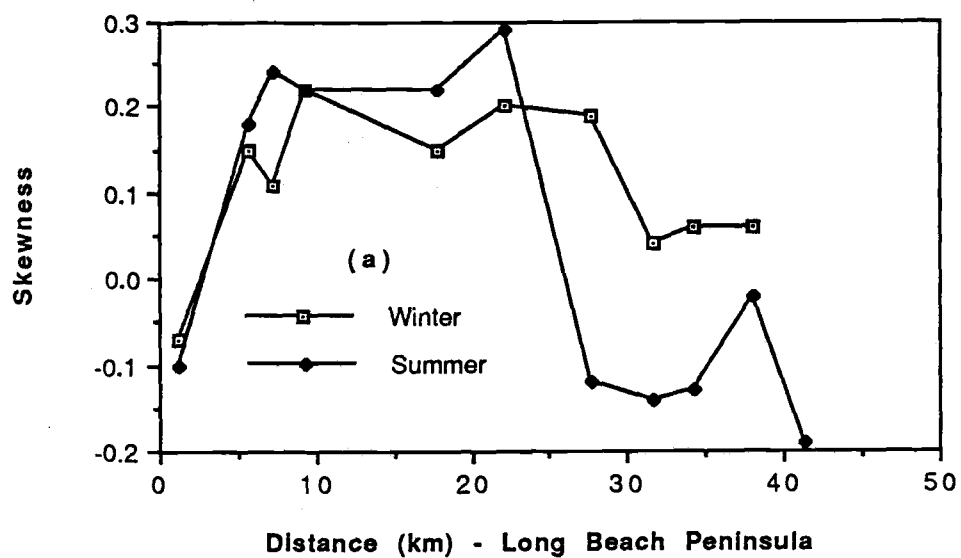
Figure 19
Skewness variation with longshore distance away from the
Columbia River mouth on Long Beach Peninsula (a) and Clatsop
Plains (b).

mm, fine sand). The median grain sizes of the winter samples are generally coarser than those of summer, but this seasonal variation is generally small. Since both winter and summer samples indicate similar trends of longshore grain size variations, and the latter shows a more regular pattern (Figure 17), this study will mainly focus on the summer samples.

It is found that beach sands on the Clatsop Plains have an average Md of 2.59φ (0.17 mm), which is generally finer than the sands on the Long Beach Peninsula (average Md of 2.38φ); a comparable north-south difference was also found by Ballard (1964). Figure 17 shows that beach sands are finer close to the source, the Columbia River mouth, and become coarser both northward and southward. The coarsest median grain sizes occur at about 10 to 15 km away from the river mouth, and then become finer at still greater distances until the end of the Clatsop Plains and the Long Beach Peninsula (Figure 17). A similar grain size variation pattern was found by Ballard (1964), but Plopper (1978) described a slightly different trend.

6.1.3 Sorting Coefficients

The variations of sorting coefficients are plotted against the longshore distance from the Columbia River mouth in Figure 18. The sorting coefficients range from 0.21 to 0.44, with a grand mean of 0.30. Of the total 35 samples, 32 or 91% have sorting coefficients smaller than 0.35. Thus the beach sands of the study area are dominantly very-well sorted. The seasonal variation of sorting is very small, the summer samples on average being slightly better sorted than the winter samples.

It is also found that sands on the Long Beach Peninsula are generally better sorted than along the Clatsop Plains, the average sorting coefficients being 0.29 and 0.33 respectively. Correponding to the finer grain sizes close to the Columbia River mouth, beach sands are slightly poorer-sorted there, with sorting coefficients reaching as high as 0.44. Away from the river mouth, sorting generally improves along the entire length of each beach section.

6.1.4 Skewness Coefficients

The variations of skewness coefficients with longshore distance are graphically presented in Figure 19. The skewness coefficient (Sk) ranges from 0.29 to -0.38. According to the scales of Folk and Ward (1957), 13 of the total 35 samples (37%) are nearly symmetrical, 12 samples (34%) are coarse-skewed with tails of fine grain sizes, 8 samples (23%) are fine-skewed with tails of coarse grain sizes, and 2 samples (5%) are very fine-skewed. Samples from the Long Beach Peninsula and the winter samples of the Clatsop Plains show a similar trend of longshore skewness variations. Beach sands are fine-skewed (negative Sk) close to the jetties and at the end of each stretch. In the central part of the beach, skewness coefficients become positive and sands are nearly symmetrical or coarse-skewed (Figure 19). Summer samples of the Clatsop Plains show an opposite trend where beach sands are coarse-skewed close to the south jetty, the skewness coefficient decreases away from the jetty, and beach sands become nearly symmetrical and fine-skewed at the mid-section of the beach. Towards the south end of the beach, the skewness coefficient is increased, and beach sands become nearly symmetrical again.

84

6.1.5 Median Grain Sizes of Individual Minerals

The major goal of this study is to investigate grain sorting processes that control longshore sediment transport and placer development in the study area. Density and grain size are the most important factors affecting the sorting mechanisms. Sieving analyses of the total samples provide only the general textural characteristics of the mixed heavy and light minerals, while textural characteristics of individual minerals are more important for understanding the actual sorting mechanisms. As outlined in Chapter 5, one of the subsamples was used to separate the heavy and light minerals, which were then sieved separately. A small amount of sand split from each sieving fraction of the heavy minerals was mounted on a microscope slide and the principal heavy minerals hornblende, augite, hypersthene and opaques (magnetite plus ilmenite) were identified and counted. These data together with the sieving data of the light minerals (quartz and feldspars) were then plotted as cumulative frequency curves and the median grain sizes determined for these major minerals. Since a sieving analysis mainly measures a particle's intermediate diameter D_b, and due to the preference of this D_b value in sediment dynamic studies (Komar and Cui, 1984; Komar and Wang, 1984), these sieving median grain sizes have been converted into particles' intermediate diameters, utilizing the relationships of equation (1) obtained in the previous chapter. These converted median grain sizes are listed in Table 7, and are plotted versus the longshore distance from the Columbia River mouth in Figure 20.

A similar pattern is found for the longshore grain-size variations of these individual minerals compared with that of the total samples. Median

Table 7   Median intermediate diameters (in φ) of the individual
            minerals for the summer samples.

Sample Number	Distance (km)	Qtz	Horn	Aug	Hyp	Opq
Clatsop Plains						
ss1	0.6	2.13	2.26	2.40	2.48	2.62
ss2	5.1	2.16	2.19	2.28	2.27	2.29
ss3	8.6	2.06	2.26	2.41	2.44	2.46
ss4	15	2.05	2.39	2.49	2.50	2.52
ss5	20.4	2.08	2.43	2.51	2.62	2.45
ss6	25.7	2.09	2.43	2.40	2.64	2.54
ss7	27.5	2.15	2.42	2.42	2.62	2.55
Long Beach Peninsula						
sn1	1.2	1.94	2.07	2.17	2.14	2.31
sn2	5.7	1.80	1.97	2.09	2.05	2.10
sn3	7.2	1.69	1.93	2.02	2.00	2.06
sn4	9.4	1.81	1.99	2.10	2.12	2.15
sn5	17.9	1.74	2.06	2.22	2.22	2.11
sn6	22.2	1.77	2.04	2.30	2.22	1.99
sn7	27.6	1.78	2.31	2.47	2.43	2.36
sn8	31.6	2.10	2.29	2.44	2.43	2.37
sn9	34.2	2.14	2.40	2.47	2.56	2.52
sn10	38.0	2.23	2.49	2.52	2.61	2.59
sn11	41.3	2.11	2.29	2.37	2.36	2.45

Qtz: quartz, Horn: hornblende, Aug: augite, Hyp: hypersthene,
Opq: opques.
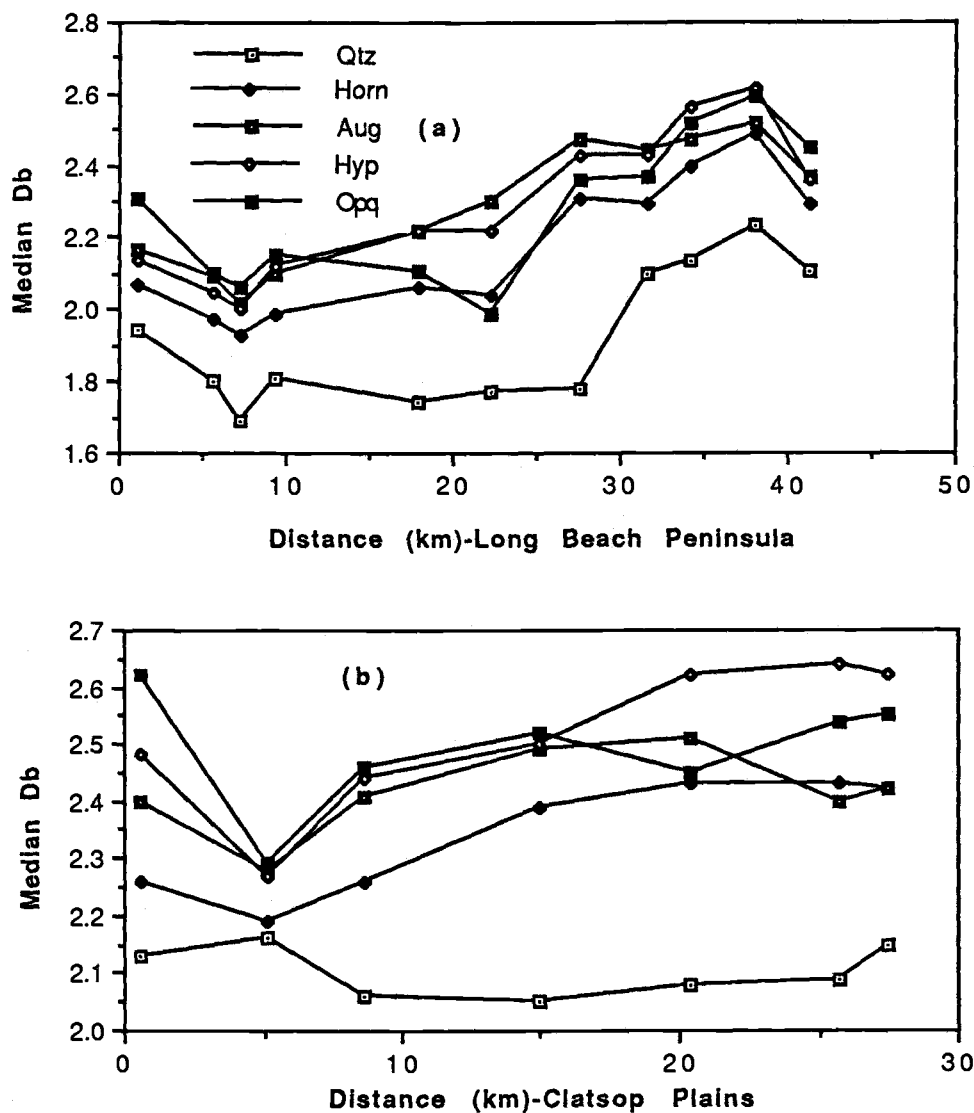
Figure 20

Longshore variation of median intermediate diameter D_b (ϕ) for the major minerals on Long Beach Peninsula (a) and Clatsop Plains (b). The diagrams show an away-from-source coarsening of medians close to the river mouth and a general fining at still greater distances. The following abbreviations have been used: Qtz-quartz (including feldspars), Horn-hornblende, Aug-augite, Hyp-hypersthene, and Opq-opaques.

grain sizes of all minerals are finer close to the sediment source (Columbia River mouth), but become coarser away from the source for the first 2 or 3 samples (Figure 20). The median grain size then decreases for the remaining distance to the end of the Clatsop Plains and Long Beach Peninsula, except for a small coarsening at the tip of each beach stretch. Figure 20 also shows that for the first 3 to 4 samples away from the sediment source, where heavy minerals are highly concentrated, median grain sizes of individual minerals are inversely correlated with their densities. For each sample, minerals of high densities are generally finer than the minerals of smaller densities. Therefore, median grain sizes for quartz, hornblende, augite, hypersthene and opaques, in a given sample, become successively smaller as their densities increase in that order. The higher density and smaller grain size are the basic factors controlling selective grain sorting and heavy mineral concentration in the study area. These observed patterns will, therefore, be discussed in detail in the following chapter where the origin of the placers is examined.

6.2 Results of Mineralogy Analyses

6.2.1 Total Heavy Mineral Concentrations

A subsample was split from each sample and heavy minerals with densities in excess of 3.00 g/cm^3 were separated from the light minerals (Appendix I). The total heavy mineral weight percentage (H%) was then obtained when the weight of the heavy fraction was divided by the weight of the entire subsample. The total heavy mineral concentrations for the summer samples are listed in Table 8, and are graphically presented in Figure 21 where the total heavy mineral concentration is plotted as a

Table 8   Weight percents (wt%) of individual minerals for the summer samples.

Sample No.	Dist. (km)	L	H	Horn	Aug	Hyp	Opq	Others
Clatsop Plains								
ss1	0.6	39.91	60.09	9.26	10.26	10.59	15.90	14.09
ss2	5.1	78.06	21.94	4.74	4.32	4.18	3.46	5.23
ss3	8.6	86.69	13.31	2.41	2.42	2.09	2.68	3.71
ss4	15.0	97.96	2.04	0.45	0.38	0.37	0.36	0.48
ss5	20.4	98.56	1.44	0.25	0.23	0.18	0.30	0.48
ss6	25.7	98.51	1.49	0.26	0.40	0.14	0.20	0.49
ss7	27.5	97.94	2.06	0.30	0.50	0.25	0.46	0.55
Long Beach Peninsula								
sn1	1.2	33.55	66.45	5.56	9.93	13.65	22.17	15.14
sn2	5.7	82.41	17.59	2.46	2.20	3.36	5.09	4.47
sn3	7.2	83.89	16.11	2.12	2.85	3.07	4.15	3.92
sn4	9.4	89.23	10.77	2.03	1.56	1.94	2.25	2.98
sn5	17.9	96.37	3.63	0.76	0.58	0.58	0.74	0.97
sn6	22.2	98.79	1.21	0.38	0.14	0.14	0.19	0.35
sn7	27.6	98.71	1.29	0.37	0.19	0.19	0.19	0.35
sn8	31.6	98.79	1.21	0.30	0.21	0.20	0.19	0.31
sn9	34.2	98.73	1.27	0.33	0.24	0.22	0.16	0.33
sn10	38.0	97.70	2.30	0.49	0.54	0.43	0.24	0.60
sn11	41.3	97.54	2.46	0.45	0.51	0.56	0.31	0.64

L: light minerals, H: heavy minerals, Horn: hornblende, Aug: augite, Hyp: hypersthene, Opq: opaques.

Figure 21
Total heavy mineral concentration plotted as a function of the
longshore distance away from the Columbia River mouth for the
Long Beach Peninsula (top) and the Clatsop Plains (bottom). Heavy
minerals are found to be highly concentrated close to the river
mouth.

function of longshore distance from the Columbia River mouth for the Long Beach Peninsula and the Clatsop Plains. Repeated analyses give an average error of ±0.2%.

Figure 21 shows that the heavy minerals are highly concentrated close to the Columbia River mouth, both on the Long Beach Peninsula and along the Clatsop Plains, reaching 66% and 60% respectively. The concentration decreases dramatically away from the river source, and becomes less than 10% at about 10 km from the river mouth. This decrease in total heavy mineral concentration with longshore distance appears to be exponential. The range of the total heavy mineral concentrations also indicates that the normal percentage units have been severely compressed at the lower end of the vertical linear scale. Therefore, the total heavy mineral percentages has been replotted on a logarithmic scale in Figure 22. This shows a linear decrease of log H% for the first 20 km longshore distance from the river. Towards the end of the beach, the total heavy mineral concentration increases slightly, but the values remain low. The decreasing trends within 20 km of the source can be expressed as logH% = 1.79 - 0.075x for the Long Beach Peninsula samples, Figure 22, and logH% = 1.88 - 0.1x for the Clatsop Plains, where x is the longshore distance in km.

6.2.2 Abundances of Individual Minerals

The number percentage of each mineral from point-counting can be converted to weight percentage according to Rubey (1933) and Young (1966). The number percentage of a chosen mineral in a given sieve fraction is first multiplied by its specific gravity to obtain its calculated
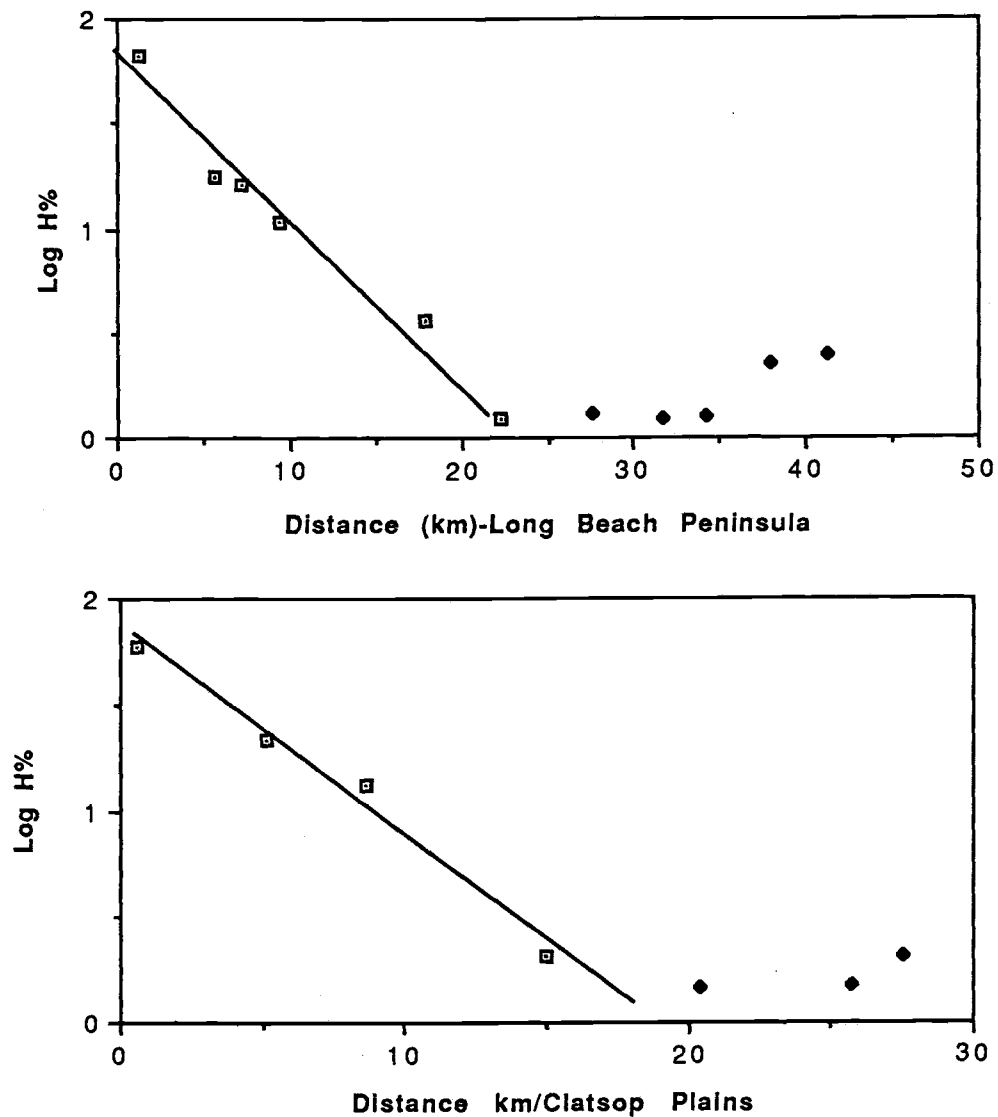
Figure 22
Log total heavy mineral weight percentages plotted as a
function of the longshore distance away from the Columbia River
mouth, showing a systematic decrease with longshore distance and
a slight increase at the ends of both beaches.

weight in the sieve fraction. The weight percentage of this mineral in the sieve fraction is then obtained by totaling the calculated weights for all the heavy minerals in the fraction and dividing the calculated weight of the individual mineral by this total weight. This weight percentage is then multiplied by the weight of the sieve fraction to obtain the actual weight of this mineral in the fraction. The weights of the mineral in the series of sieve fractions are added to obtain the total weight of the mineral in the sample. Finally, the weight percentage of the mineral in this sample can be obtained when its total weight is divided by the total weight of the sample. The weight percentage of each major heavy mineral derived in this way is multiplied by the total heavy mineral percentage H% in each sample to give the wt% of that mineral in the total sample. The weight percentages (wt%) of major individual minerals for the total summer samples are listed in Table 8, while the weight percents of major heavy minerals within the heavy fraction alone are given in Table 9.

The weight percentage of each mineral in the total sample is plotted as a function of the longshore distance from the Columbia River mouth in Figure 23a for the Long Beach Peninsula and Figure 23b for the Clatsop Plains. These plots show that the heavy minerals are mainly concentrated close to the river mouth, and become progressively diluted with distance from this source. In contrast, the abundance of quartz and feldspars systematically increases with longshore distance from the river. It is also found that within the placer deposits (averaging first samples on both sides of the river mouth), the opaques are the most abundant heavy mineral with an average of 19.0%. The average weight percentages of other heavy minerals are 12.1% for hypersthene, 10.1% for augite, and 7.4% for

Table 9   Weight percents (wt%) of individual heavy minerals within the heavy fraction for the summer samples.

Sample No.	Distance (km)	Horn	Aug	Hyp	Opq	Others
Clatsop Plains						
ss1	0.6	15.41	17.07	17.62	26.46	23.44
ss2	5.1	21.60	19.70	19.06	15.79	23.86
ss3	8.6	18.12	18.17	15.69	20.11	27.91
ss4	15.0	22.09	18.48	18.04	17.66	23.73
ss5	20.4	17.65	15.63	12.38	20.82	33.52
ss6	25.7	17.19	27.02	9.52	13.12	33.15
ss7	27.5	14.68	24.26	11.85	22.37	26.83
Long Beach Peninsula						
sn1	1.2	8.37	14.94	20.54	33.36	22.78
sn2	5.7	14.01	12.52	19.09	28.92	25.44
sn3	7.2	13.16	17.69	19.07	25.73	24.35
sn4	9.4	18.88	14.49	18.02	20.93	27.67
sn5	17.9	20.97	15.93	16.10	20.40	26.61
sn6	22.2	31.77	11.85	11.72	15.87	28.79
sn7	27.6	28.89	14.39	14.91	15.02	26.79
sn8	31.6	24.76	17.64	16.56	15.29	25.76
sn9	34.2	25.63	18.72	16.95	12.41	26.28
sn10	38.0	21.43	23.25	18.73	10.32	26.26
sn11	41.3	18.15	20.68	22.59	12.59	25.99

Horn: hornblende, Aug: augite, Hyp: hypersthene, Opq: opaques.

Figure 23

Weight percentages of major individual minerals in the total

sample plotted against the longshore distance from the Columbia

River mouth for the Long Beach Peninsula (a) and the Clatsop Plains

(b). The results show higher concentrations of the heavy minerals

and depletion of quartz close to the river mouth.
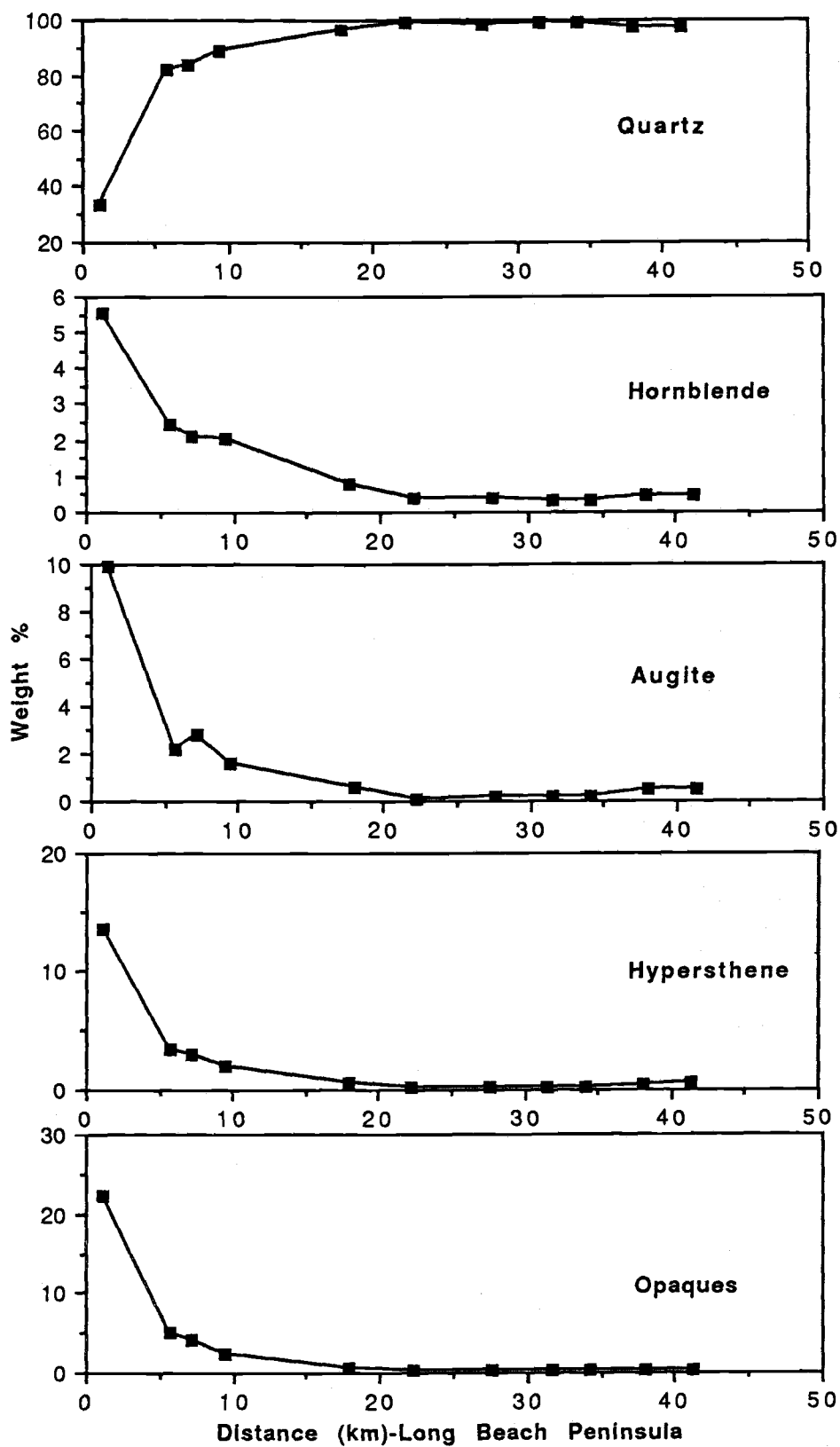
Figure 23a
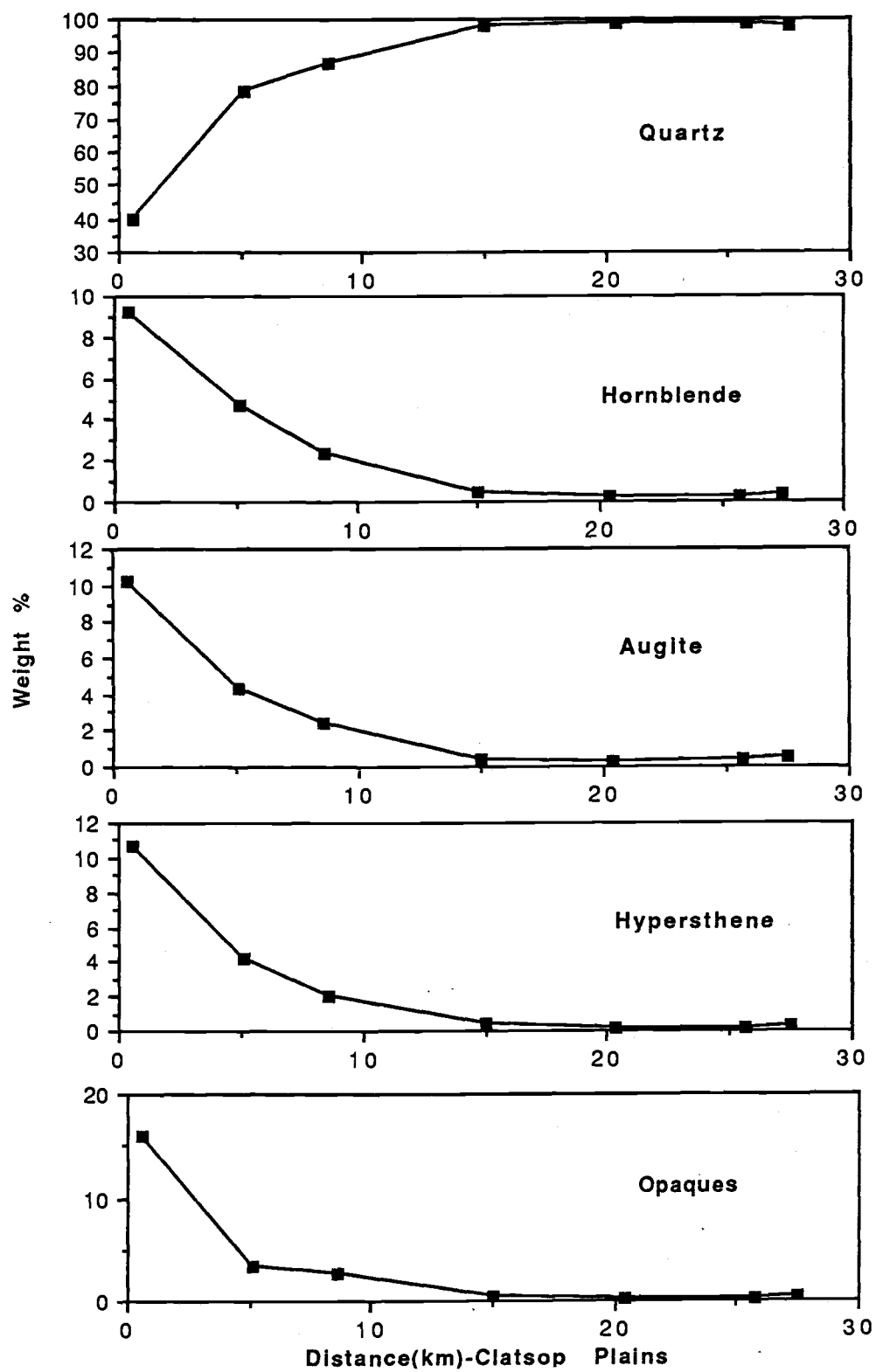
Figure 23b

hornblende.

The longshore variations of the heavy minrals are presented in Figure 24 as the abundance of each major heavy mineral within the heavy fraction of the samples. It is found that the longshore variation of individual mineral abundance is related to the density and grain size of the mineral. The opaques have the highest density (4.8 g/cm^3) and generally smaller grain sizes (Figures 20), and are most highly concentrated close to the Columbia River mouth, while the abundance decreases dramatically alongshore. This trend is stronger on the Long Beach Peninsula, while the data for the Clatsop Plains are scattered with a less apparent overall trend. Hypersthene has a density of 3.5 g/cm^3 and relatively finer grain size among the four major heavy minerals. It is more abundant both close to the Columbia River mouth and at the northern end of the Long Beach Peninsula, while the minimum concentration occurs at the middle part of the peninsula to yield a V-shaped distribution pattern (Figure 24a). In contrast, hornblende possesses a lower density (3.2 g/cm^3) and a relatively coarser grain size, and it is less concentrated close to the river mouth and at the end of the Long Beach Peninsula and the Clatsop Plains. Its maximum concentration occurs at about the mid-point of each beach, yielding an inverted-V distribution pattern. Augite has an intermediate density (3.4 g/cm^3) and grain sizes, and its concentration does not show any significant trend for the first 20 km away from the Columbia River mouth. Further north and south, the abundance of augite does increase for the remaining stretch of each beach section. One exception to the above description is the distribution of hypersthene on the Clatsop Plains. Instead of showing a V-shaped longshore pattern, its concentration is high

Figure 24

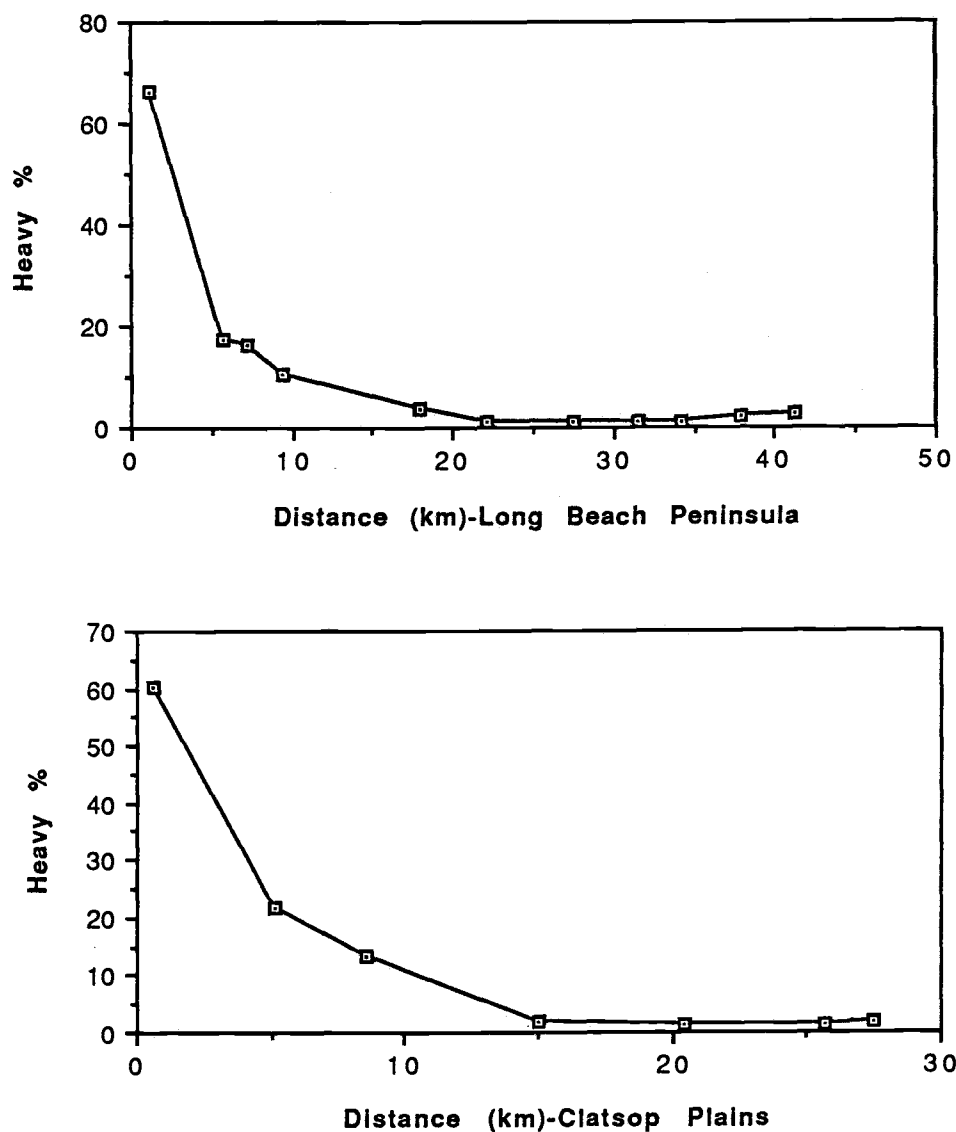The abundance of each major heavy mineral within the heavy fraction alone plotted as a function of the longshore distance from the Columbia River mouth for the Long Beach Peninsula (a) and the Clatsop Plains (b).
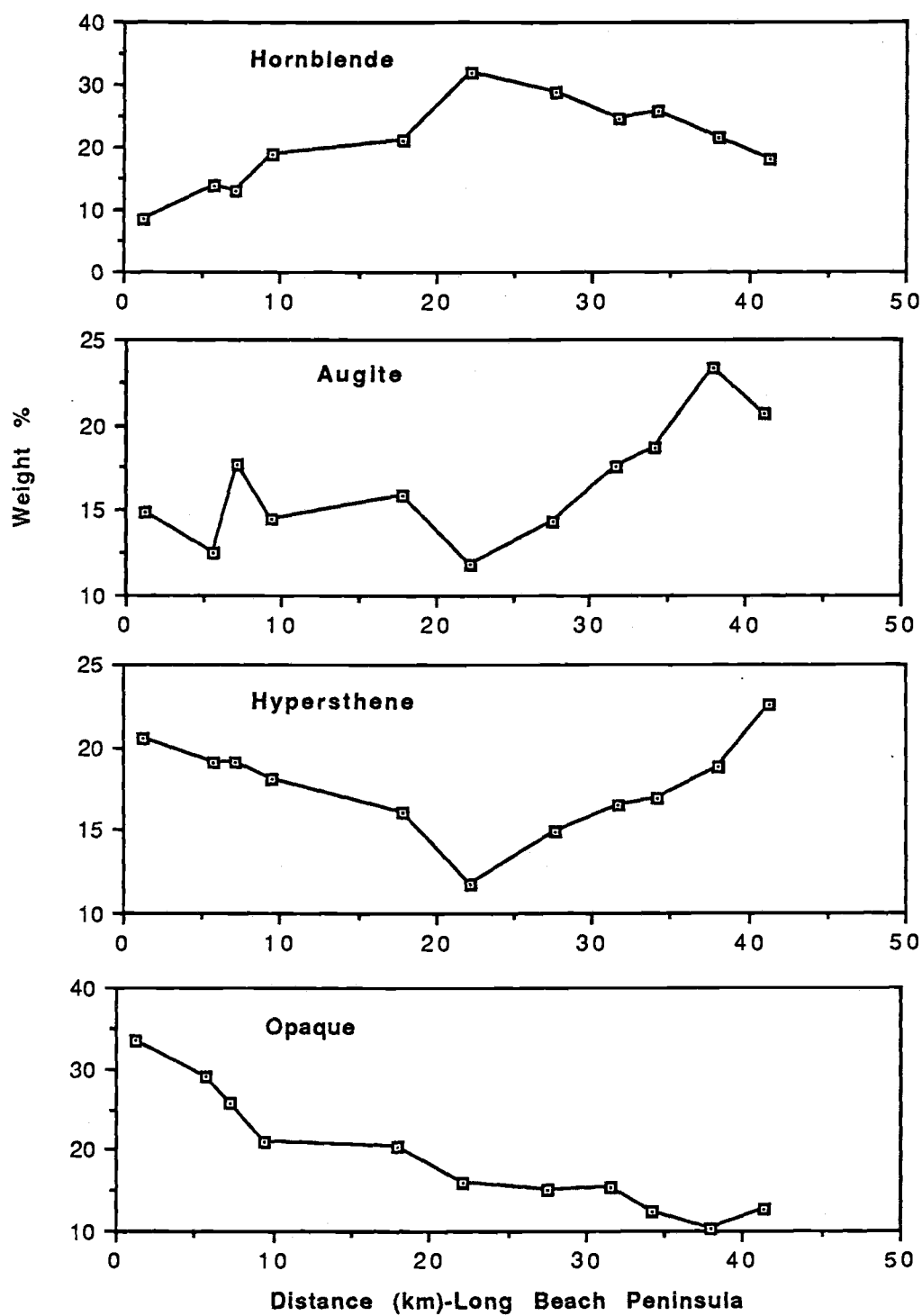
Figure 24a
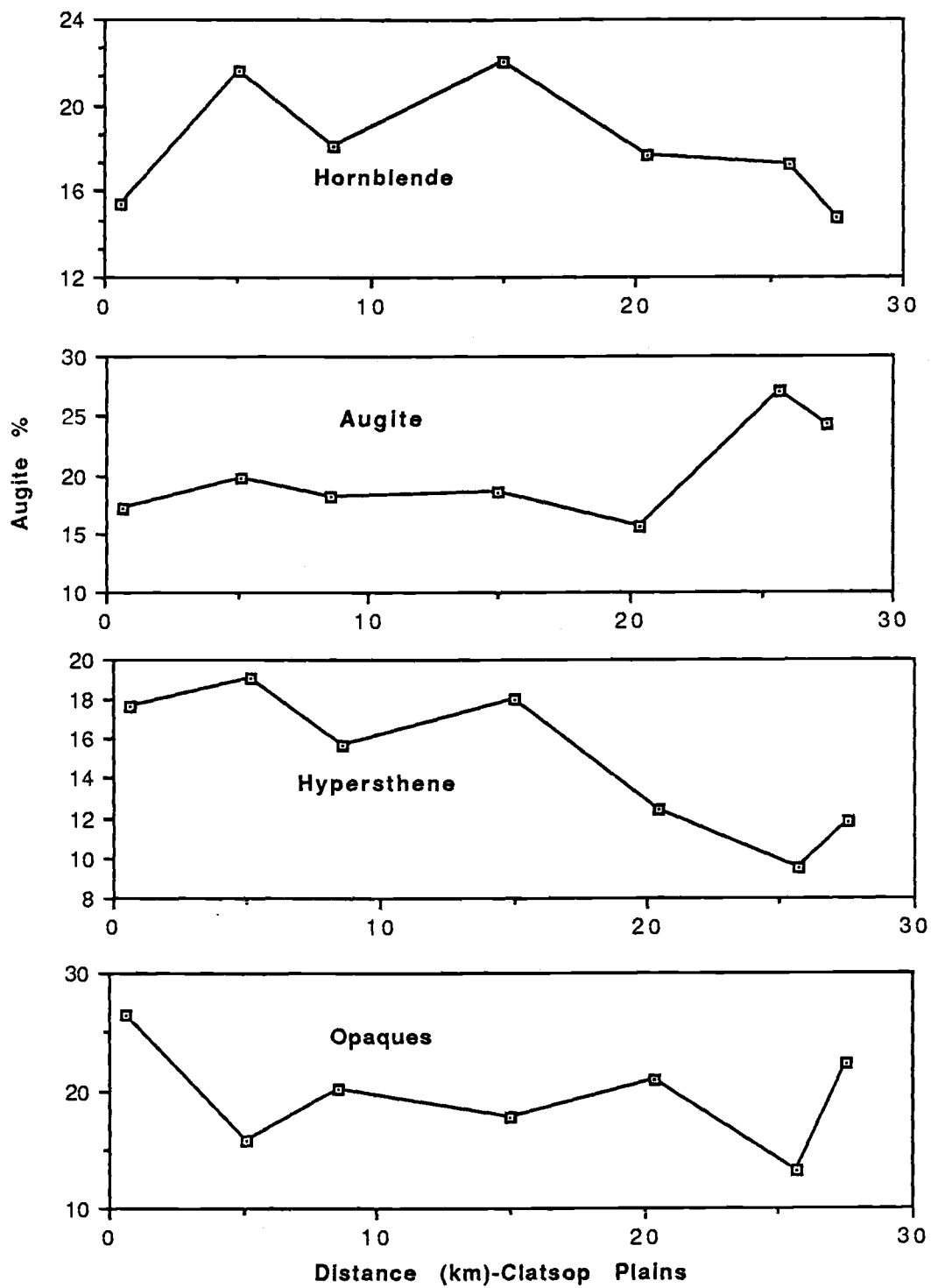
Figure 24b

close to the Columbia River mouth and generally decreases all the way to the end of the Clatsop Plains (Figure 24b).

6.3 Comparison With the Columbia River Sediments

The sediment source and longshore sediment transport pattern can also be evaluated by comparing the mineralogy of the beach samples with the mineralogy of the Columbia River sediments. According to Plopper (1978), the mineralogical dissimilarity between a beach sample and the Columbia River sediment can be defined as:

$$Ds = (\Sigma(X_{ib}-X_{ir})^2)/100n \qquad (8)$$

where Ds is the dissimilarity coefficient of a given beach sample, i refers to the heavy mineral species, X_{ib} and X_{ir} are weight percents of the mineral i for the beach and river samples respectively, and n is the number of mineral species used in the comparison. As sediments are transported away from the source, mineral sorting and new sediment inputs will gradually alter their mineralogy. Therefore, this dissimilarity coefficient should increase systematically with the transport distance away from the source.

Three major heavy minerals (hornblende, augite and hypersthene) are used in this calculation so that n = 3 in equation (8). The X_{ib} weight percentages of hornblende, augite and hypersthene of beach samples are recalculated from the values in Table 9 by excluding the opaque minerals. The average weight percentages of these three minerals given in Table 3 of Chapter 2 are used as the X_{ir} values in the river sands. The dissimilarity coefficients calculated in this way are plotted in Figure 25
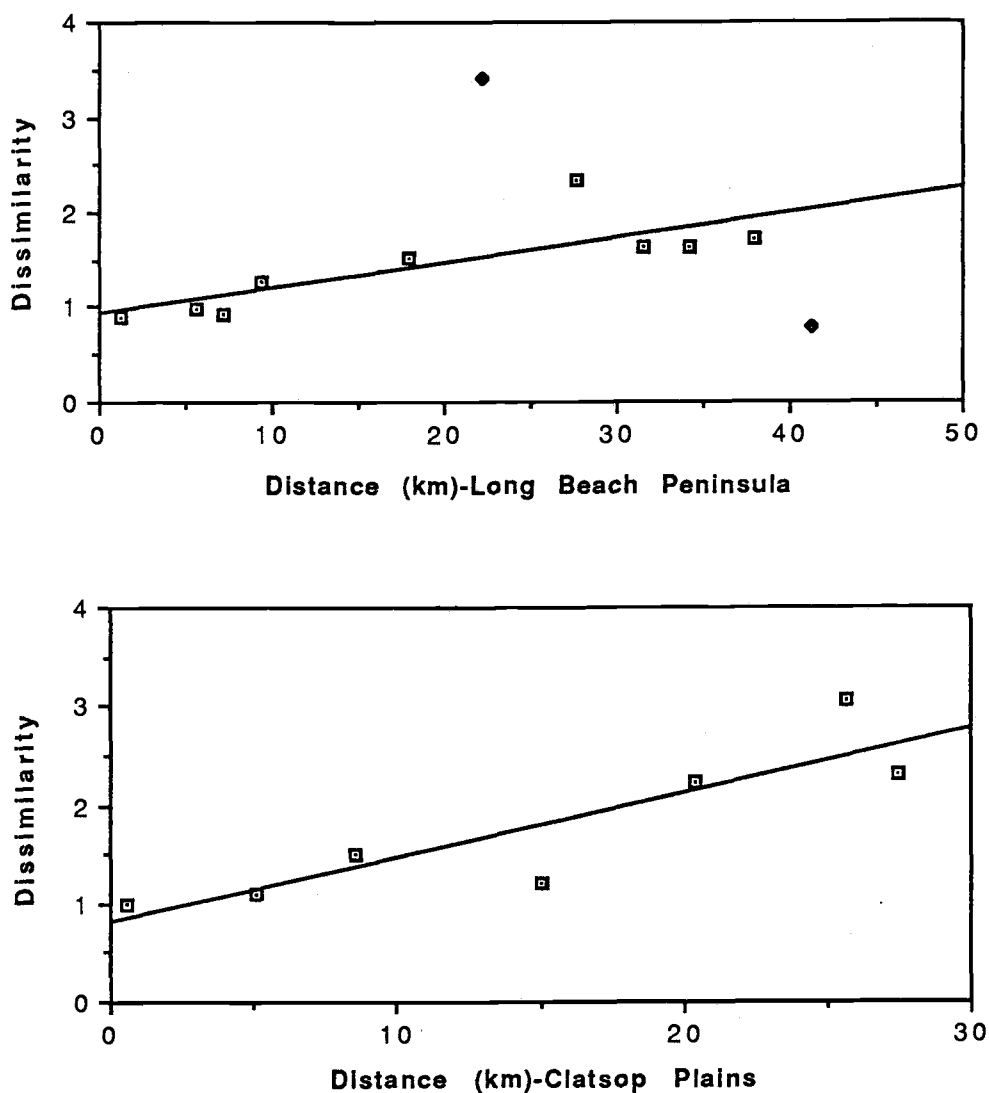
Figure 25
Variation of the mineral dissimilarity coefficient with
longshore distance for the Long Beach Peninsula (top) and the
Clatsop Plains (bottom), showing that mineral compositions of
beach sands progressively diverge from that of the Columbia River
sediment.

reconfirm that the Columbia River is the major sediment source to the study area, and that these sediments are then transported northward along the Long Beach Peninsula and southward along the Clatsop Plains. Peterson and Binney (1988) have estimated that the placer volume on the Clatsop Plains is only about half that on the Long Beach Pennisula, suggesting that the river-derived sediments are dominantly transported to the north, with only one third transported to the south. This general pattern is also supported by the systematic increase of mineralogical dissimilarity with longshore distance between the beach sands and the Columbia River sediments (Figure 25).

The sediment transport is also partially affected by blockage by the south jetty. Due to its considerable seaward extention, the south jetty has reached such a depth that waves and currents are less effective in moving the coarser sediments and mainly transport finer-grained sediments around the jetty and southward to the Clatsop Plains. This may explain why the average median grain size on the Clatsop Plains is finer than that of the Long Beach Peninsula (Figure 17). Jetties also provide some sheltering to the areas immediately adjacent to them, reducing the wave conditions. The reduced flow stresses and the mixture of light and heavy minerals on the beaches close to the Columbia River mouth are responsible for the generally poorer sorting of beach sands in these areas (Figure 18).

Finer particles of a given mineral usually have lower settling velocities and require smaller flow stresses for entrainment, and it is believed that longshore currents will transport them farther away from the source, while coarser grains will be left behind to produce a trend of

decreasing grain size with transport distance (normal sorting and transport processes). It is found that the median grain sizes of both the total samples (Figure 17) and the individual minerals (Figure 20) are finer close to the Columbia River mouth and become coarser with longshore distance until about the 10 km mark. This away-from-the source increase of sediment grain size must be explained by selective grain sorting and sediment transport processes. The median grain sizes of individual minerals in Figure 20 show that minerals with higher densities are generally finer than the minerals with lower densities in each sample within about 10 km to both directions from the Columbia River mouth. This probably implies that minerals in the river discharge are settling-equivalent due to the offset of the reverse correlation between grain size and density (an assumption demonstrated to be correct in Chapter 7). Under settling-equivalence, heavy minerals are finer than the light minerals due to the higher densities of the heavy minerals. This means that they require higher flow stresses for entrainment (Miller and Byrne, 1966; Fenton and Abbott, 1977; Li and Komar, 1986; Komar and Li, 1986). Under certain conditions, coarser-grained light minerals are selectively transported away from the source area and the finer-grained heavy minerals are left behind to form the placer deposits. At still greater distance, Figures 17 and 20 both show systematic decreases in median grain sizes. This indicates that normal grain sorting and sediment transport processes become more important on the remaining part of the beach and finer mineral grains have outdistanced the coarser grains during the longshore transport process. Figure 21 shows that heavy minerals are mainly concentrated within 10 km of the Columbia River mouth, and this

coincides with the extent of the increasing grain size away from the source, indicating that the selective grain sorting and sediment transport processes are responsible for the placer formation in the immediate vicinity of the Columbia River mouth.

This longshore transformation from selective to normal grain sorting and sediment transport processes is probably caused by flow stress variations and mineral compositional changes. It has been shown that low to medium flow stresses will enhance the efficiency of selective grain sorting and sediment transport processes (Slingerland, 1977; Komar and Wang, 1984). The higher heavy mineral contents, and lower flow stresses due to jetty sheltering and wave shoaling on the delta may favor the selective sorting mode close to the Columbia River mouth . The depletion of heavy minerals and high flow stresses on the open beaches may cause the dominance of the normal sorting mode on the remaining part of the beach.

Figure 22 shows that the total heavy mineral concentration is highest close to the Columbia River mouth and also slightly increases at the ends of the Long Beach Peninsula and the Clatsop Plains. This longshore variation is mainly determined by the beach-erosion pattern which is then controlled by a bi-directional selective grain sorting and longshore sediment transport model caused by the seasonal shifts of longshore current directions. A similar model has been used by Peterson et al. (1986) to explain the consistent maximum placer developments south of headlands on the central Oregon beaches. Observations of wave direction (Chapter 1) and longshore wave energy flux analyses (Ballard, 1964) have shown that major storm waves generally approach the coast

from the southwest sector and produce high-velocity northward longshore currents in the winter. For the Long Beach Peninsula, this northward longshore current transports sediments both offshore and northward away from the beach close to the jetty to cause seasonal erosion in this area. During this erosion process, coarse-grained light minerals are selectively removed and transported offshore and northward away from the Columbia River mouth, while finer-grained heavy minerals are left behind to cause the high concentration of heavy minerals close to the river mouth. During major storms, a small amount of heavy minerals could be transported to the north end of the Long Beach Peninsula. Here the longshore currents are deflected by the Willapa Bay tidal currents and these heavy minerals are deposited (Tillamook Head deflects the southward summer longshore currents and thus will play the same role on the Clatsop Plains). Erosion at the Leadbetter Point due to the migration of the tidal channel probably has caused the initial concentration of heavy minerals at the north end of the Long Beach Peninsula. In the summer, distant storms produce smaller waves that mainly come from the northwest and generate low-velocity longshore currents to the south. This southward longshore current now will selectively remove and transport the coarse-grained light minerals back towards the south. This will further increase the concentration of the heavy minerals at the north end of the Long Beach Peninsula. Since the Columbia River is the sediment source to the study area and very small amount of heavy minerals has reached the north end of the Long Beach Peninsula, this increase of heavy mineral concentration is much smaller than the high concentration found close to the river mouth. The reverse procedures should occur on the Clatsop Plains.

The unique longshore variations of individual mineral concentrations shown in Figure 24 can also be explained by this bi-directional sorting and transport model. Since the Clatsop Plains and the Long Beach Peninsula show similar patterns, only the Long Beach Peninsula is used in the following discussion. Due to its highest density and finest grain size among the major heavy minerals, the opaques (magnetite and ilmenite) will probably require very high flow stresses for their entrainment and transport. Winter longshore currents are not strong enough to effectively transport these opaque minerals northward and most of them are left close to the Columbia River mouth. Thus they are highly concentrated close to the river mouth and the abundance decreases systematically northward to the end of the Long Beach Peninsula. In comparing hypersthene and hornblende, the former has relatively higher density and finer grain size than the latter, and thus probably requires higher threshold flow stresses for entrainment and transport. Therefore, the winter longshore currents will selectively remove and transport the coarser-grained hornblende northward away from the source area to deplete its concentration close to the river, while the finer-grained hypersthene is left behind to cause its high concentration close to the Columbia River mouth. In the summer, southward longshore currents will selectively remove and transport the coarse-grained hornblende back towards the south and the finer-grained hypersthene is again left behind to form another high concentration at the northern end of the Long Beach Peninsula. The combination of these opposite winter and summer processes has resulted in the v-shaped longshore distribution pattern of hypersthene and the inverted v-shaped pattern of hornblende shown in

Figure 24.

Augite has a density and grain size between hypersthene and hornblende. Close to the Columbia River mouth, denser and finer-grained opaque minerals are abundant and selective sorting of the northward winter longshore currents are ineffective on augite. Thus its concentration does not show any significant change for the first 20 km away from the river mouth. At the northern end of the peninsula, however, the concentration of the opaques is dramatically reduced and selective sorting processes become effective on augite. Thus, summer longshore currents tend to selectively remove the coarser-grained quartz and hornblende southward, while augite is left behind to be relatively concentrated at the northern end of the Long Beach Peninsula (Figure 24).

Chapter 7
PROCESSES OF SELECTIVE GRAIN SORTING

7.1 Physical Processes of Mineral Sorting

The processes of selective grain sorting depend mainly on the densities, sizes and shapes of the minerals involved. These processes occur whether or not valuable minerals are present. Many previous studies have focused on the sorting processes under unidirectional currents as found in rivers, but close parallels exist between marine and fluvial environments (Komar, 1989). The grain sorting processes described below thus apply to both waves and unidirectional flows. These processes (as diagramed in Figure 2) include settling sorting, selective entrainment sorting, differential transport sorting, and dispersive-pressure sorting. It is believed that more than one process is generally involved in the development of a placer.

7.1.1 Settling Equivalence and Grain Sorting

It has long been known that within a multiple-mineral deposit representing a narrow range of hydrodynamic conditions, the denser minerals are generally finer-grained than the lighter minerals (Mackie, 1923). However, Rubey (1933) is credited with originating the concept of settling equivalence. When analyzing the mineralogy of two Pleistocene terrace deposits, Rubey stated that conditions which have permitted the deposition of quartz grains of a certain size would also permit the deposition of smaller grains of denser minerals having the same settling velocity.

For two minerals of different densities, assuming for the moment

that their settling is in the Stokes range so that equation (3) applies, the equivalence of their settling velocities requires:

$$(D_h/D_l) = [(\rho_l - \rho)/(\rho_h - \rho)]^{1/2} \qquad (9)$$

where subscripts l and h refer respectively to the light and heavy minerals. For ilmenite versus quartz, their densities are ρ_h = 4.8 and ρ_l= 2.65, and their equivalent diameter ratio according to equation (9) is D_h/D_l = 0.66. Thus, in the Stokes range ilmenite grains must be 0.66 times smaller than the quartz grains if they are to have the same settling velocity. For coarser particles, the necessity of evaluating the drag coefficient C_d in equation (1) complicates the comparison, but the principle is the same as derived here for the Stokes range.

Although the concept of settling equivalence is theoretically sound, most investigations have found that the heavy and light minerals in natural deposits seldom have equal settling velocities (Rittenhouse, 1943; McIntyre, 1959; Hand, 1967; Lowright, et al., 1972; Slingerland, 1977). This deviation has been explained as resulting in part from size restrictions of the minerals as derived from the source rocks (Briggs, 1965). However, it is more likely caused by other selective sorting processes that change the equivalence after deposition (Hand, 1967; Lowright, et al., 1972; Slingerland, 1977; Komar, 1989).

If heavy and light minerals are settling-equivalent in the original sediment derived from the source, then free settling itself will not sort the grains. However, grain settling can still be important because it governs the overall grain-size distribution in the deposit which will be subsequently sorted by other processes to lead to the heavy mineral concentration and placer formation. If the original sediment supply

contains minerals of unequal settling velocities, grains with different sizes , densities and shapes will fall through the water column with contrasting velocities, so that grain sorting occurs. When sediment is transported away from the source under this situation, the mean settling velocity of each mineral should decrease as the distance increases away from the source.

7.1.2 Sorting by Selective Entrainment

As the velocity and bottom stress of a current progressively increase over a bed of sediments, a condition will eventually be reached where individual grains are dislodged and transported from their resting positions. This first sediment movement is commonly referred to as the threshold of sediment movement or grain entrainment. Natural sediments often contain grains of different sizes, densities and shapes and thus require different flow stresses for their entrainment. This selective entrainment will cause sorting and separation of minerals according to their sizes and densities.

Grain entrainment has been studied extensively over the past half century, but nearly all of these previous investigations are based on flume experiments using uniform grains in a flat bed. These measurements have been compiled by Miller et al., (1977) and Yalin and Karahan (1979) to provide up-dated versions of the threshold curves. However, those standard threshold curves are not strictly applicable to the selective sorting processes leading to the development of placers since they are based on experiments using grains of uniform sizes and densities. As diagrammed schematically in Figure 26, the formation of a placer involves the entrainmnent of a finer-grained heavy mineral particle (dotted grain)

Figure 26

Effects of relative exposure and pivoting angle Φ on the selective
entrainment of a finer-grained heavy mineral particle (dotted grain)
among larger quartz grains. It is more difficult to entrain the heavy
mineral grain due to its larger pivoting angle and relatively lower
exposure to the flow.
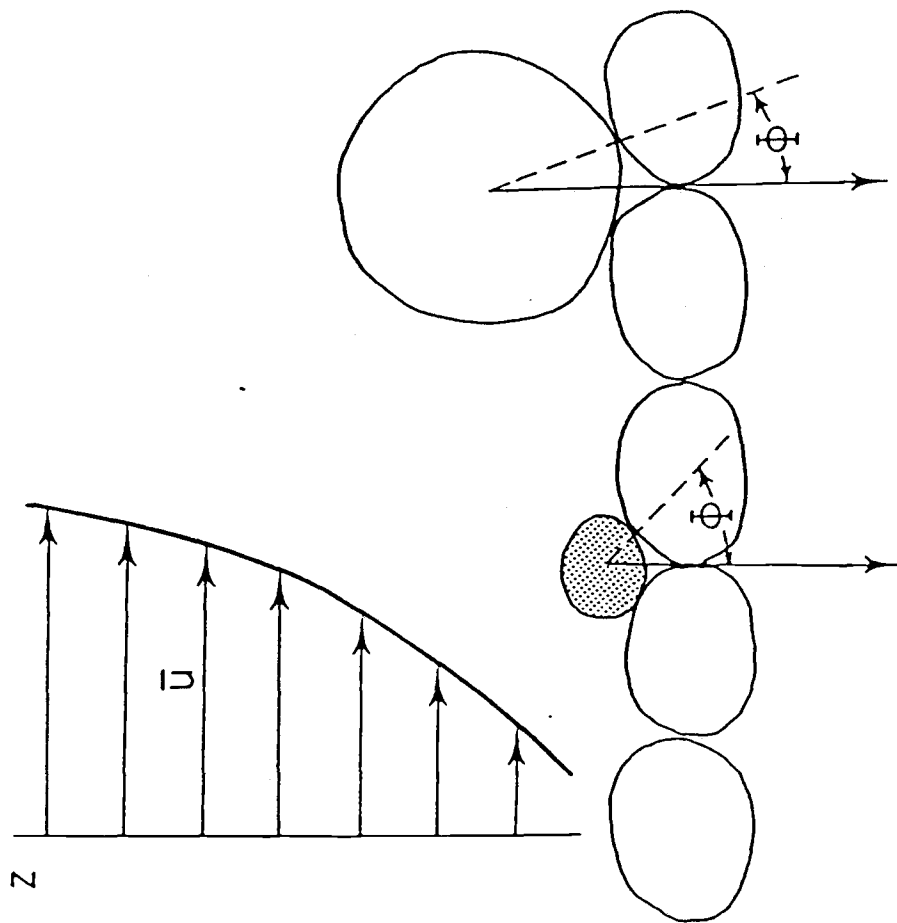
Figure 26

compared with the movement of the large quartz grains. Three factors are involved in determining the mobility of minerals in this selective entrainment process: mineral density, particle exposure to the flow, and the pivoting angle Φ of the grain over the underlying particles. The higher density of the heavy mineral is of course important in offsetting its smaller grain size, but the smaller size itself is also important. The entrainment process involves a pivoting of the grain out of its resting position, and Figure 26 shows that the smaller heavy mineral grain has a larger pivoting angle than the larger quartz grain, making its entrainment more difficult. In addition, Figure 26 shows that the larger quartz grain protrudes higher into the flow and experiences greater drag and lift forces. Thus, in a deposit of mixed minerals and grain sizes, a current may be able to entrain and transport the coarse-grained light minerals, while the finer-grained heavy minerals are left behind to develop into placer deposits.

Slingerland (1977) and Komar and Wang (1984) have developed models to analyze the selective entrainment of grains from a deposit of mixed sizes and densities. By balancing the moments of the fluid drag force and the immersed weight of the particle to be entrained, the basic entrainment relationship is

$$\tau_t = k(\rho_s - \rho) \, g \, D \, \tan\Phi \tag{10}$$

where τ_t is the threshold stress, k is an empirical coefficient, and D is the diameter of the particle that is to be entrained; Φ is conventionally called the angle of repose, but the more descriptive term "pivoting angle" has been suggested by Li and Komar (1986) for this particular application. Figure 26 shows that Φ is the angle between the vertical and the line that

connects the center of the grain to the pivot point. For a deposit of mixed grain sizes, experiments by Miller and Byrne (1966) and more recently by Li (1986) and Li and Komar (1986) have shown that

$$\Phi = e \, (D/K)^{-f} \tag{11}$$

where D is the diameter of the grain being entrained and K is the median grain size of the bottom particles, while e and f are empirical coefficients which generally depend on grain shape, overall grain size, and packing characteristics such as imbrication. Based on these analyses, Slingerland (1977) and Komar and Wang (1984) have attempted to quantify the selective entrainment processes involved in placer development. By deriving a semi-empirical critical velocity equation, Slingerland (1977) found that the boundary Reynolds number and the relative grain protrusion can be successfully used to explain experimental and natural heavy-mineral concentrations. More comparable to the present work is the study of Oregon beach placers by Komar and Wang (1984), who used the relationships

$$\tau_t = 0.00515(\rho_s - \rho) \, g \, D^{0.568} \tan \Phi \tag{12a}$$

$$\Phi = 61.5 \, (D/K)^{-0.3} \tag{12b}$$

Equation 12a was derived originally by Miller et al. (1977) for threshold of uniform grains of diameters smaller than 1 mm, and equation 12b was given by Miller and Byrne (1966) for natural beach sands. For uniform grains, D/K equals to 1 and this model gives the threshold stress under normal sorting process. For sediments of mixed grain sizes, the combination of these two relationships predicts that an increase of D/K will cause a decrease of the pivoting angle Φ so that the threshold stress τ_t will be reduced, thereby accounting for selective entrainment and

transport of the coarse-grained light minerals and the sheltering and concentration of the finer-grained heavy minerals inherent in placer formation. Since a grain exposure (protrusion) factor is not included in this model, it may over-predict the entrainment stresses (Komar, 1989). Nevertheless, this model has been used by Komar and Wang to calculate a series of threshold curves for minerals found within beach placers on the Oregon coast. Furthermore, it was shown that the relative entrainment stresses of the various minerals were directly related to their degrees of concentration within the placers.

7.1.3 Grain Sorting by Differential Transport

Following entrainment, various size and density fractions of a mixed sediment will be transported at different rates, leading to further separation (Figure 2). Sediment transport can occur as a combined bedload and suspended load. Grain movement in suspension partly depends on its settling velocity, while bedload transport involves episodic "stop and go" movements of mineral grains (repeated entrainments). Thus transport sorting actually encompasses aspects of other sorting processes.

Suspension transport can lead to the fractionation of grains of different settling velocities into different levels above the bed, and therefore lead to their subsequent separation during deposition. Based on the Rouse equation (Rouse, 1950), Slingerland (1984) obtained a relationship to calculate concentrations of heavy and light minerals at any fixed elevation in the flow:

$$(C/C_a)_h = (C/C_a)_l^{w_h/w_l} \tag{13}$$

where C is the concentration of suspended load at any elevation, C_a is a reference concentration at an elevation a, w is the settling velocity, and

the subscripts l and h again refer to the light and heavy minerals. When a suspended load is transported by a current, grains with lower settling velocities will be transported at greater rates than grains with higher settling velocities. Sorting and concentration of heavy minerals will occur only if the settling velocities between the heavy and light minerals are significantly different.

When the settling velocities of the grains are sufficiently high, they will be transported close to the bed. This grain movement mode is called bedload transport, which mainly involves grain rolling and saltation. Bedload and suspended load transports are divided by the criterion $W_s/u_* = 0.8$ to 1.5 where u_* is the flow's shear velocity (Francis, 1973; Abbott and Francis, 1977). Slingerland (1984) and Komar and Wang (1984) have used Einstein's bedload function (Einstein, 1950; 1964) to analyse the role of transport sorting in placer formation. This model considers selective entrainment as well as different transport rates. By including a hiding facter, the model also accounts for smaller grains being sheltered by larger grains. Therefore, this approach simulates the transport of finer-grained heavy minerals from a bed of mixed sediments. Slingerland (1984) has calculated the transport rates for different size fractions in a 90% quartz, 10% magnetite sand mixture under different bed roughnesses k_s and shear velocities u_*, the mixure being constructed in such a way that quartz and magnetite are roughly settling-equivalent. It was found that for a given u_*, transport rates for all sizes and both minerals decrease with increasing roughness, and that the relative concentration of magnetite in the moving bedload increases with increasing u_* for a given roughness and decreases with increasing roughness for a given u_*. Similar

calculations have been undertaken by Komar and Wang (1984) in their study on Oregon beach placers. They found that the transport rates of all of the minerals are increased with an increase in flow stress, and that minerals with higher densities and smaller grain sizes are transported at lower rates. It was also found that this transport sorting is more effective at low to medium flow stresses than at high flow stresses.

Limited data from flume experiments supports the analysis results described above. Meland and Norrman (1966) conducted flume experiments to measure the transport velocities of glass spheres over fixed beds of ideally packed uniform spheres. Sizes of both the transported sphere and those in the bed were varied to study the effects of bottom roughness on the transport rates. It was found that for a fixed bottom roughness, larger grains move faster than smaller ones; for a given u_*, the highest transport rates occur for the largest grains moving over the smallest bottom roughness. In a similar experiment, Steidtmann (1982) investigated the effects of both density and relative grain size D/K. He similarly found that grain transport velocities increase with increasing D/K for a given u_*, and with increasing u_* for a fixed D/K. He also found that for a given D/K, the transport velocity of the light mineral is greater than the heavy mineral, and the difference increases with increasing D/K values. Thus for a sediment of mixed minerals and sizes, coarse-grained light minerals will be transported at higher rates and farther away from the source area, while the finer-grained heavy minerals will have lower transport rates and thus be left behind to form placer deposits.

7.1.4 Dispersive-Pressures and Shear Sorting

High concentrations of heavy minerals are often found at the bases

of thin laminations within beach deposits (Emery and Stevenson, 1950; Clifton, 1969; Sallenger,1979). It is believed that this segregation is caused by a shearing of the bedload layer on the beach during backwash of waves. Studies by Bagnold (1954, 1956) have shown that when a sediment-laden flow is sheared by fluid forces, grain interactions will create an upward force perpendicular to the plane of shearing, a force that is termed the "dispersive pressure". Experiments proved that this pressure is greater on larger grains than on smaller grains at any given horizon. Thus when grains of mixed sizes are sheared, coarser grains tend to migrate upward toward the surface while the finer grains move downward toward the bed. Since heavy minerals usually are finer-grained than the associated light minerals, the size grading will be accompanied by the concentration of heavy minerals toward the base of the layer. The term "shear sorting" was coined by Inman et al. (1966) to represent this vertical segregation.

Based on Bagnold's studies, Sallenger (1979) developed the concept of grain-dispersive equivalence, and proposed that particles riding in the same horizon in a sheared sediment flow should have equal dispersive pressures. He showed that their respective diameters are then governed by

$$D_h / D_l = (\rho_l/\rho_h)^{1/2} \tag{14}$$

indicating an inverse relationship between grain size and density.

7.2 Previous Work on Grain Sorting and Beach Placers

Selective grain sorting processes and their effects on placer formation have been extensively studied (McIntyre, 1959; Hand, 1967; Lowright et al., 1972; Stapor, 1973; Slingerland, 1977, 1984; Komar and

Wang, 1984). Most of these studies have focused on beach placers and attempted to determine which sorting processes are responsible for the heavy mineral concentration. Some of the recent studies of direct significance to the present investigation are reviewed below.

The thesis study of Trask (1976), subsequently published by Trask and Hand (1985), examined longshore mineral sorting on the beach along the eastern side of Lake Ontario. Sieving analysis indicated a northward decrease in grain size for the first 17 km, and a coarsening north of that distance. A fraction having a fall velocity equivalent to a 2ϕ quartz grain was separated using a settling tube. Heavy mineral abundances and their hydraulic ratios versus the light minerals were obtained for this settling-equivalent fraction. The heavy mineral percentage was found to decrease in the direction of transport. It was also established that the degree to which each heavy mineral lags behind the light mineral is a function of the ratio of their effective densities (mineral density minus fluid density). Since the sampling procedure had eliminated the possible effect of sorting by grain settling , this longshore mineral sorting was concluded to result from differential entrainment and transport processes in which heavy minerals were less entrainable and transportable than their light companions due to their smaller sizes and higher densities.

Plopper (1978) collected samples from the southernmost two-thirds of the Washington coast to study hydraulic sorting and longshore sand transport on these beaches. Textural and mineralogical analyses were first carried out, and it was found that heavy mineral concentrations and mean grain sizes generally decrease northward along the Long Beach Peninsula, indicating a net northward longshore sediment transport. Similar to the study of Trask and Hand (1985), a fraction having

a fall velocity equivalent to a 2φ quartz grain was separated using a settling tube. Hydraulic ratios of various mineral pairs were calculated for the settling-equivalent splits in order to understand the hydraulic sorting processes. This hydraulic ratio is defined as the weight of any heavy mineral divided by the weight of any light mineral multiplied by 100 (Rittenhouse, 1943), and thus it is a measure of availability of heavy minerals for deposition. By analyzing changes in hydraulic ratios with distance from the Columbia River and their relationship with mineral density, Plopper was able to confirm the existence of a hydraulic lag and to draw the conclusion that longshore distribution of heavy minerals on the Washington coast is caused primarily by hydraulic sorting during transport.

In contrast to the longshore grain sorting studies of Plopper (1978) and Trask and Hand (1985), Komar and Wang (1984) collected a series of samples across an Oregon beach profile to study cross-shore selective grain sorting and placer formation during an erosion event. Sieving and mineralogy analyses showed that the heavy minerals are highly concentrated in the landward-most sample in the upper swash zone. The overall concentration of heavy minerals decreased systematically offshore, while the median grain sizes of both the heavy and the light minerals increased progressively in the offshore direction. Though all the heavy minerals tended to be concentrated in the placer in the upper swash zone, analysis of individual heavy mineral concentrations revealed that the sorting processes leading to placer formation are more efficient in concentrating denser and finer-grained minerals, while transporting the less dense and coarser-grained minerals offshore. In determining the possible sorting processes, Komar and Wang directly measured the settling

velocities of individual mineral grains. It was found that all of the minerals in the sediments have approximately the same settling rates, precluding their selective sorting by differences in settling. A process-oriented selective entrainment model and Einstein's bed-load approach were used to evaluate the selective entrainment stresses and bedload transport rates of the individual minerals. By comparing these results with the degree of concentration of each mineral in the placer, they concluded that selective entrainment and differential transport are the dominant sorting processes in the development of that Oregon beach placer.

The present investigation has aspects that are similar to the studies of Plopper (1978), Trask and Hand (1985) and Komar and Wang (1984). Like Plopper and Trask and Hand, this study examines grain sorting that occurs in the longshore direction. It differs from those studies in undertaking analyses of the complete grain-size and settling-velocity distributions of the principal minerals in the deposits, not being limited to the 2ϕ quartz-equivalent size physically extracted from a settling suspension. The present study is similar to that of Komar and Wang in its attempt to relate the observed patterns of grain sorting to measured settling velocities and estimated grain-entrainment stresses. It differs from Komar and Wang in examining sorting in the longshore direction rather than in the cross-shore.

7.3 Effects of Sorting by Differential Settling
7.3.1 Settling Velocity Distribution In The Original Sediment Supply

The median grain sizes listed in Table 7 are the result of selective grain sorting and longshore transport of the original sediment supplied by

the Columbia River. In analyzing the sorting mechanisms, it is useful to examine the grain size distribution of major minerals in the source sediments. A direct approach would be to analyze samples collected from the Columbia River estuary. However, longshore transport mainly occurs on the beach and in the surf zone. The grain size data of sands that have reached the beaches is more important to longshore grain sorting study than that of the estuarine samples. Therefore, the approach used here is to remix the longshore samples to obtain the median grain sizes of the major minerals in the original sediment supply, before it was reworked by longshore selective grain sorting and transport processes. Sorting mechanisms responsible for placer development can then be evaluated by examining the settling velocities, selective entrainment stresses, and transport rates of the major minerals in this original sediment supply. In order to do this, the median intermediate diameters given in Table 7 and relative abundances of heavy and light minerals given in Table 8 are used to remix the longshore samples so that a weighted average D_b can be obtained for each mineral to represent its median grain size in the original sediment supply. For instance, the median grain size of hornblende in the original sediment on the Clatsop Plains can be calculated as:

$$Db\text{-Hornblende} = \frac{(Db \times Wt\%)ss1 + (Db \times Wt\%)ss2 + ... + (Db \times Wt\%)ss7}{(Wt\%)ss1 + (Wt\%)ss2 + ... + (Wt\%)ss7}$$

$$= 0.209 \text{ mm} \qquad\qquad (15)$$

where Wt% is the weight percentage of the mineral for a given sample. The original median diameters calculated this way for each of the major minerals are listed in Table 10 together with their assumed densities.

The opaques in this study are mainly magnetite and ilmenite (densities 5.2 and 4.8 g/cm^3 respectively). Examination under the microscope has shown that a significant number of the opaque mineral grains are weathered. This weathering tends to decrease mineral's density and thus a lower density of 4.8 g/cm^3 has been used in this study.

The intermediate diameter D_b of each mineral listed in Table 10 is first used to calculate their spherical settling velocity Ws according to Warg (1973), and their measured settling velocities W_m were then obtained from equation 7. This W_m can be defined as the settling velocity of each mineral in the original sediment supply, and are also listed in Table 10. These data indicate that minerals of higher densities also settle faster than minerals with lower densities in the original sediment supply. In order to understand if settling equivalence exists among these minerals in the original sediment, their settling velocities relative to the settling velocity of augite (W_m/ W_m-Aug) have been plotted versus their densities in Figure 27. If these minerals are settling equivalent, their settling velocity ratios with that of augite should closely follow the constant line of W_m/ W_m-Aug = 1, being uncorrelated with the density. Figure 27 shows that settling velocity ratios of minerals with densities greater than augite (hypersthene and opaques) are roughly equal to one, indicating that they are in settling equivalence with augite in the original sediment supply. However, minerals of lower densities (quartz and hornblende) give lower settling velocity ratios. This signifies that they have lower settling velocities than other minerals in the original sediment source. Therefore, settling sorting is probably responsible for the overall

TABLE 10
Summary of important parameters in Selective Sorting of Placer Minerals

Minerals	ρ_s (g/cm3)	Db (mm)	C.F.	Settling Vel. (cm/s)	Entrain. (τ_t) (Dynes/cm2)	Transp. Rate at $\tau_o =$: 5	10	25
North								
Quartz	2.7	0.264	0.34	2.57	2.01	.076(1)	.8(1)	3.74(1)
Hornblende	3.2	0.241	18.56	2.66	2.65	.014(.18)	.44(.55)	3.04(.81)
Augite	3.4	0.225	69.24	2.99	2.95	.0072(.10)	.28(.35)	2.71(.73)
Hypersthene	3.5	0.228	96.25	3.09	3.06	.006(.08)	.27(.34)	2.73(.73)
Opaques	4.8	0.218	140.65	3.06	5.21	.00014(.002)	.01(.12)	2.49(.66)
South								
Quartz	2.7	0.233	0.40	2.30	1.87	.023(1)	.47(1)	2.89(1)
Hornblende	3.2	0.209	36.44	2.39	2.48	.0036(.15)	.20(.42)	2.32(.81)
Augite	3.4	0.194	45.58	2.59	2.76	.00098(.04)	.12(.25)	2.06(.71)
Hypersthene	3.5	0.185	74.60	2.58	2.93	.00061(.03)	.10(.21)	1.53(.53)
Opaques	4.8	0.175	81.32	2.55	5.02	.00007(.003)	.05(.11)	1.21(.42)
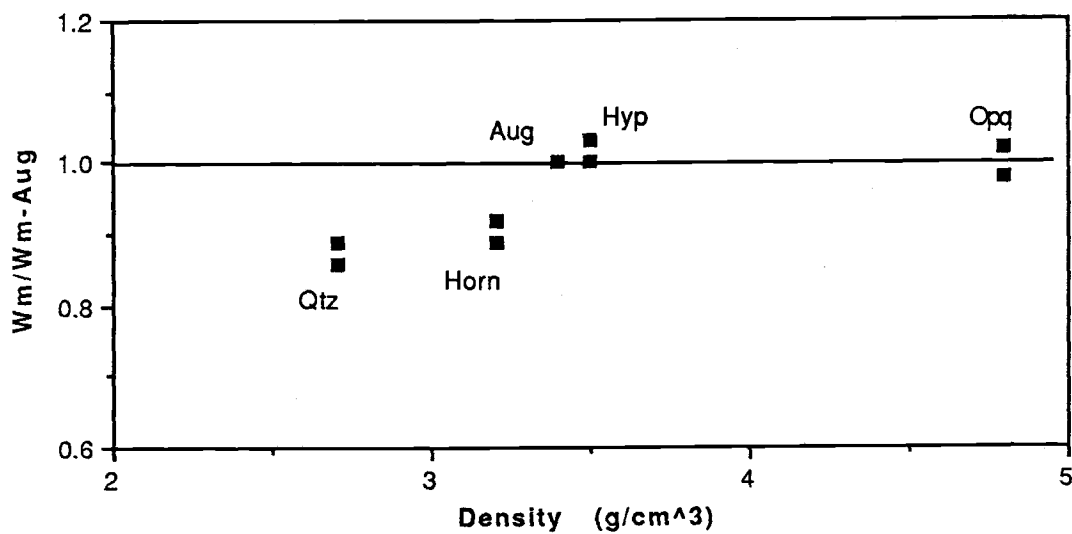
Figure 27
Settling velocities of major minerals normalized to that of augite,
plotted as a function of their densities, showing a general settling
equivalence among the heavy minerals and slower-settling quartz
and hornblende in the original sediment source.

separation of the heavy minerals from the light minerals close to the Columbia River mouth, since slower-settling light minerals will outdistance the faster-settling heavy minerals during longshore sediment transport. However, the separation of augite, hypersthene and opaques (Figures 24a and 24b) cannot be explained by this settling-sorting process, since theses minerals are in settling equivalence in the original sediment supply.

7.3.2 Settling Velocity Versus the Concentration Factor

To further examine the effects of settling sorting on mineral separation and placer formation, the settling velocity of each mineral in the original sediment supply has been compared with its concentration factor, C.F. in the placer deposit. This concentration factor is computed as the percentage of each heavy mineral in the placer samples (ss1 and sn1), divided by its lowest percentage in the longshore samples. The percentages are the mineral abundances in the overall sample, including both the heavy and the light minerals, so that this concentration factor is actually a direct measure of the degree to which a mineral has been concentrated in the placer deposit. These C.F. values are listed in Table 10 separately for the Clatsop Plains and the Long Beach Peninsula. It is seen that quartz (the light minerals) has the lowest concentration factors, being less than unity. This indicates that most of the quartz has been moved away from the source area. The concentration factors increase systematically from hornblende to augite and hypersthene, indicating that they become more concentrated in the placer deposits in that order. The opaques (ilmenite and magnetite) have the highest C.F. values, and thus are most highly concentrated in the placer deposits, with very little being

transported alongshore away from the river source.

The concentration factors of major minerals are plotted in Figure 28 as a function of their settling velocities W_m in the original sediment supply, separately for the Clatsop Plains and the Long Beach Peninsula. It is found that the concentration factor first increases with an increase in settling velocity. However, as the settling velocity is further increased, the C.F. curve approaches a constant value. This pattern suggests that light minerals of lower settling velocities could have been transported more effectively away from the source area, leaving the heavy minerals to be concentrated in the placer deposits. Minerals of high settling velocities are nearly settling-equivalent, and therefore their settling velocities are not correlated with their concentration factors. It can be concluded that sorting by differential settling may have played some role in controlling the general longshore sorting of light versus heavy minerals, but plays no significant role in further separations among the heavy minerals themselves.

7.3.3 Longshore Variations of Settling Velocities

The discussion thus far has focused mainly on settling velocities in the original sediment supply. Settling sorting effects can also be evaluated by examining the settling velocities of major minerals after they were reworked by longshore selective sorting and transport processes. The median grain sizes given in Table 7 have been used to calculate the settling velocities of the major minerals for all beach samples . These calculated W_m values are listed in Appendix IV and are plotted in Figure 29 against the longshore distance from the Columbia River mouth for each mineral. It is seen that the settling velocity for each
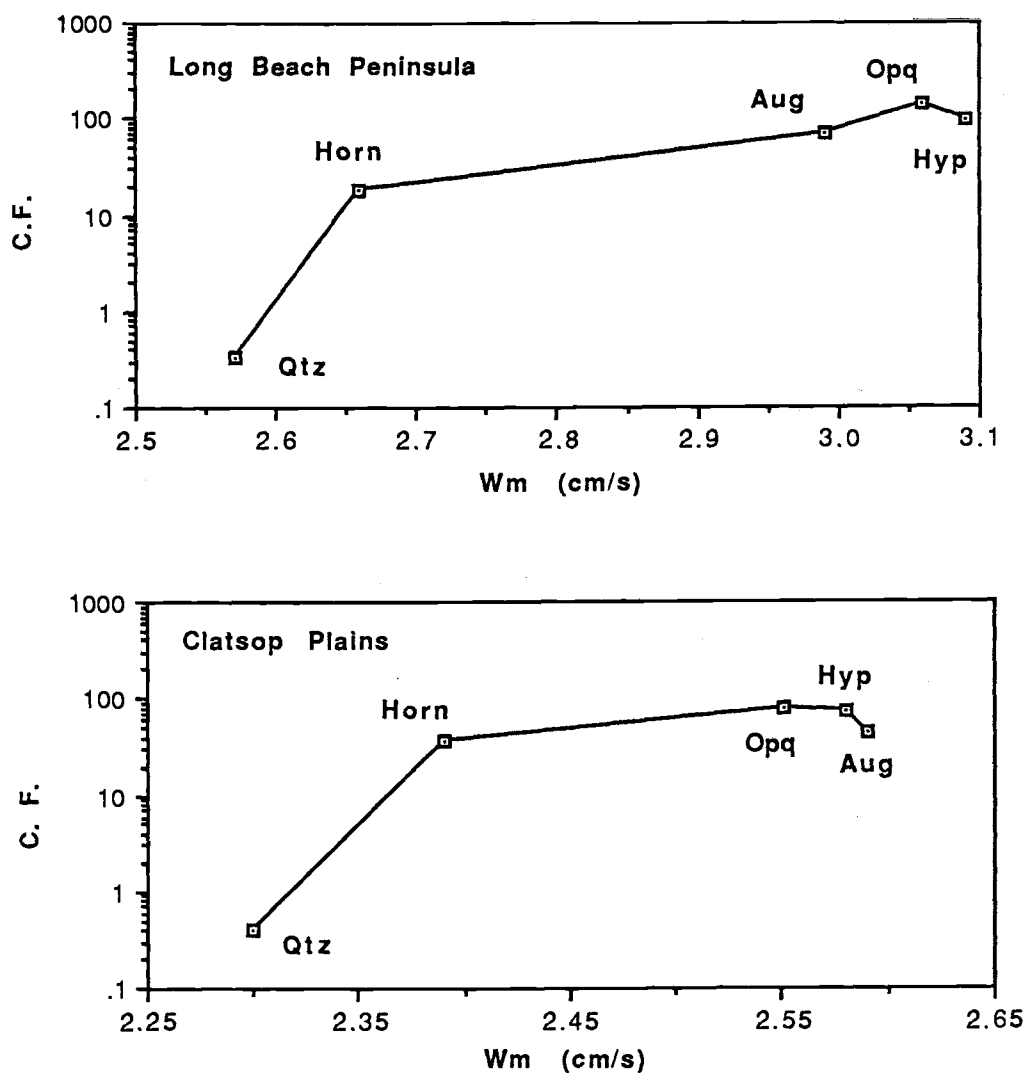
Figure 28

Mineral concentration factors (C.F.) in the placer plotted against their settling velocities in the original sediment supply. The lower settling velocity of quartz may have resulted in its depletion in the placer deposits, but the settling velocities of the heavy minerals are poorly correlated with their concentration factors.

Figure 29

Settling velocity (W_m) variations of each major mineral as a

function of longshore distance from the Columbia River mouth on

the Long Beach Peninsula (a) and Clatsop Plains (b), showing an

unusual away-from-source increase of settling velocity close to the

river mouth and a general decrease at still greater distances.
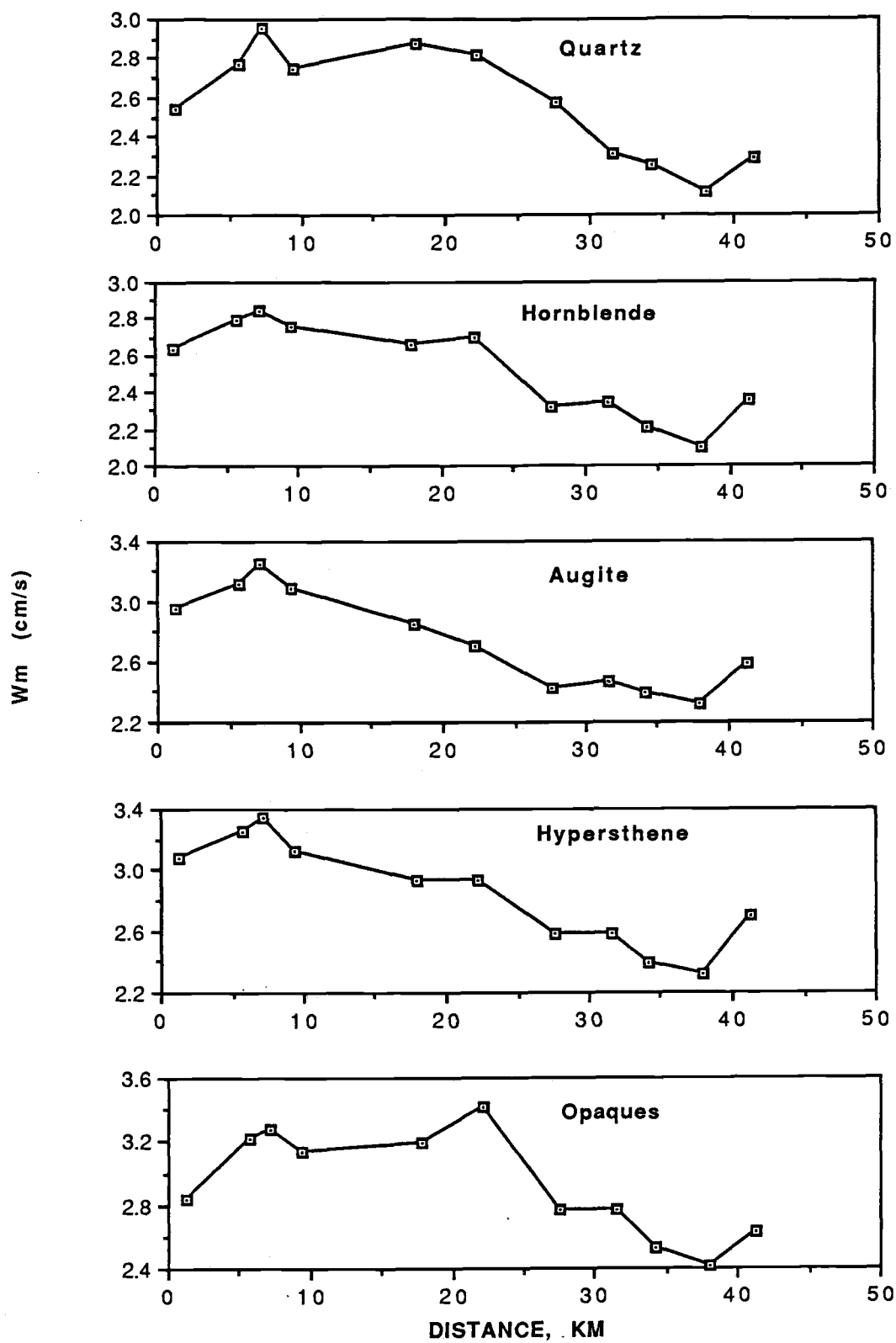
Figure 29a
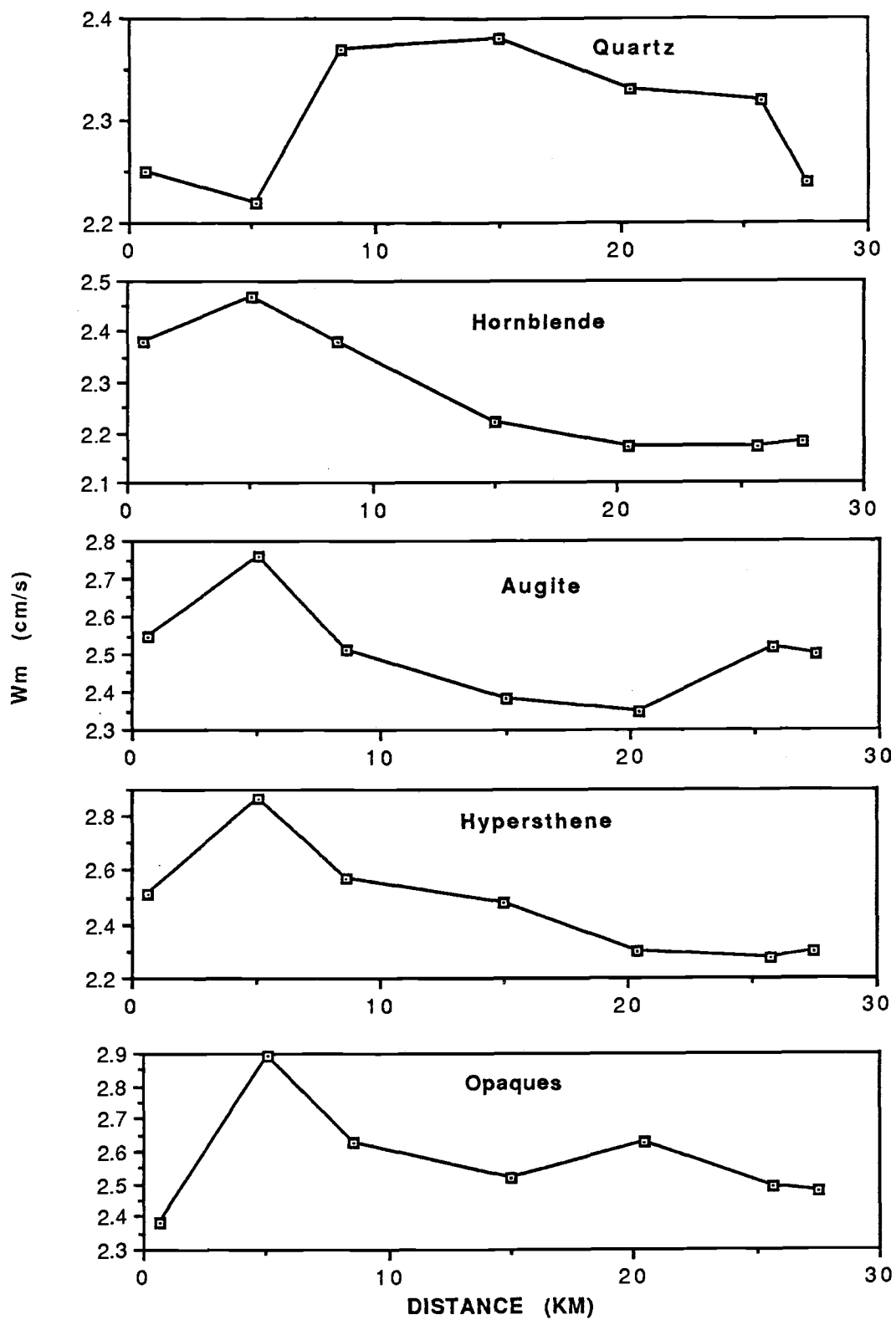
Figure 29b

mineral is low close to the Columbia River mouth, and increases away from the river to a distance of about 5-8 km. With greater longshore distance, the settling velocity W_m generally decreases toward the end of each beach section, except for a slight increase at the very ends of the Clatsop Plains and the Long Beach Peninsula. If relative grain settling plays a significant role in the mineral sorting and placer development, minerals with high settling velocities should deposit closer to the source area while minerals with lower settling velocities should be transported farther away from the Columbia River mouth. The opposite trend in the placer samples shown in Figure 29 indicates that settling sorting plays little if any role in the concentration of heavy minerals close to the river mouth. The general decrease in settling velocity starting at about 5-8 km longshore distance, however, indicates that grain sorting due to differential settling is important for the remaining length of the beach. Along those portions of shore, mineral grains with higher settling velocities are generally outdistanced by mineral grains with lower settling velocities.

7.4 Selective Entrainment and Differential Transport

7.4.1 Threshold Stresses of the Original Sediment

The general settling equivalence of heavy minerals in the original sediment supply occurs because minerals of higher densities are generally finer-grained than minerals of lower densities (Table 10). This inverse relationship between grain size and density suggests that selective entrainment and differential transport can be important mechanisms in sorting the grains, leading to placer development in the study area. In order to understand the effects of selective entrainment, the intermediate

diameters (D_b) of each major mineral listed in Table 10 have been used in equations 12a and 12b to calculate their entrainment stresses in the original sediment. Since heavy minerals constitute only about 10% of the original sediment, the intermediate diameter of quartz is assumed to be K the median grain size of the original sediment mixture (K = 0.26 mm for the Long Beach Peninsula and 0.23 mm for the Clatsop Plains). The entrainment stresses calculated this way are listed for each mineral in Table 10, where it is seen that minerals of higher densities and finer grain sizes generally require higher flow stresses to be entrained than minerals of lower densities and coarser grain sizes. The threshold stress increases in sequence for quartz, hornblende, augite, hypersthene and the opaque minerals.

The selective entrainment stresses are plotted as a function of the concentration factor of each mineral in Figure 30 for the Clatsop Plains and Long Beach Peninsula. Both show a similar pattern – minerals of lower entrainment stresses correspond to lower concentration factors in the placer. Quartz has the lowest entrainment stress, and its concentration factor is also the lowest, being less than unity. As the entrainment stresses increase from hornblende to augite, hypersthene and opaques, their concentration factors correspondingly increase. This pattern implies that minerals of lower selective entrainment stresses are more easily removed from the original sediment, and transported away from the source area. As a result, they are less concentrated in the placer deposits. This relationship between higher placer concentrations and high mineral entrainment stresses strongly suggests that selective entrainment sorting plays an important role in the processes of heavy mineral concentration and placer formation in the study area.

Figure 30

Mineral concentration factors (C.F.) plotted against their selective entrainment stresses in the original sediment supply for sands on the Long Beach Peninsula (a) and Clatsop Plains (b). Both show a positive correlation that minerals of higher selective entrainment stresses are more concentrated in the placer deposits.
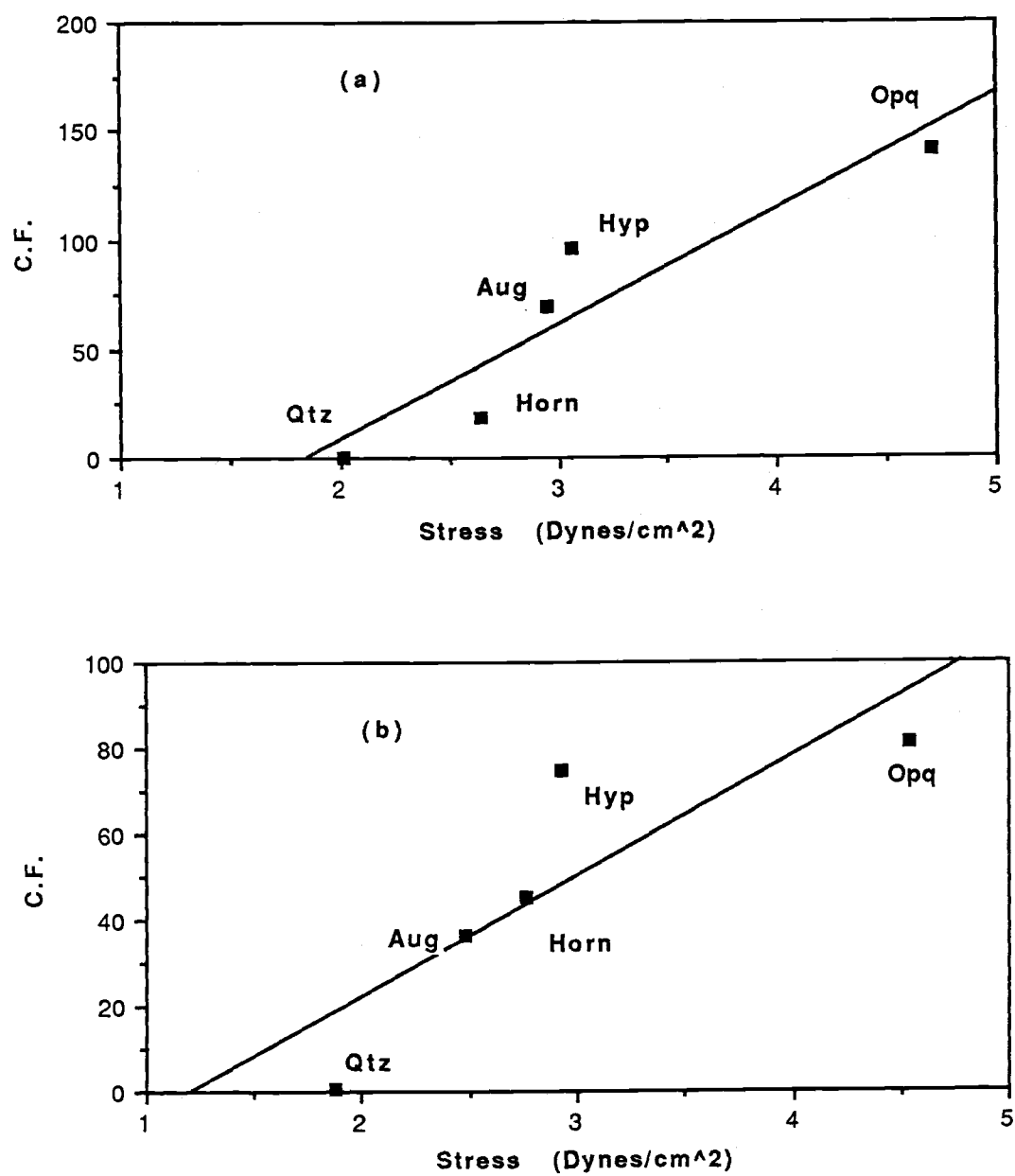
Figure 30

7.4.2 Stress Variation with Longshore Distance

The effects of sorting due to selective entrainment can also be studied by examining the longshore variation of threshold stress of each mineral. It is expected that mineral grains with lower threshold stresses should be transported farther than grains with higher threshold streesses. The D_b values of hornblende for the Long Beach Peninsula (Table 7) have been chosen for a test evaluation. These D_b values and $K = 0.26$ mm are used in equations 12a and 12b to calculate their selective entrainment stresses τ_t in the original sediment source. These entrainment stresses are plotted against the longshore distance in Figure 31. If selective sorting mechanism is effective along the entire beach length, a systematic trend of decreasing τ_t with longshore distance from the source should exist. The results show that for the first three samples (about 8 km northward of the Columbia River mouth), the selective entrainment stress of hornblende decreases with longshore distance. After this, its entrainment stress increases systematically to the end of the Long Beach Peninsula. The entrainment stresses of other minerals show similar variations with longshore distance. This longshore variation pattern suggests that sorting due to selective entrainment is only dominant close to the Columbia River mouth. Finer mineral grains require higher flow stresses for entrainment than coarser grains, and thus are left close to the source area, yielding the systematic decrease of τ_t for the first 2 or 3 samples away from the river mouth. The trend of increasing τ_t with longshore distance further away from the source area indicates that mineral grains requiring higher selective entrainment stresses in the
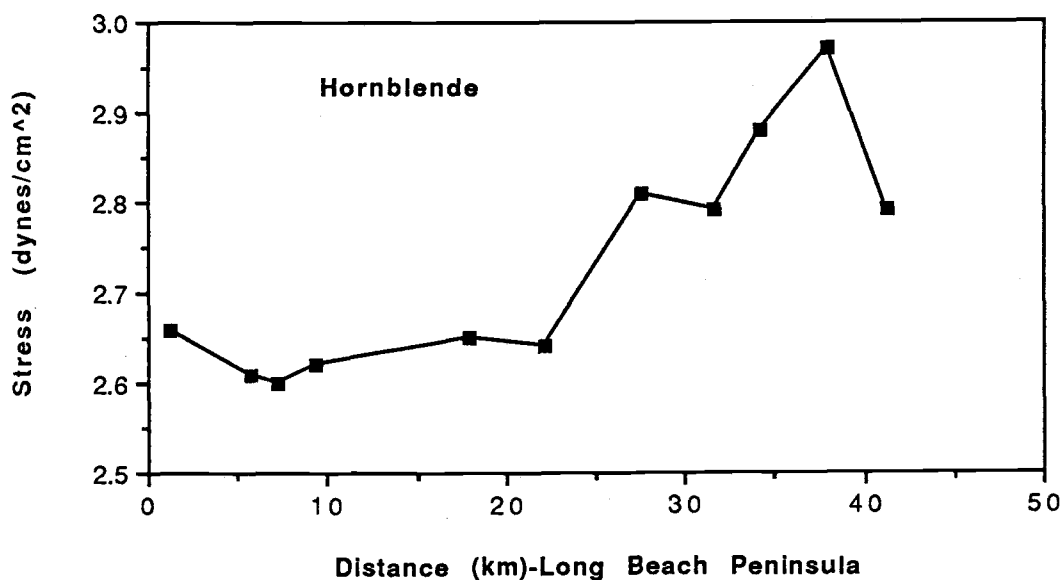
Figure 31
Longshore variation of entrainment stress for hornblende
calculated using the selective entrainment model and the median
grain size of the mineral in each sample. Except for the first three
samples, the entrainment stress increases with longshore distance,
suggesting that the selective entrainment model is not applicable to
this part of the beach.

original sediment supply were transported further away from the source, which is certainly unlikely. This suggests that equations 12a and 12b might be unsatisfactory to predict τ_t values, and thus selective entrainment sorting is probably not effective for these beach sections. This agrees with the conclusion reached from grain size and mineralogy analyses in chapter 6, which predicts that selective grain sorting is effective close to the Columbia River mouth, and that normal processes of sediment transport become more important away from this source area.

7.4.3 Differential Transport Rates and Mineral Separation

After being entrained by a current, various minerals can be further separated due to their differential transport rates. In order to evaluate the significance of differential transport in placer development, the intermediate diameters D_b given in Table 10 have been used in the Einstein's bedload function (Einstein, 1950, 1964) to calculate the bedload transport rates of the five major minerals in the original sediment mixture. This approach involves various equations and graphs. The detailed procedures and necessary graphs are given in Appendix V. The transport rates(in grams/s/cm) are calculated for flow stresses τ_o = 5, 10 and 25 dynes/cm^2 in order to examine this sorting mechanism under different flow conditions. The results are listed in Table 10. These calculated transport rates are then normalized to the transport rates of quartz. These ratios are also listed in Table 10 (in brackets) and should serve as an indication of each mineral lagging behind the fastest-transporting quartz, which has a ratio of one.

An examination of these results shows that the transport rate of

each mineral increases with the increase of the flow stress τ_o. For example, the transport rate of augite on the Long Beach Peninsula increases from 0.0072 to 0.28 and then 2.71 g/cm/s as the flow stress increases from 5 to 10 and 25 dynes/cm^2. For any fixed flow stress, the transport rates decrease with an increase in mineral density and decrease of grain size. The degree of lag behind quartz increases from hornblende to augite, hypersthene and opaques. It is also found that at very high flow stresses, mineral sorting due to differential transport is not effective. For instance, at τ_o = 25 dynes/cm^2, the transport rate of augite is 0.73 times that of quartz, and even opaques are significantly transported, their rate being 0.66 times that of quartz along the Long Beach Peninsula. In contrast, at τ_o = 5 and 10 dynes/cm^2, the transport rates of augite are 0.1 and 0.35 times of that of quartz on the Long Beach Peninsula. Thus, it can be concluded that differential transport sorting is more effective at low to medium flow stresses, a conclusion also reached by Komar and Wang (1984).

The effect of transport sorting on placer development can be better examined by comparing the transport rates of the various minerals in the original sediment supply with their degrees of concentration in the placer deposits. In Figure 32 the concentration factor of each mineral is plotted against its transport rate at τ_o=10 dynes/cm^2. It is seen that the concentration factor progressively decreases with increasing transport rate. Quartz, with the highest transport rate, corresponds to the lowest concentration factor in the placer, since most of it has been transported away from the source area. As the transport rates decrease from hornblende to augite and hypersthene, their concentration factors

Figure 32

Relationship between mineral concentration factors (C.F.) in the placer deposits and their longshore transport rates (g/s/cm) in the original sediment supply, indicating that minerals having lower longshore transport rates are more highly concentrated in the placer deposits.
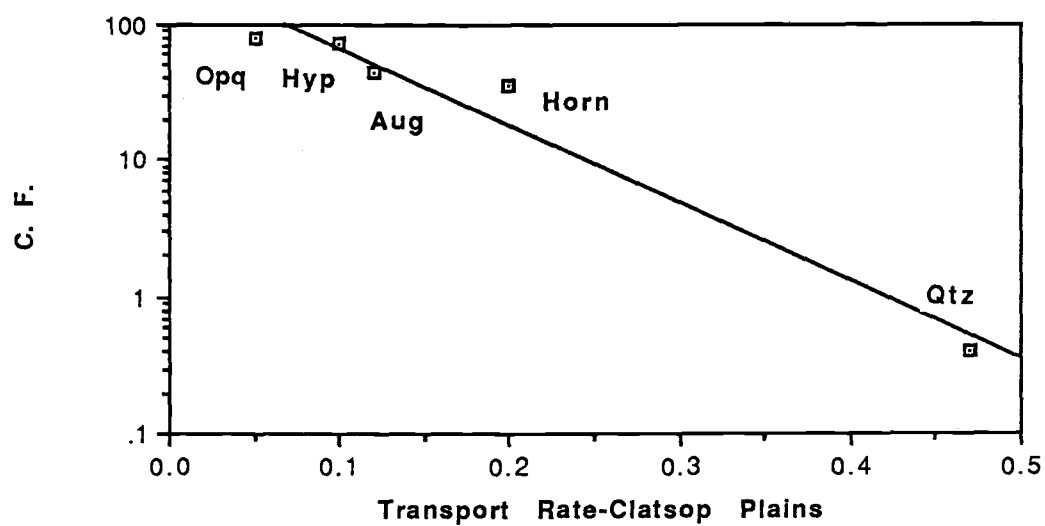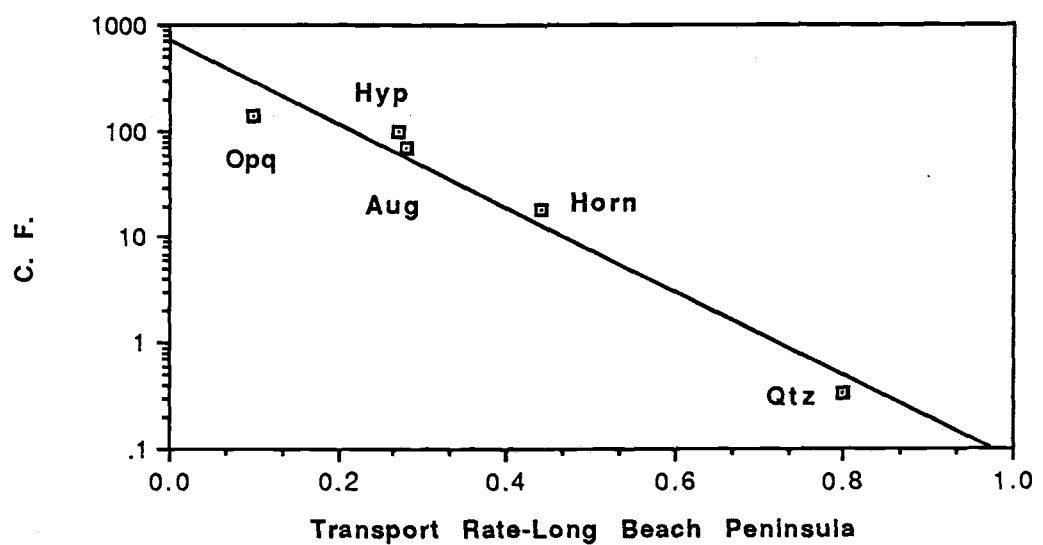
Figure 32

increase, indicating stronger lagging behind in the placer deposits. The opaques show the lowest transport rate and largest concentration factor, so that most of it remains close to the source area to be highly concentrated in the placer deposits. This inverse correlation between mineral concentration factors and transport rates suggest that differential transport as well as selective entrainment are important sorting mechanisms in mineral separation and placer formation in the study area.

7.4.4 Hydraulic Ratios

Analyses presented in section 7.3 (Effects of Sorting by Differential Settling) indicated that differential settling does not play a significant role in heavy mineral separation and placer development. This can be further confirmed by evaluating mineral sorting under an equivalent settling velocity and calculating the hydraulic ratios for the major minerals in that settling-equivalent fraction. Hydraulic ratio was first defined by Rittenhouse (1943). McMaster (1954) used hydraulic ratios to determine sediment sources and transport directions on beaches along the New Jersey shoreline. Plopper (1978) and Trask and Hand (1985) have also analyzed the longshore variations of hydraulic ratios of major mineral pairs on Washington beaches and the eastern shore of Lake Ontario, respectively. They found that hydraulic ratios decrease with distance from the sediment source, indicating that the abundances of the denser minerals decrease relative to the lighter minerals in the transport direction. The rate of decrease for a given heavy mineral was found to be proportional to the density difference between the heavy and light minerals.

In order to calculate hydraulic ratios in this study, the frequency curve of Wt% vesus grain size has to be converted to the frequency curve of accumulative percentage versus the settling velocity. As described in Chapter 5, equation (1) is first used to convert the sieve D_{sv} to mineral D_b for each sieving fraction. The settling velocity W_m is then calculated according to equations (4) through (7). The settling velocity W_m of each sieving fraction is then plotted against the cumulative weight percentage Wt% to obtain the settling velocity frequency curve. Settling velocity frequency curves have been determined for each major mineral and plotted for each sample. The curves of sample sn7 are presented in Figure 33 as an example. A representative settling velocity band ranging from 2.25 to 2.50 cm/s is chosen so that the weight percentage of each mineral in this range can be calculated. The relative abundances of the major minerals within this settling-velocity fraction can then be obtained and their hydraulic ratios calculated.

The longshore variations on the Long Beach Peninsula of mineral abundances under equivalent settling velocity are plotted for the total sample in Figure 34 and for the heavy fraction alone in Figure 35. Figure 34 shows that even for an equivalent settling velocity, all the heavy minerals are concentrated close to the river mouth while the abundance of quartz (light minerals) increases away from the source area. This pattern establishes that when settling-sorting can be ruled out, selective entrainment and differential transport still cause mineral sorting leading to a relative concentration of heavy minerals close to the Columbia River mouth. If Figure 35 is compared with Figure 24a, similarities are readily apparent: the dense opaques and hypersthene are concentrated close to the jetty, the less-dense hornblende is depleted close to the jetty, while

Figure 33

Settling velocity (W_m) frequency curves of the major minerals for sample sn7 derived from the sieve size frequency curves. A representative settling velocity band ranging from 2.25 to 2.5 cm/s is indicated by the vertical lines. This band is used to calculate the relative abundances of major minerals under the equivalent settling velocity.
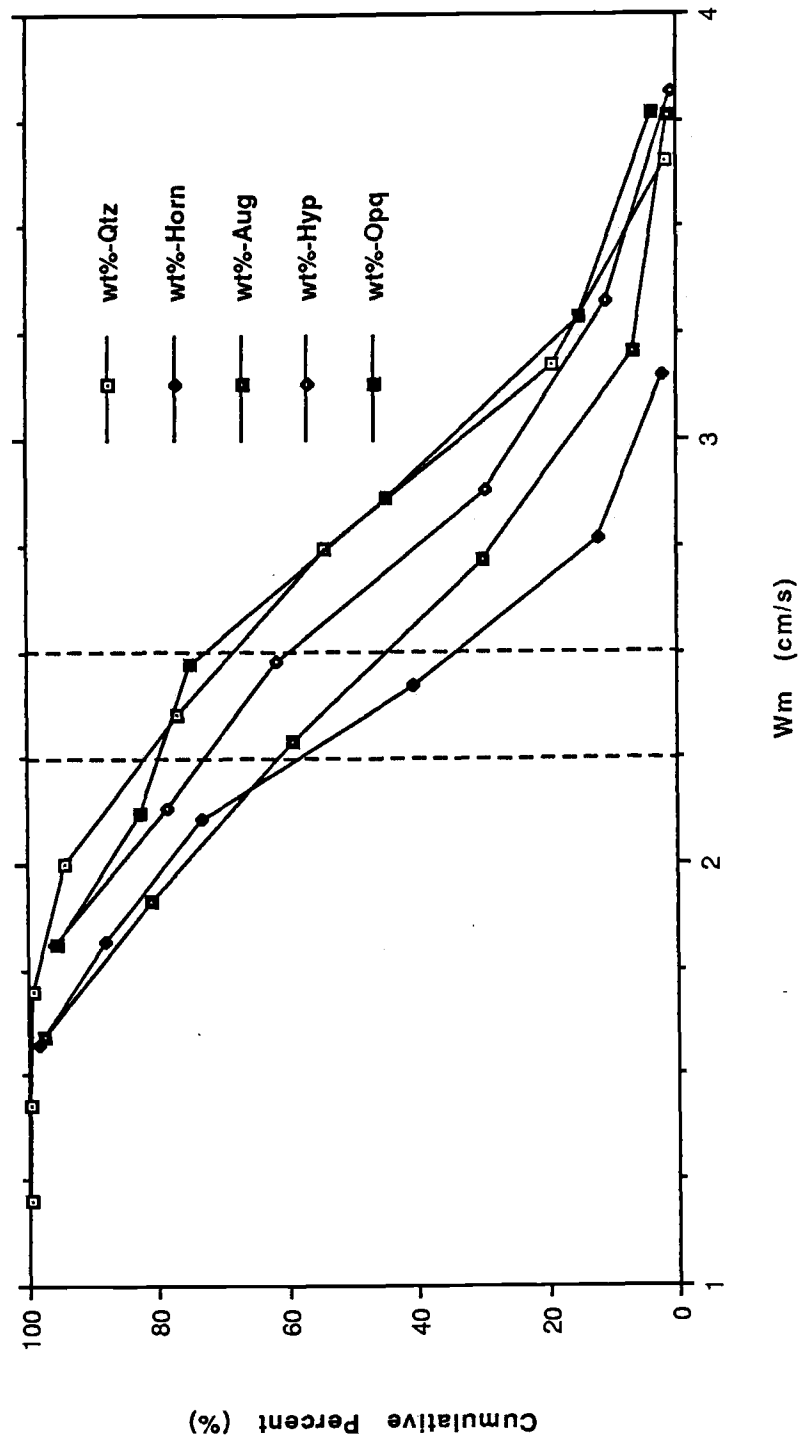
Figure 33

Figure 34

Longshore variation of mineral abundances under equivalent settling velocity in the total samples from the Long Beach Peninsula. These trends are similar to those presented in Figure 23, indicating that even when settling sorting is eliminated, selective entrainment and differential transport sorting still causes mineral separation and the concentration of heavy minerals close to the river mouth.

149
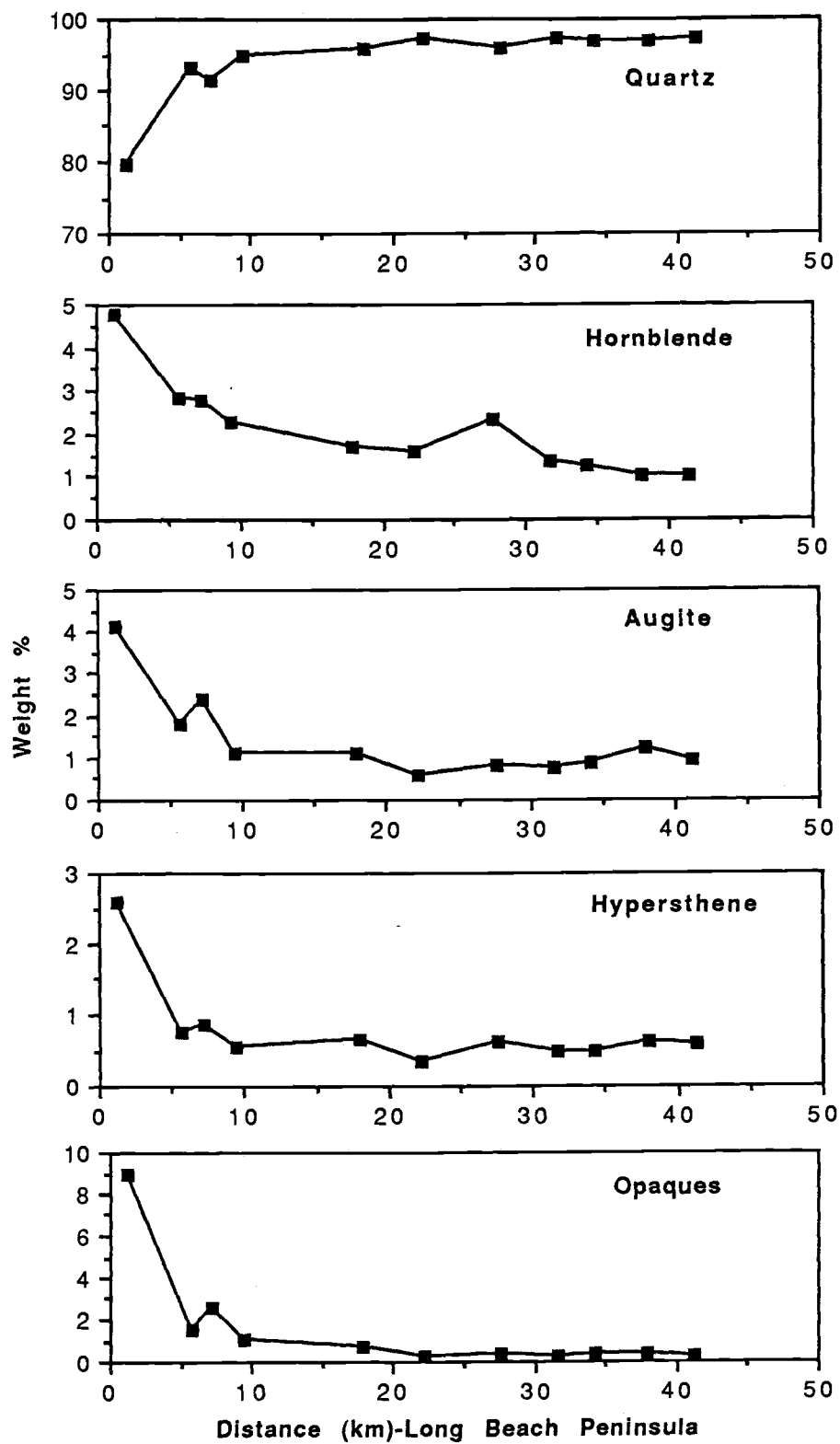
Figure 34

Figure 35

Longshore variation of mineral abundances under equivalent settling velocity in the heavy fraction alone, Long Beach Peninsula. The similarity of the trends between this figure and those in Figure 24 indicates that selective grain sorting is the cause for the further separation of the heavy minerals.
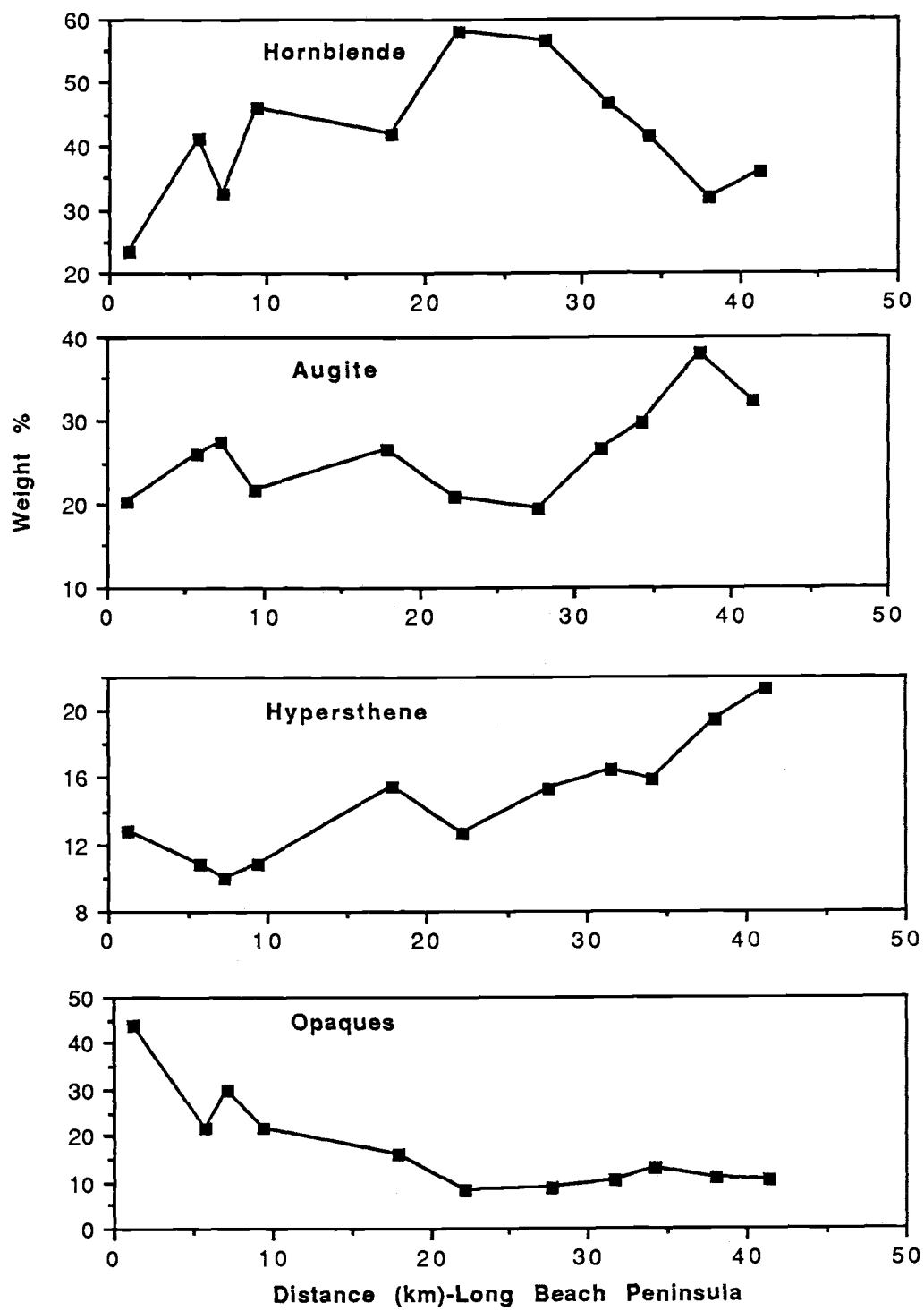
Figure 35

augite does not show any apparent trend. These similarities confirm that further separation among the heavy minerals is mainly caused by the selective entrainment and differential transport grain-sorting processes.

The hydraulic ratios of various mineral pairs are plotted on a logarithmic scale in Figure 36 as a function of the longshore distance for the Long Beach Peninsula. Data from the Clatsop Plains show similar patterns. This diagram shows that nearly all hydraulic ratios decrease northward along the Long Beach Peninsula until about 20-25 km, where a discontinuity occurs and the trends vary depending on different mineral pairs. This pattern indicates that within 20-25 km of the Columbia River, the abundance of the denser (numerator) minerals decrease relative to the lighter (denominator) minerals in each pair. Since settling sorting has been eliminated by obtaining these data from a settling-equivalent condition, selective entrainment and differential transport processes must be responsible for this lag of the heavier minerals. For the northern half of the Long Beach Peninsula, hydraulic ratios of most mineral pairs do not show any significant pattern of longshore variations, indicating that sorting due to selective entrainment and differential transport is not effective on this part of the beach. This agrees with the conclusion obtained previously. An exception to this pattern is the hydraulic ratios for mineral pairs opaques/hornblende, hypersthene/hornblende and augite/hornblende, all of which show systematic increases with longshore distance (Figure 36). This trend of increasing hydraulic ratios implies that the abundances of opaques, hypersthene and augite, relative to that of hornblende, increase with longshore distance along this half of the Long Beach Peninsula. This is not surprising, as it agrees with the longshore variation pattern of heavy minerals presented in Figure 24. As described

Figure 36

Hydraulic ratios (HR) of various mineral pairs on a logarithmic scale plotted against the longshore distance from the Columbia River mouth on Long Beach Peninsula. Linear regression line and slope m are also given for each mineral pair.
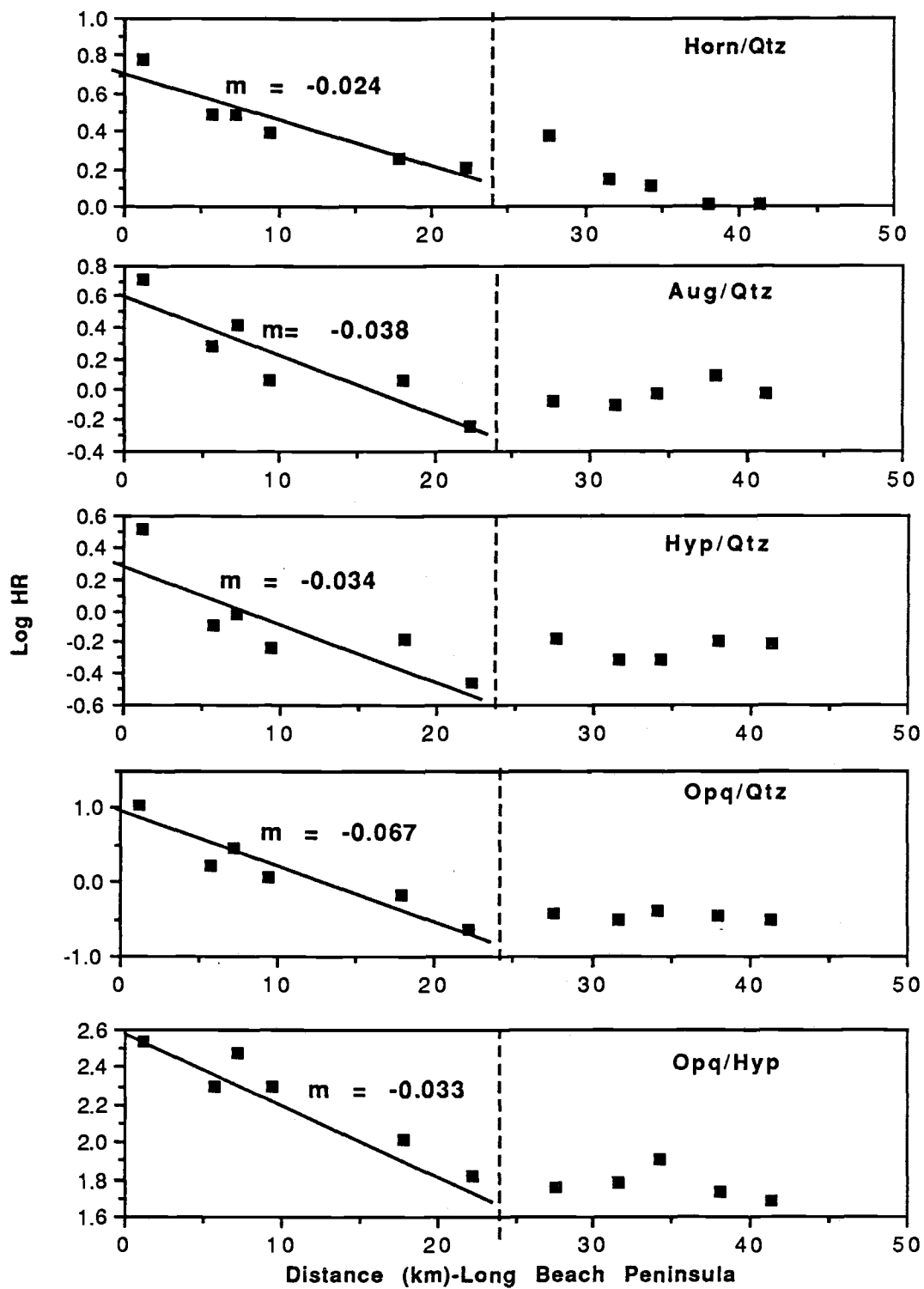
Figure 36
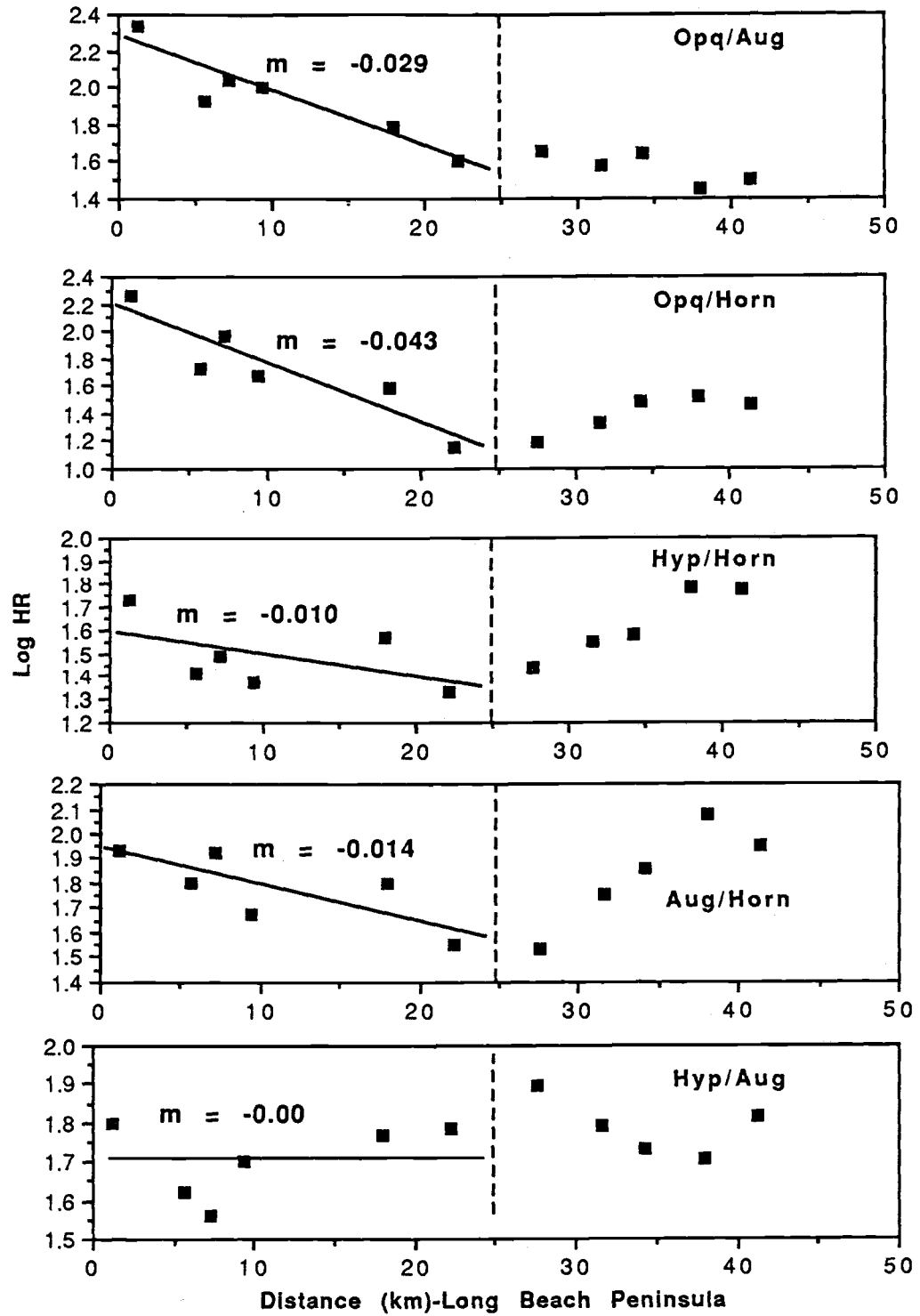
Figure 36 (continued)

in Chapter 6, the explanation for this trend is that after a small amount of heavy minerals has arrived at the north end of the Long Beach Peninsula during the northward transport under winter storms, beach erosion at the Leadbetter Point has caused the initial concentration of heavy minerals in this area. The southward summer longshore currents will then selectively entrain and transport the lighter and coarser-grained hornblende back toward the river mouth, while other finer-grained heavy minerals are left behind so as to become relatively concentrated with respect to hornblende. However, since the trend presented in Figure 36 is obtained under settling-equivalent conditions, it can now be stated that selective entrainment and differential transport are again the mechanisms for this reversed trend.

Linear regressions have been fitted to the longshore variations of log hydraulic ratios of the various mineral pairs. The regression lines and their slopes m are shown in Figure 36. The slope of each best-fit line represents the rate of decrease in hydraulic ratio with distance from the Columbia River mouth — therefore, it can be taken as a transportability coefficient, representing the transport disadvantage of the denser mineral versus the lighter one in the pair (Plopper, 1978; Trask and Hand, 1985). A larger m value indicates that the denser mineral is transported more slowly than the paired lighter mineral. Referring to Figure 36, there appears to be a relationship between the slopes of the regression lines and the density differences of the paired minerals. This shows that greater density differences correspond to larger differences in mineral longshore transportability. This relationship is better evaluated by plotting the transportability coefficients m against their corresponding density ratios in Figure 37. It is seen that the transportability coefficient is inversely
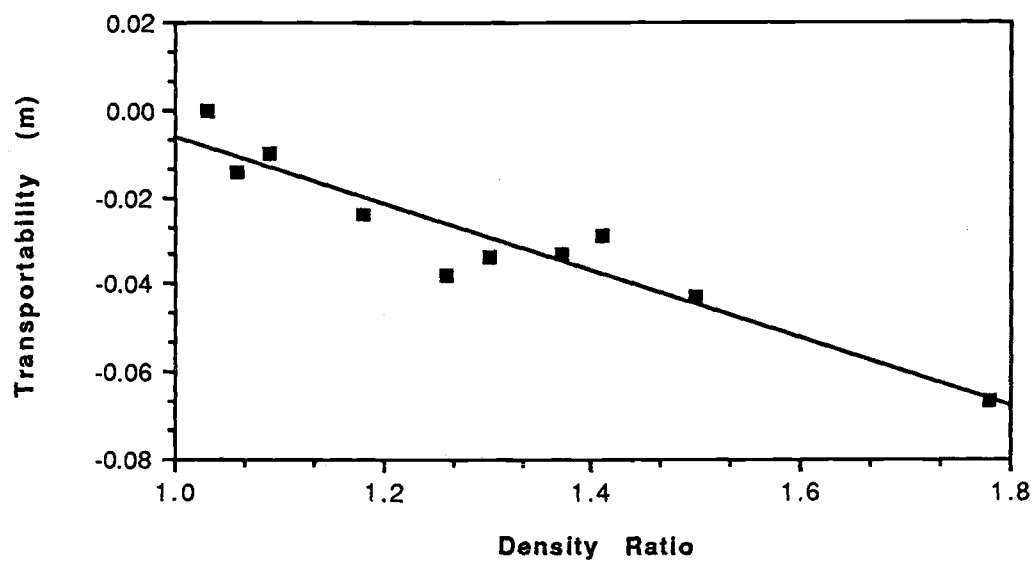
Figure 37
Transportability coefficient m plotted as a function of
density ratios of various mineral pairs for the Long Beach Peninsula
samples, indicating that minerals of higher densities are
transported alongshore at slower rates.

correlated with the density ratio. The best-fit line from linear regression is:

$$m = 0.071 - 0.077X_1 \qquad (R^2 = 0.89) \qquad (16)$$

where X_1 is the density ratio of the mineral pairs. This relationship predicts that as the density ratio between two minerals increases, their transportability coefficient decreases, so that the concentration of the heavier mineral relative to that of the lighter mineral decreases more rapidly with longshore distance, a stronger lag during longshore transport. Similar relationships have been obtained by Plopper (1978) and Trask and Hand (1985).

The efficiency of selective sorting of a mineral is not solely controlled by its density. Its grain size also plays an important role. Referring to Figure 20 and Table 10, it is seen that mineral grain size is inversely correlated with its density in the placer deposits as well as in the original sediment mixture. It has been noted earlier that higher densities and finer grain sizes of heavy minerals are the basic factors controlling selective grain sorting and placer formation in the study area. This grain size effect is better presented in Figure 38, where the mineral transportability coefficient m is plotted as a function of its grain size ratio X_2, which is defined as the D_b of the heavier mineral divided by D_b of the lighter mineral (see Table 10). Figure 38 shows that a mineral's transportability increases systematically with its grain size ratio X_2, and the function is best described by a linear regression line:

$$m = -0.264 + 0.256 \, X_2 \qquad (R^2 = 0.62) \qquad (17)$$

This relationship indicates that the smaller the relative grain size of a heavy mineral, the smaller (more negative) its transportability versus
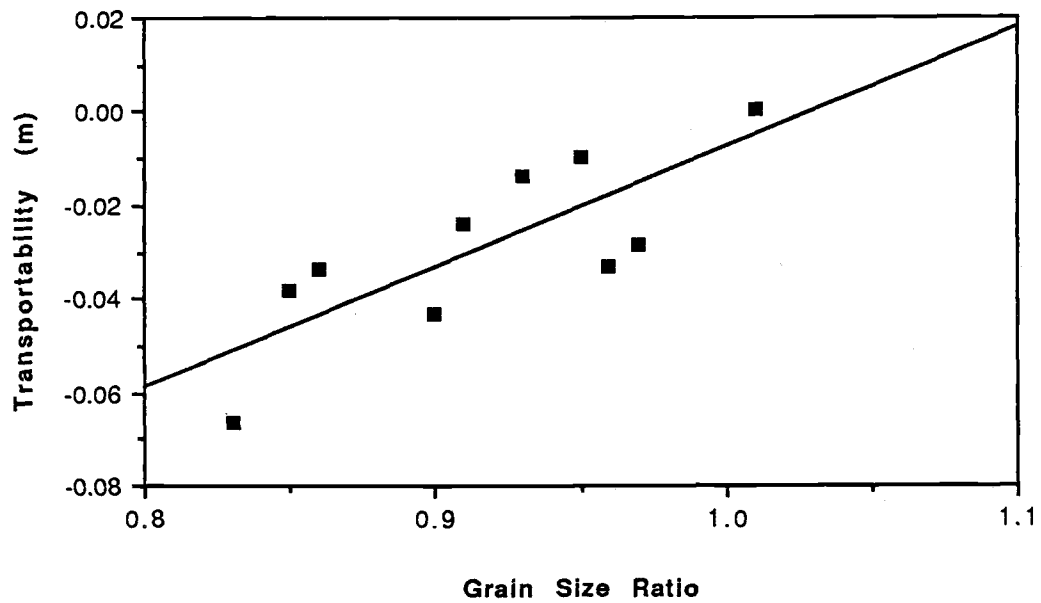
Figure 38
Transportability coefficient m plotted as a function of grain size ratios of various mineral pairs for the Long Beach Peninsula samples. Minerals of finer grain sizes in the original sediment source are shown to have slower alongshore transport rates.

that of the lighter mineral. Therefore, the heavy mineral is more effectively concentrated in the placer deposits while the light mineral is transported farther away from the Columbia River mouth. It can be concluded that mineral density and grain size are primary factors controlling the selective sorting processes.

7.4.5 Flume Experiments on Selective Entrainment

The selective entrainment model employed in this study, equations 12a and 12b, is based on the threshold data for uniform grains (Miller et al., 1977). These data were empirically fitted to equation 10 by Komar and Wang (1984), and the resulting model was then used in their placer study. However, the model has not been tested with data for selective entrainment of sediments from a bed of mixed grain sizes. Textural and mineralogical analyses, and entrainment stress calculations in previous chapters, have already suggested that dominant sorting processes may vary with longshore distance away from the Columbia River mouth, and this variation is most likely caused by changes in flow conditions and heavy mineral abundance in the beach sands. The purposes of the flume experiments presented here are first to simply test the validity of the selective entrainment model under mixed grain-size conditions, and secondly to investigate how flow stresses and heavy-mineral contents may control the efficiency of selective sorting processes. A schematic diagram of the apparatus used in these experiments is shown in Figure 39. The flume consists of a pump, flexible hoses, head tank, fiber-glass channel and a settling tank. The water channel itself is 230 cm long, 10 cm wide and about 50 cm high.

The first set of experiments was to measure threshold stresses for
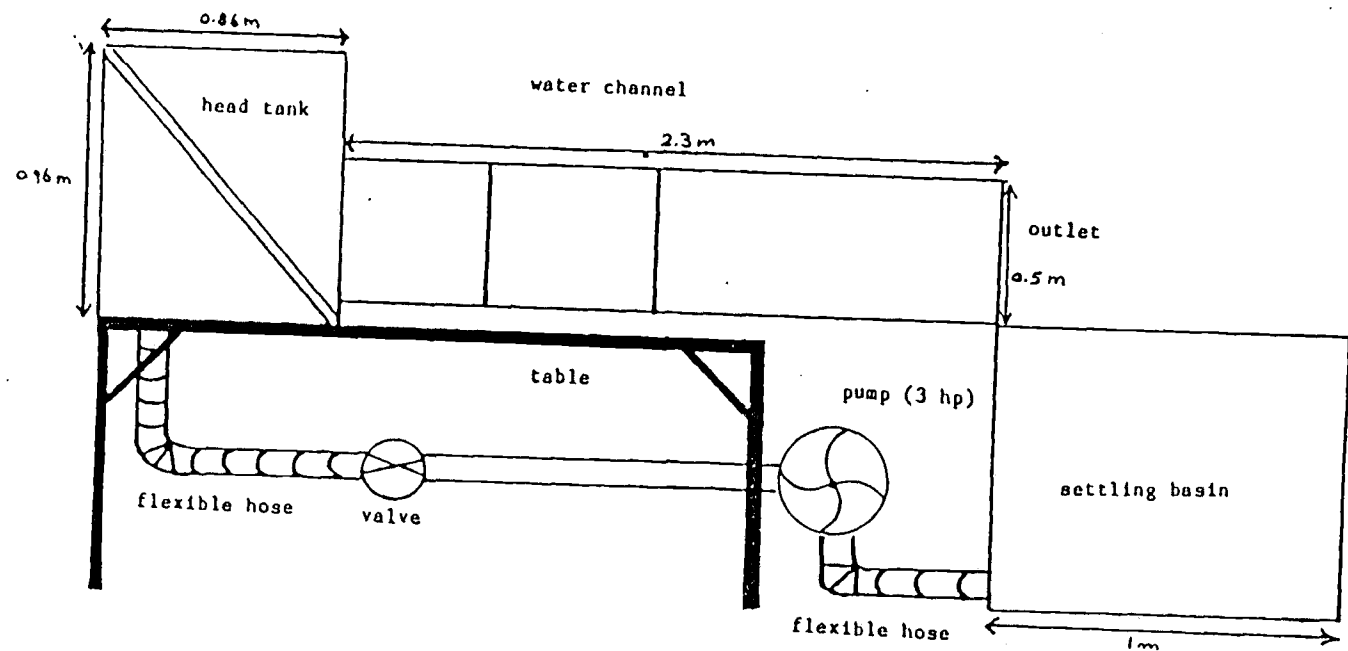
Figure 39   Schematic diagram showing the flume facility used in the
present study.

variable relative grain size D_b/K, so that the selective entrainment model represented by equations 12a and 12b can be tested. A uniform layer of quartz sand with a mean intermediate axial diameter of 0.239 mm (the K value) was glued to the surface of a hard-wood board, which was then placed on the bottom of the flume at a fixed slope of 0.0007. Quartz grains of intermediate diameter D_b were spread as a thin layer on this fixed-grain bed. The flume was run under a range of discharges for each D_b/K. Mean flow depth h and water surface slope S_e measured using a point gauge were used to calculate the flow stress from $\tau_o = \rho g R S_e$, in which g is the gravity acceleration and R is the hydraulic radius defined as the ratio of the cross-sectional area to the wetted perimeter. The bedload transport rates q_B (in milligrams/minute/cm) were measured for these runs and were plotted against the flow stresses to obtain the threshold stress τ_t at an extrapolated zero transport rate. The selective entrainment model was examined by using grains of different D_b diameters, one at a time, to yield a range of D_b/K ratios.

The mean flow depth h, water surface slope S_e, flow stress τ_o and bead load transport rate q_B are listed for variable relative grain size D_b/K in Table 11. The flow stresses are plotted in Figure 40 versus their corresponding bedload transport rates for various D_b/K values. Excellent correlations have been found between stresses and transport rates for each D_b/K value, and they all confirm that higher flow stresses cause higher bedload transport rates. Linear regression has yielded the best-fit relationship for each D_b/K ratio, and the threshold entrainment stress was

Table 11 The mean flow depth h (cm), water surface slope S_e, flow stress τ_0 (dynes/cm^2) and bedload transport rate q_B (milligram/min./cm) for variable relative grain size D_b/K in part I of the flume experiments.

D_b/K	Depth h	Slope S_e	Flow Stress τ_0	Bedload Transp. Rate, q_B
0.59	1.463	0.00229	2.54	11.50
	1.540	0.00244	2.82	24.80
	1.615	0.00244	2.93	35.21
	1.753	0.00260	3.31	53.74
0.71	1.311	0.00213	2.16	5.50
	1.494	0.00229	2.57	38.71
	1.539	0.00244	2.81	47.86
	1.676	0.00244	3.00	61.15
0.84	1.250	0.00213	2.08	7.60
	1.311	0.00229	2.33	22.00
	1.356	0.00244	2.54	37.67
	1.417	0.00259	2.79	45.50
1.00	1.219	0.00183	2.02	9.40
	1.265	0.00213	2.11	15.17
	1.250	0.00244	2.39	33.29
	1.433	0.00244	2.66	45.10
1.19	1.189	0.00198	1.86	4.30
	1.250	0.00213	2.08	21.00
	1.356	0.00229	2.40	37.50
	1.433	0.00244	2.66	55.00
1.41	1.280	0.00213	2.13	14.00
	1.387	0.00213	2.27	21.83
	1.433	0.00213	2.33	26.16
	1.615	0.00244	2.92	48.14

Figure 40

Flow stresses (dynes/cm^2) versus the bedload transport rates (milligrams/minute/cm) for various D_b/K values. Linear regression equations are included in each diagram and are used to calculate the threshold stress τ_t at a zero transport rate.
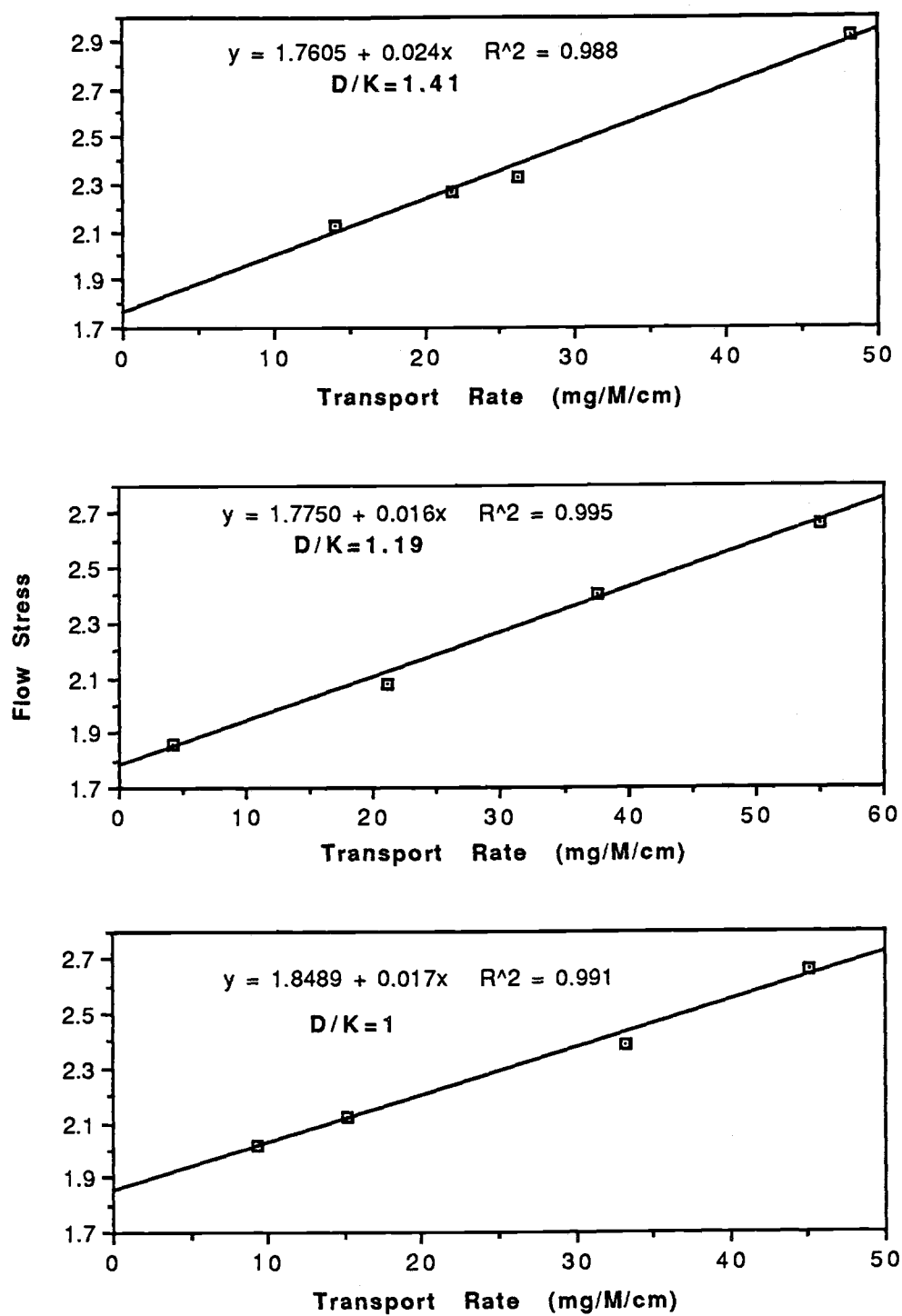
Figure 40
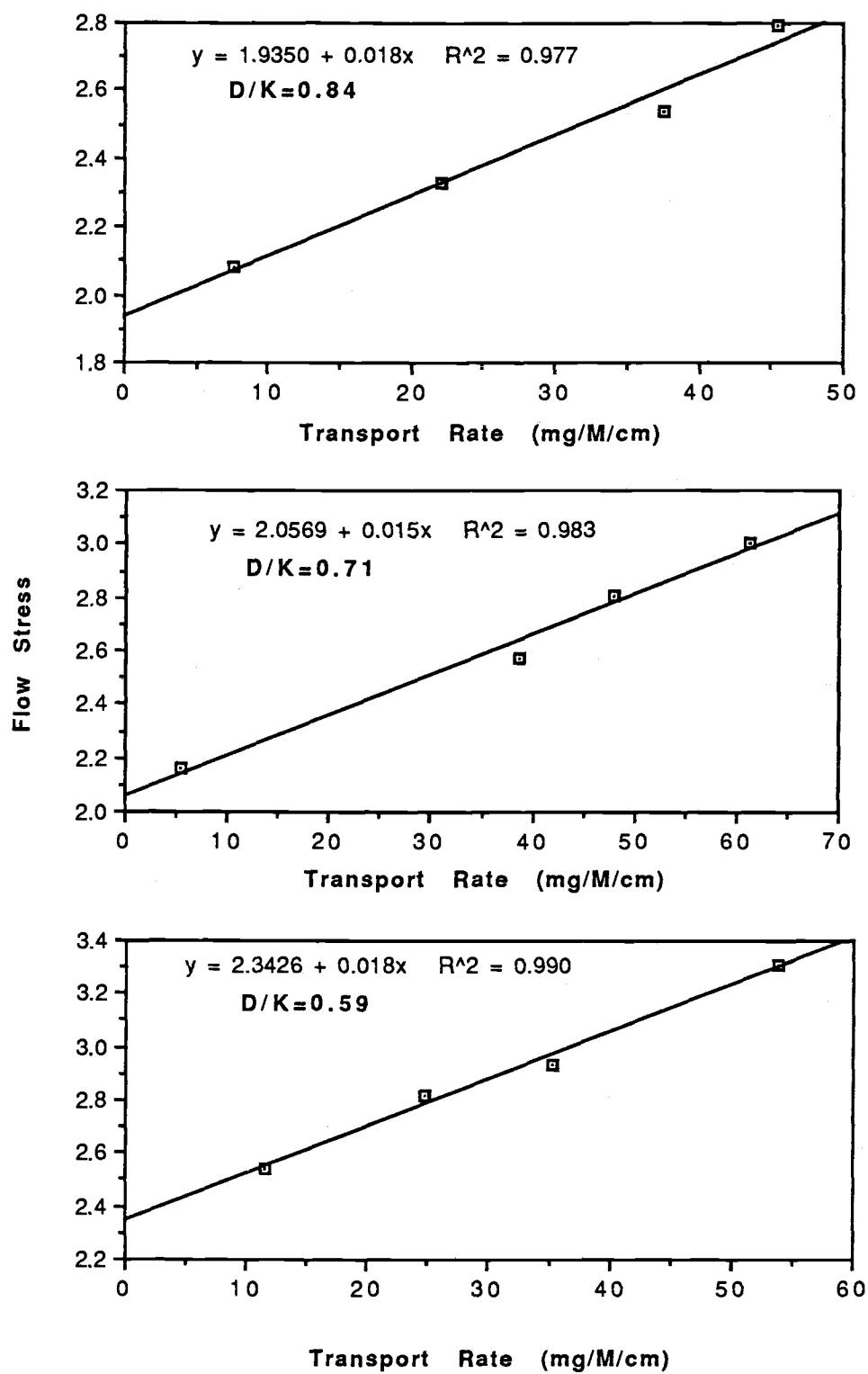
Figure 40 (continued)

then obtained by extrapolating the relationship to a zero transport rate. These selective entrainment stresses are listed in Table 12, together with the relative grain sizes D_b/K and the selective entrainment stresses predicted by equations 12a and 12b. These measured selective entrainment stresses are plotted in Figure 41 as a function of the relative grain size D_b/K, and stresses predicted by the model (equation 12) are also included for comparison. As predicted by the general pivoting model,

Table 12   Measured selective entrainment stress (τ_t, measured) and entrainment stress predicted by equation 12 (τ_t, predicted) for vaiable relative grain size D_b/K.

D_b/K	τ_t measured	τ_t predicted
0.59	2.34	2.30
0.71	2.06	2.05
0.84	1.94	1.93
1.00	1.85	1.84
1.19	1.78	1.80
1.41	1.76	1.77

Figure 41 shows that the entrainment stresses for $D_b/K < 1$ are much higher than the threshold stress for grains at $D_b/K = 1$. The selective entrainment stresses decrease as the relative grain size increases, due both to the decreasing pivoting angles and higher grain protrusions into the flow (Figure 26). Figure 41 also shows that at large D_b/K values, the effect of relative grain size becomes less important and the entrainment

Figure 41

Measured selective entrainment stresses plotted as a function

of relative grain size D_b/K. It shows that an increase in D_b/K

causes a progressive decrease in selective entrainment stress.

Selective entrainment stresses predicted by the model (equation

12) are also plotted for comparison.
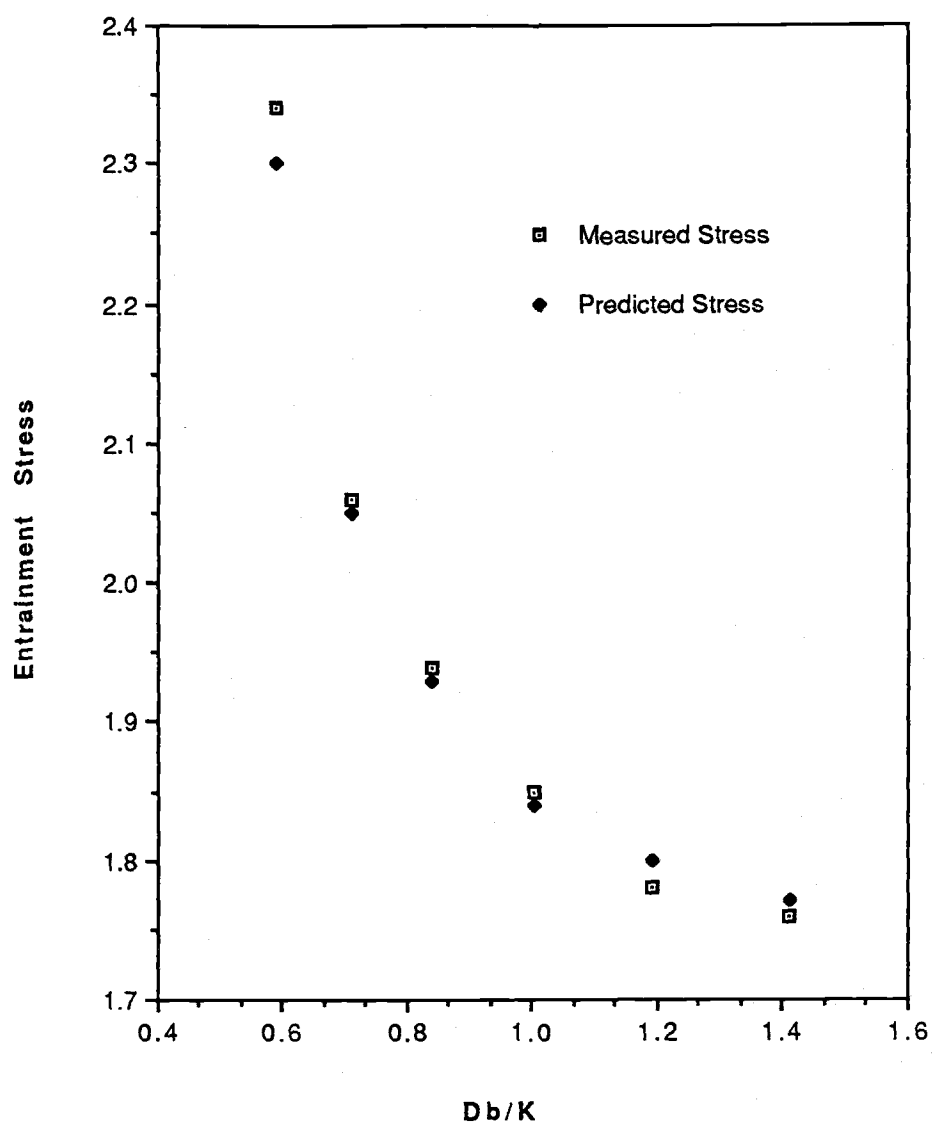
Figure 41

stress approaches a constant value. This agrees with the selective entrainment model which actually predicts that at still larger D_b/K ratios, the threshold stress may increase with the relative grain size. Nevertheless, the flume experiments have shown that the selective entrainment model is generally correct.

Close examination of Figure 41 indicates that for $D_b/K < 1$, the measured threshold stresses are slightly above the model-predicted values, and for $D_b/K > 1$ the opposite situation occurs. This difference can be better seen in Figure 42 where measured selective entrainment stresses are plotted against the predicted stresses from equation (12). This clearly shows that the selective entrainment model may under-predict the threshold stresses when $D_b/K < 1$, and systematically over-predict them when $D_b/K > 1$. A reasonable explanation would be that the model has only incorporated the pivoting angle factor, and does not include the effects of grain exposure (protrusion) which is another important factor in selective entrainment process (Fenton and Abbott, 1977). For $D_b/K < 1$, the pivoting grain is significantly sheltered by the larger bottom particles and is less exposed to the flow. Therefore, the inclusion of grain protrusion would increase the predicted τ_t values. In contrast, the pivoting grain will protrude higher into the flow when $D_b/K > 1$ and this would further lower the τ_t predicted by the current model. In order to improve the model, the measured selective entrainment stresses have been used in an iterative calculation to find the best-fit exponential coefficient in equation 12b which controls the effect of relative grain size D_b/K. It is found that when this coefficient is increased from 0.3 to
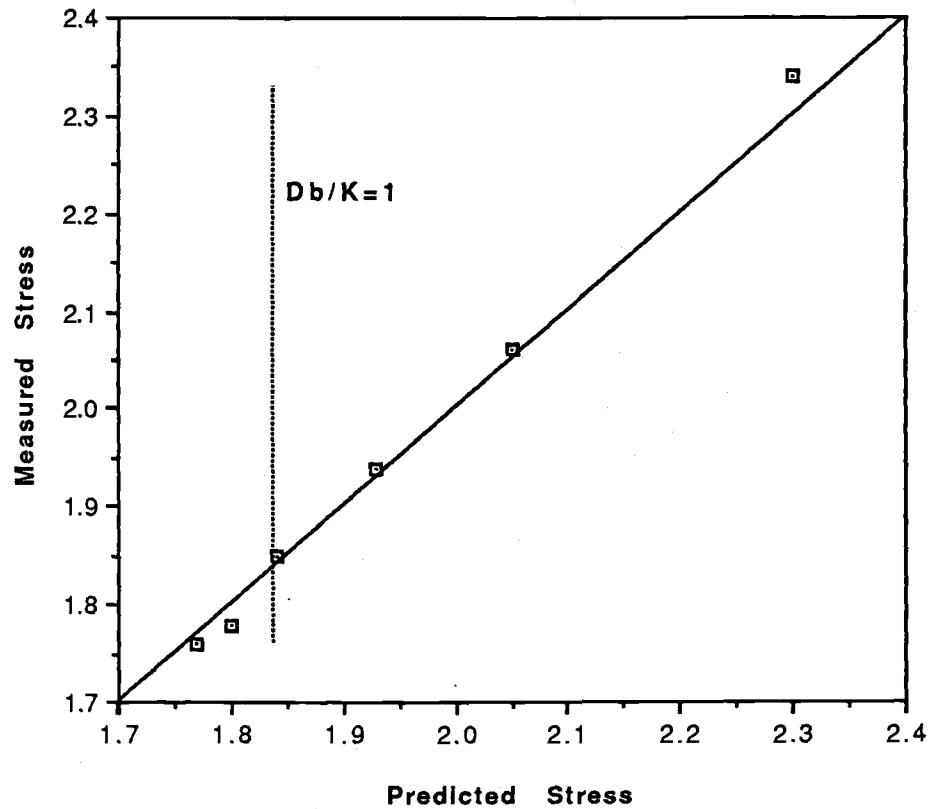
Figure 42
Correlation between measured and model-predicted selective
entrainment stresses for variable relative grain sizes D_b/K. It is
seen that the model under-predicts the threshold stress for $D_b/K <1$
and over-predicts it for $D_b/K >1$.

0.313, the improved model will decrease the standard deviation of the predicted τ_t from 0.0219 to a minimum of 0.0118.

The second series of flume experiments involved various flow stresses with sands having different heavy mineral concentrations, so that their effects on selective grain sorting and placer development could be evaluated. A mixture of 2% heavy minerals and 98% quartz (including feldspars) was first created. The heavy minerals included 20% opaques (density 4.8 g/cm^3) and 80% other heavy minerals (average density 3.4 g/cm^3). The median grain size of the quartz sands was 0.232 mm, and according to equation (9), median diameters of 0.195 and 0.155 mm have been used respectively for the non-opaque heavy minerals and the opaques so that the mixture is settling equivalent. This selection of sediment sizes, therefore, eliminates the possibility for sorting due to differential grain settling. Another mixture of 10% heavy minerals and 90% quartz was made with the same settling-equivalent median diameters. The overall median grain size for the 2%-mixture is 0.173 mm (2.53ϕ), and 0.172 mm (2.54ϕ) for the 10%-mixture. Three runs were undertaken with each sediment mixture. The flow stresses were 3.21, 3.80 and 6.89 dynes/cm^2 for the three runs using the 2%-mixture, while the three runs with the 10%-mixture were at flow stresses of 3.27, 6.50 and 8.15 dynes/cm^2. About 380 grams of mixture sands were evenly spread on the bottom of the upstream portion of the flume, and were eroded and transported down-flume during each run which usually lasted for 5-10 minutes. After each run, samples were collected at 5, 35, 70 and 105 cm down-flume from the source, as well as from the sediment trap at the end of the flume. Ripples developed during almost every run, and heavy minerals were observed to be concentrated on the stoss-sides of the ripples, mostly

close to the crest lines. Therefore, samples were taken across the whole length of a ripple to eliminate this small-scale local sorting. Sieving and heavy mineral separation analyses were then carried out on these samples.

The median grain sizes and heavy mineral concentrations of along-flume samples are listed in Tables 13 and 14 for the 2%- and 10%-heavy mixtures, respectively. The median grain sizes and weight percentages of the heavy minerals in each sample are shown respectively as functions of the transport distance in Figures 43 and 44. These figures show that the sands are generally finer and contain more heavy minerals at the upstream end of the flume. As the transport distance increases (down-flume), sands become progressively coarser and the heavy mineral concentrations systematically decrease. These trends prove that under settling-equivalent conditions, selective entrainment and transport sorting processes have preferentially moved the coarser-grained quartz down-flume, while the finer-grained heavy minerals have been concentrated at the upstream portion of the flume. The degree of selective grain sorting and mineral separation, however, also depends on the magnitude of the flow stress. For low to medium flow stresses (top and middle diagrams in Figures 43 and 44), sands at the upstream end of the flume are generally finer and more concentrated in heavy minerals than for high flow stress conditions (bottom diagrams in Figures 43 and 44). For example, the median grain sizes at the upstream end of the flume in Figure 44a increase from 0.176 mm (2.51ϕ) and 0.170 mm (2.56ϕ) to 0.178 mm (2.49ϕ) as the flow stress increases from 3.21 and 3.8 dynes/cm^2 to 6.89 dynes/cm^2, while heavy mineral percentages decrease from 4.25% and 5.18% to only 2.73% (Figure 44a). This dependence on flow stress is further examined in Figure 45, where the regression slopes in

Table 13   Median grain sizes and heavy mineral concentrations of along-flume samples for the 2%-heavy mixture under variable flow stress τ_o (dynes/cm^2).

Flow Stress τ_o	Down-flume Distance, cm	Median ϕ	Heavy Mineral %
3.21	5	2.51	4.25
	35	2.48	3.59
	70	2.50	4.09
	105	2.48	3.10
	140	2.47	
3.80	5	2.56	5.18
	35	2.54	5.03
	70	2.51	4.34
	105	2.51	3.12
	140	2.47	
6.89	5	2.49	2.73
	35	2.50	2.83
	70	2.48	3.00
	105	2.48	2.73
	140	2.49	

Table 14 Median grain sizes and heavy mineral concentrations of along-flume samples for the 10%-heavy mixture under variable flow stress τ_o (dynes/cm^2).

Flow Stress τ_o	Down-flume Distance, cm	Median ϕ	Heavy Mineral %
3.27	5	2.53	13.10
	35	2.55	15.05
	70	2.51	11.30
	105	2.49	10.57
	140	2.42	
6.50	5	2.59	14.40
	35	2.52	17.41
	70	2.49	12.37
	105	2.50	11.13
	140	2.47	
6.89	5	2.53	11.63
	35	2.55	14.00
	70	2.49	12.28
	105	2.49	12.43
	140	2.46	

Figure 43

Median grain size (Md, in ϕ) versus downflume transport distance (cm) for the 2%-heavy mixture (a) and the 10%-heavy mixture (b). Flow stresses and linear regression relationships are included in each diagram.
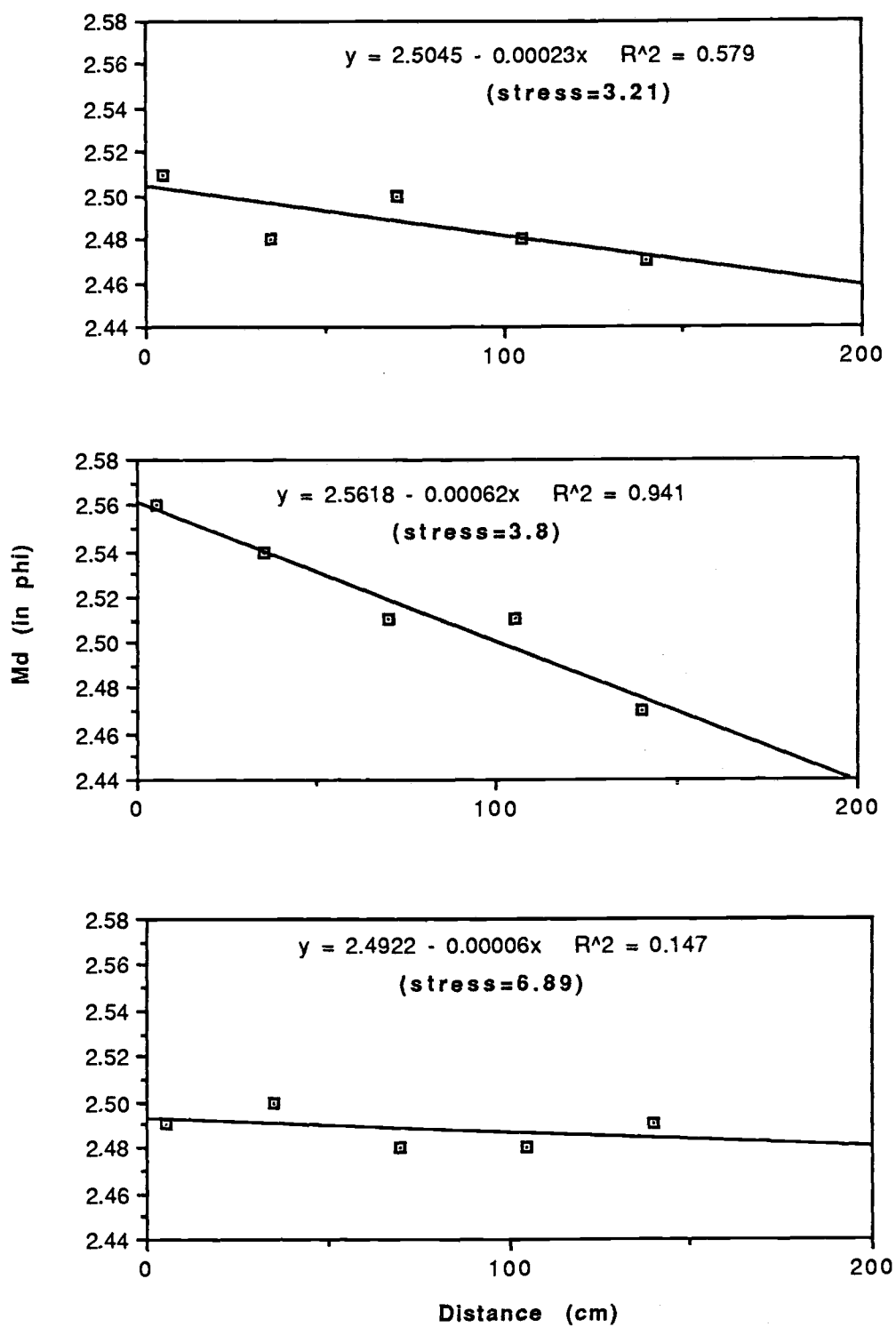
Figure 43a
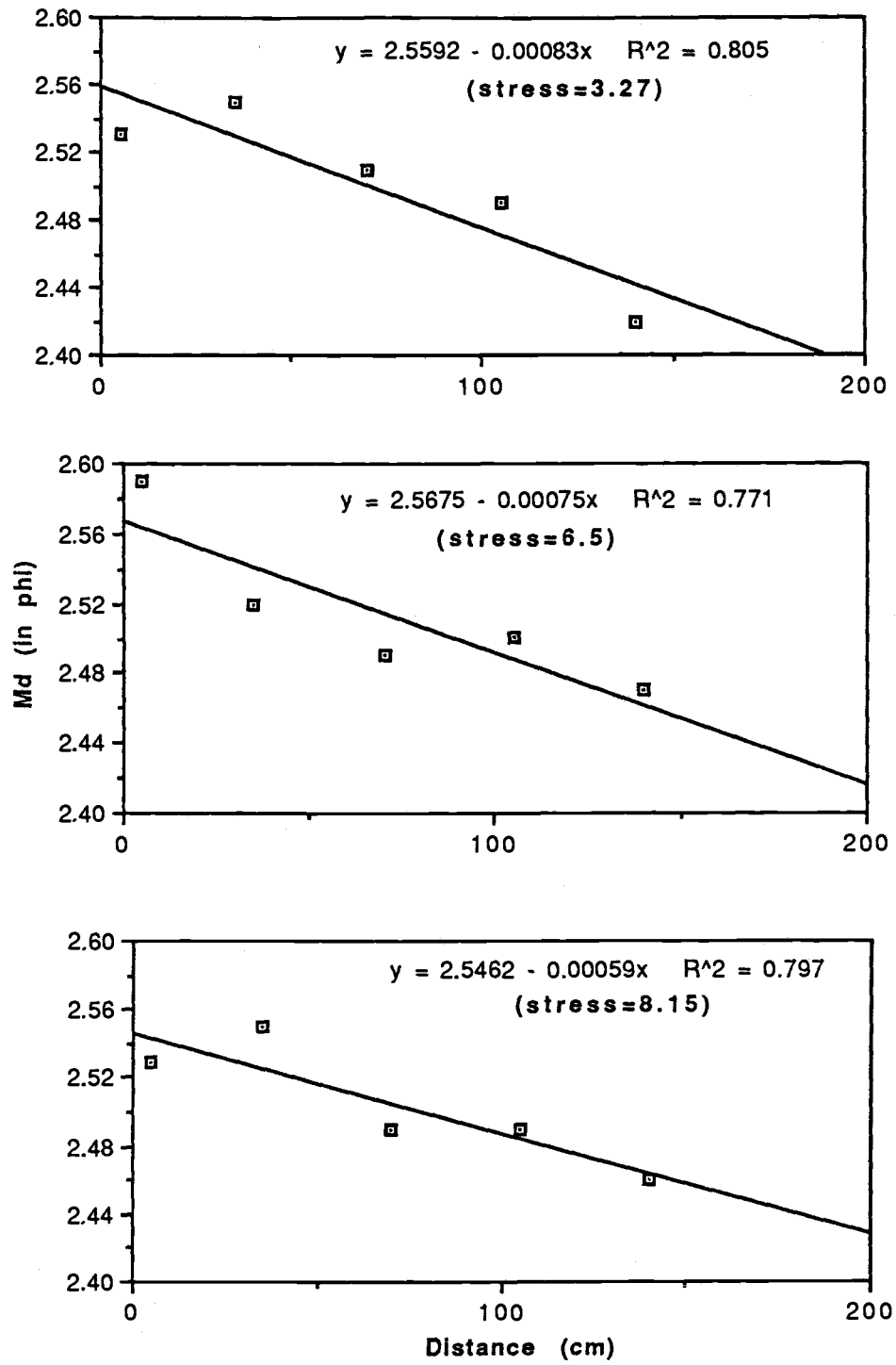
Figure 43b

Figure 44

Heavy mineral weight percentage (%) plotted against the
down-flume transport distance (cm) under various flow stresses,
(a) for the 2%-heavy mixture and (b) for the 10%-heavy mixture.
Linear regression equations are given in each diagram.

Figure 44a

181
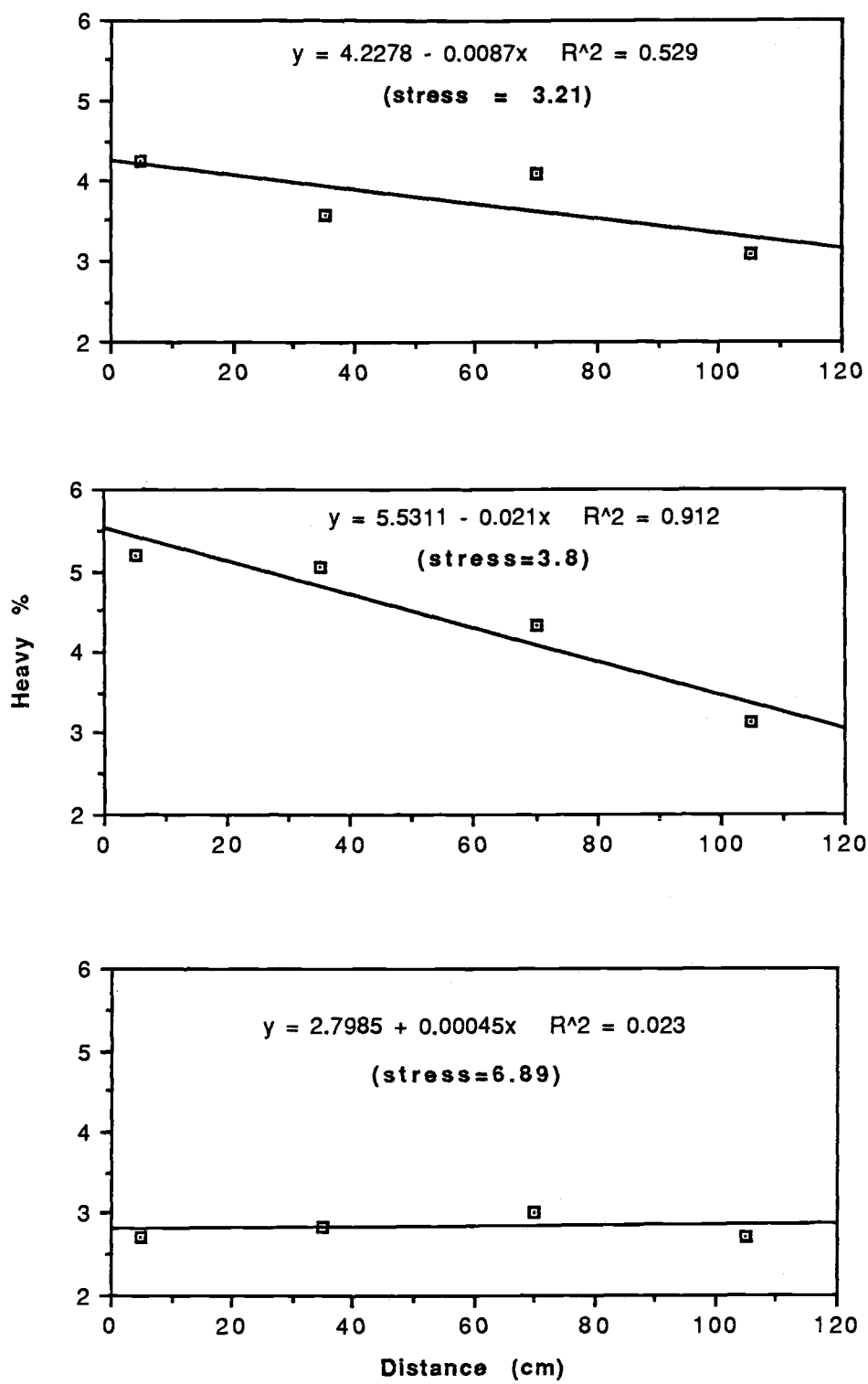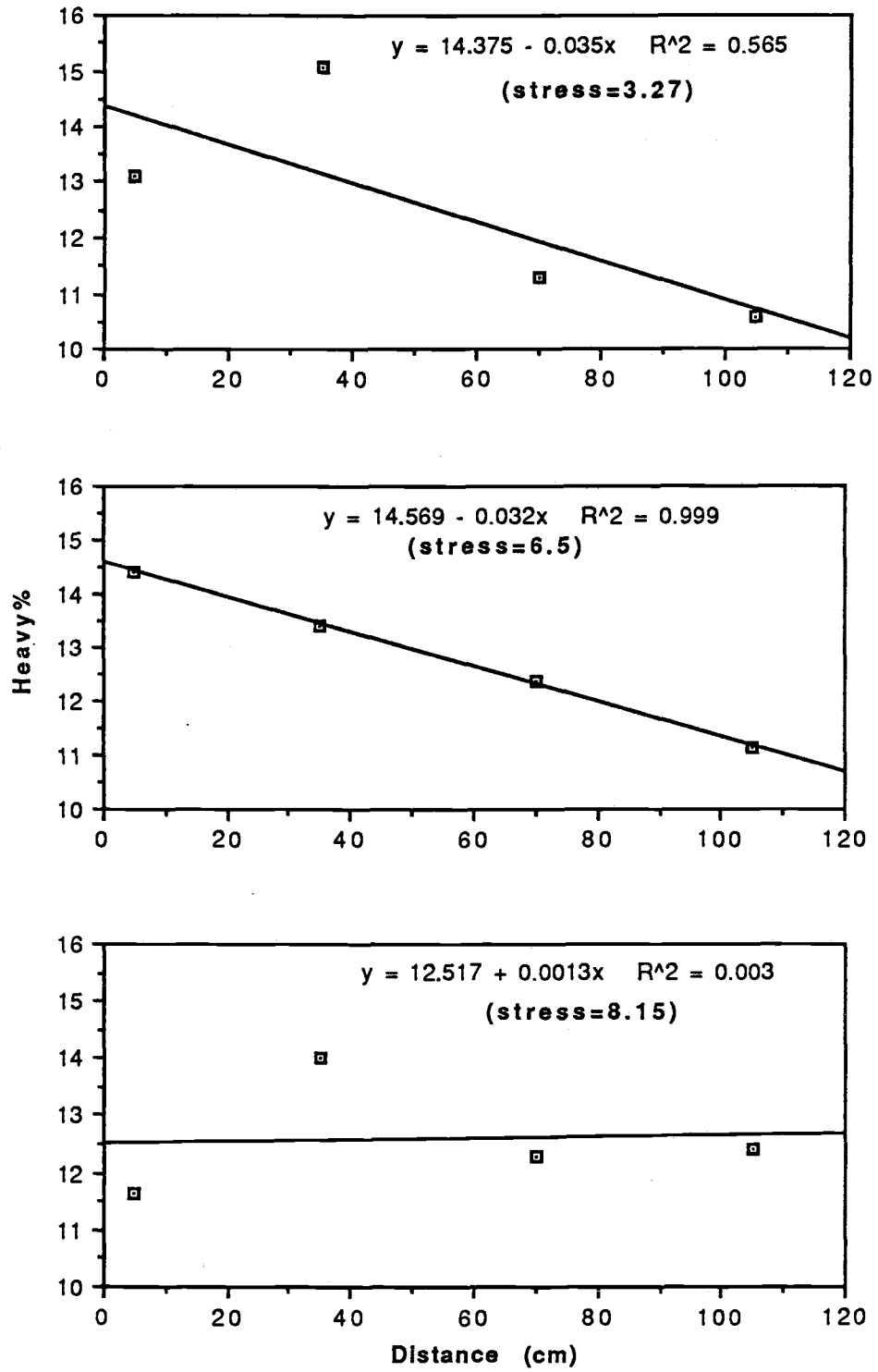
Figure 44b

Figures 43 and 44, defined here as a size-sorting coefficient and a heavy-mineral concentration coefficient, are plotted as a function of the flow stress, (a) for the 2% mixture and (b) for the 10% mixture. Although there are only three data pairs, they roughly show that selective grain sorting is more effective at low to medium flow stresses than at high flow stresses. The reason for this dependence on flow stress is that the low to medium flow stresses are probably sufficiently strong to transport the coarser-grained quartz, but are less or only marginally higher than the threshold stresses of the heavy minerals, and thus cannot cause their significant transport. At high flow stresses, strong flows have exceeded the threshold stresses for all minerals, so they are transported at roughly equal rates and selective grain sorting efficiency correspondingly decreases.

Another objective of these flume experiments is to understand how heavy mineral concentration in the sediment may affect selective grain sorting efficiency. The variations in median grain sizes and heavy-mineral percentages with transport distance are compared in Figure 46 for the 2% and 10% mixtures. Figure 46a shows that under roughly equal flow stresses, the residual sands at the upstream end of the flume are not only much finer for the 10% mixture, but the median grain sizes also increase with down-flume distance at faster rates than with the 2% mixture. As shown in Figure 46b, the heavy mineral percentages in the residual sands are apparently higher for the 10% mixture than for the 2% mixture due to the higher abundance in the original source. Under similar flow stresses, heavy mineral abundances also decrease much faster with transport distance in the case of the 10% mixure, the slopes being 0.035 versus 0.0087 for low flow stresses, and 0.032 versus virtually 0 for medium

Figure 45

Grain size sorting coefficient and heavy mineral concentration coefficient versus flow stresses for the 2% and 10% heavy mixtures. Selective grain sorting processes are generally more effective at low to medium flow stresses.
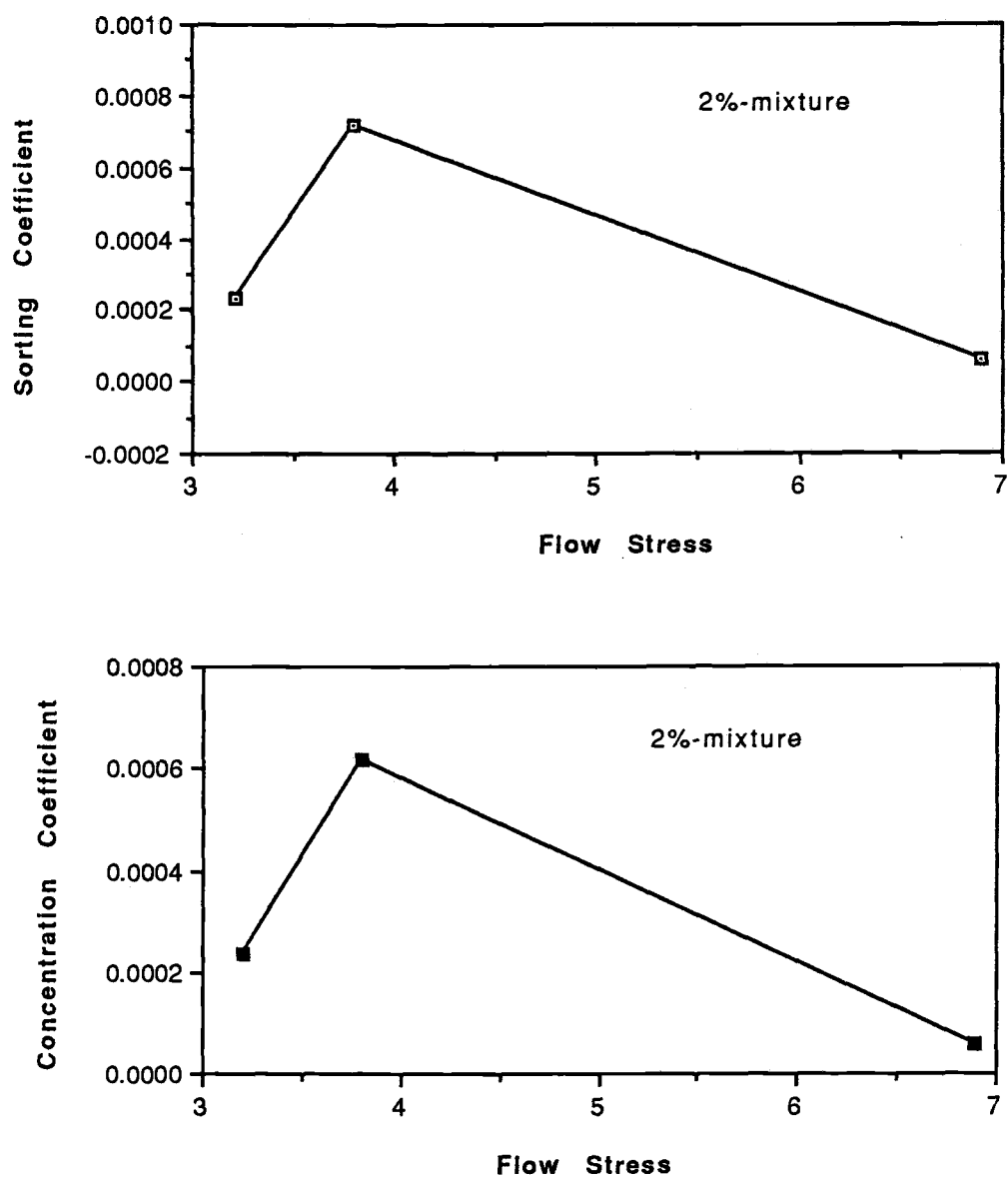
Figure 45
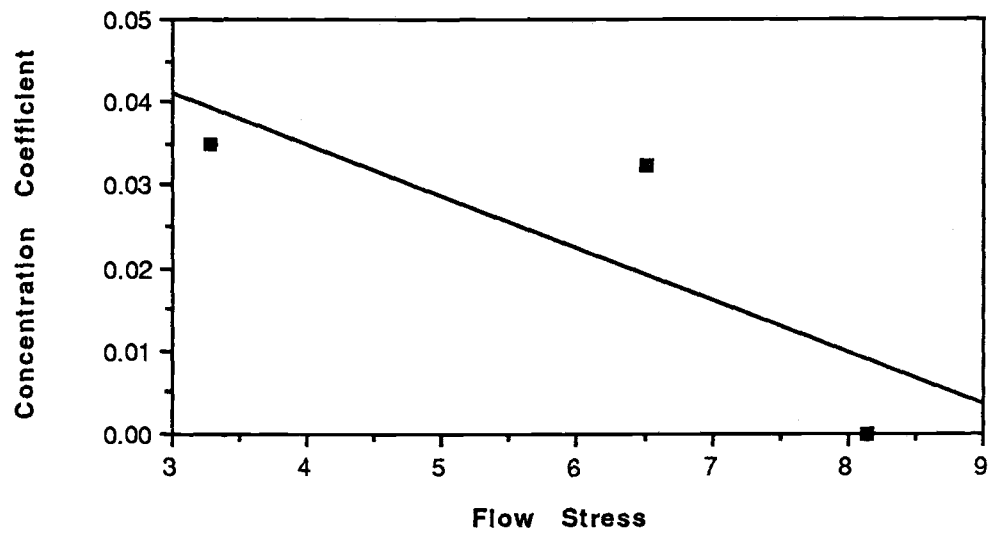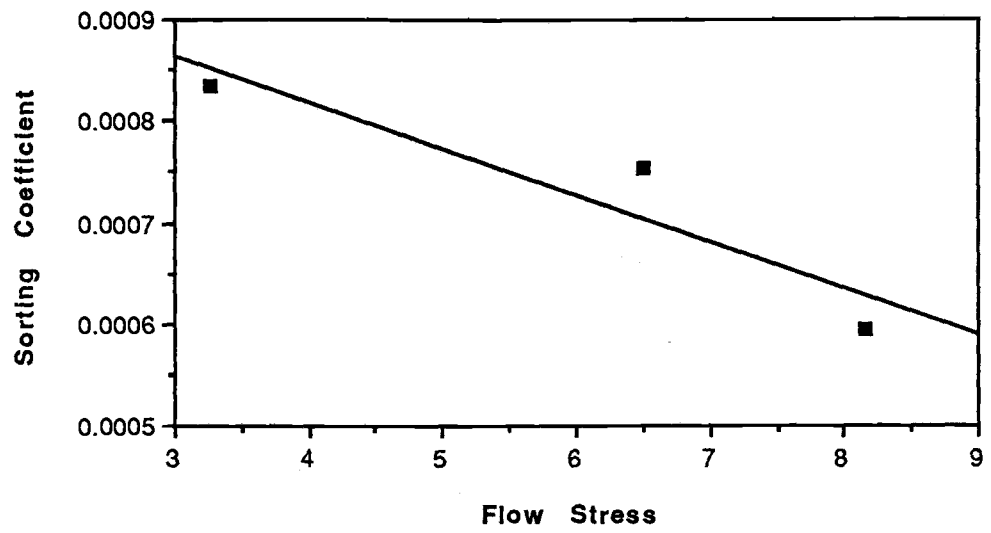
Figure 45 (continued)

Figure 46

The median grain size (a) and heavy mineral weight percentage
(b) versus the transport distance (cm), compared between the 2%-
and 10%-heavy mixtures under similar flow stresses. The
median grain sizes are in ϕ units. Squares represent the
2%-heavy mixture and the diamonds the 10%-heavy mixture.

$$y = 2.5592 - 0.00083x \quad R^2 = 0.805$$
(stress=3.27   10%H)

$$y = 2.5045 - 0.00023x \quad R^2 = 0.579$$
(stress=3.21   2%H)

$$y = 2.5675 - 0.00075x \quad R^2 = 0.771$$
(stress=6.5   10%H)

$$y = 2.4922 - 0.00006x \quad R^2 = 0.147$$
(stress=6.89   2%H)

Figure 46a

y = 14.375 - 0.035x   R^2 = 0.565
(stress=3.27   10%H)

y = 4.2278 - 0.0087x   R^2 = 0.529
(stress=3.21   2%H)

y = 14.569 - 0.032x   R^2 = 0.999
(stress=6.5   10%H)

y = 2.7985 + 0.00045x   R^2 = 0.023
(stress=6.89   2%H)
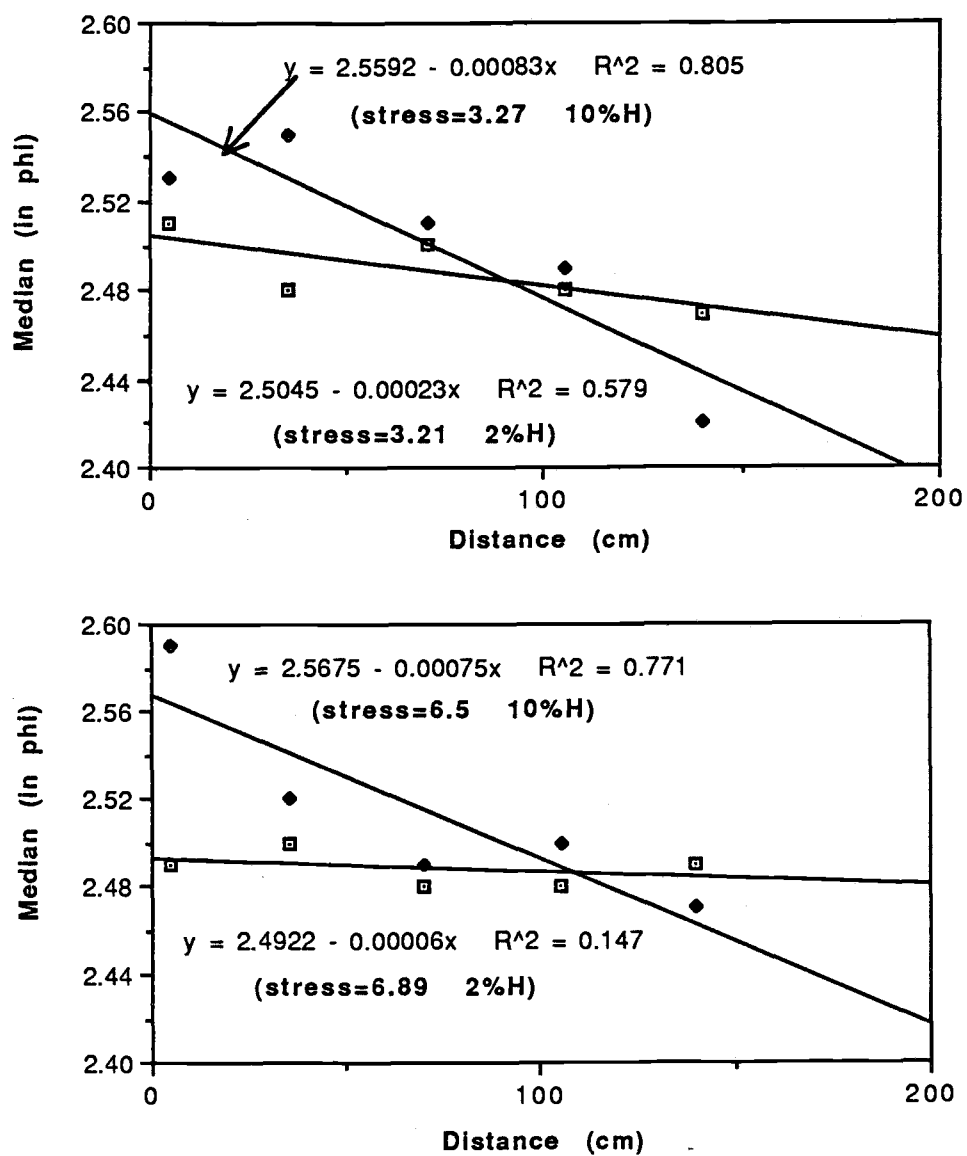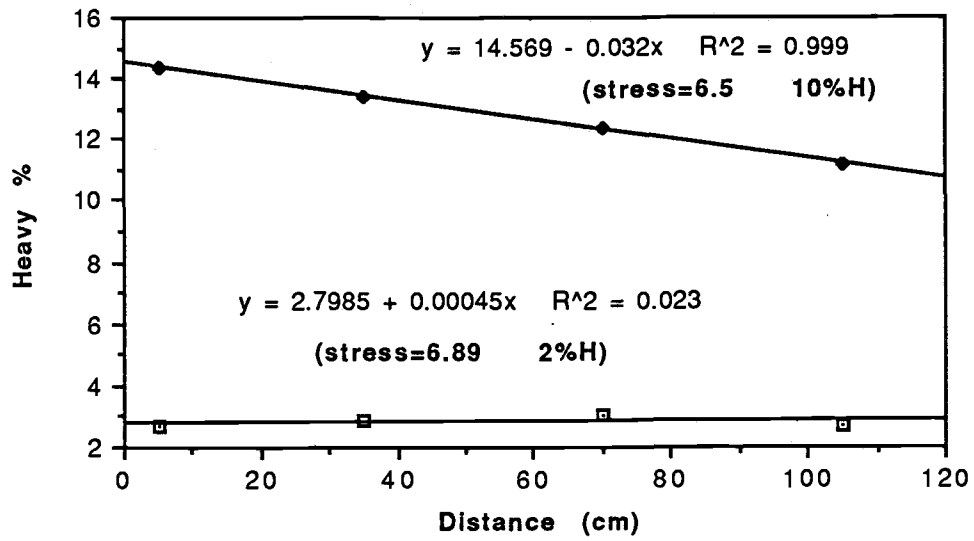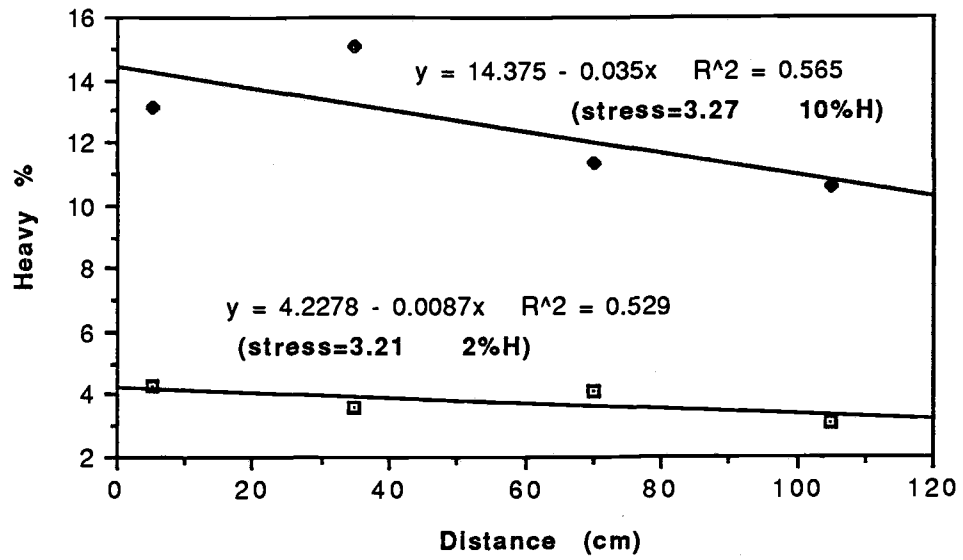
Figure 46b

flow stresses. This suggests that for a given flow stress, the selective grain sorting and heavy mineral separation processes are more effective for sands of higher heavy mineral concentrations. A probable explanation is that for heavy-mineral depleted sands, the mode is generally dominated by the sorting process in the light-mineral fraction in which the grain size range is usually small and effects of density sorting do not exist. Therefore, selective grain sorting is not significant and heavy minerals will not be highly concentrated. As heavy mineral percentages increase in the original source, the sorting mode in the heavy fraction becomes more important. The increased size range and density differences will cause stronger selective entrainment and transport, and thus higher heavy mineral concentrations may form in the residual sands.

Chapter 8

DISCUSSION AND SUMMARY OF CONCLUSIONS

8.1 Shoreline Evolution and Effects on Placer Formation

The formation of the Clatsop Plains and Long Beach Peninsula occurred primarily following the Holocene rise in sea level, that is, within the last few thousand years. Both land areas are formed of sediment derived from the Columbia River. Toward the end of the Holocene sea-level rise (about 3000 years B.P), the transgression reached 3 km farther inland from the present shoreline on the Clatsop Plains. As the outward flow of the Columbia River spread its bedload fanwise, pronounced shoaling and a northward-projecting spit developed in front of the eroded bluff. Sediments were continuously supplied by the Columbia River, and ridge after ridge accreted to form the Clatsop Plains. The history of the Long Beach Peninsula is slightly different than the Clatsop Plains. Because of the dominant northward transport of the Columbia River sediments, a more-sizeable beach initially existed offshore during the late stages of the Holocene transgression. As sea level rose, that beach migrated landward and formed a proto-spit extending northward from Cape Disappointment. Transport of sand from the Columbia River caused the progressive seaward progradation of the spit, a growth that continues today in spite of dam construction on the river and the placement of major jetties at the river mouth.

Construction of the jetties, initiated about a hundred years ago, produced rapid beach accretion adjacent to the river mouth, leading to the formation of Clatsop Spit and Peacock Beach, Figure 10. Those beaches are

the areas of maximum placer development in the study area. A period of intensive erosion has been found close to the jetty on the Clatsop Spit after the jetty extension (Kidby and Oliver, 1966). Similar erosion period may also have occured on Peacock Beach after the construction of the north jetty, though this has not been documented. Placer deposits are usually associated with beach erosions (Rao, 1957; Woolsey, 1975; Frihy and Komar, 1990), therefore these periods of beach erosion are at least partly responsible for the maximum placer developments in these areas. Exploratory drillings on Clatsop Spit and Peacock Beach have qualitatively shown that the placer is limited mainly to the modern beach, and that black sand concentrations decrease markedly landward. Based on the placer volume and annual heavy mineral supply from the Columbia River, the age of the placer deposit is estimated to be about 66 years, which roughly coincides with the completion of jetty construction in 1917. These analyses, therefore, indicate that jetty construction and the associated shoreline changes have played an important role in placer development in the study area.

8.2 Longshore Grain Sorting
and the Origin of Placer Deposits

Sediments discharged from the Columbia River are transported northward along the Long Beach Peninsula and southward on the Clatsop Plains. The analyses undertaken in this study show that there are generally systematic decreases in sediment grain sizes and total heavy mineral concentrations away from the river mouth (Figures 20 and 21). The northward longshore currents of the winter are generally stronger than the southward summer currents. Therefore, more sediment is

transported to the north to the Long Beach Peninsula than to the south and the Clatsop Plains. As a result, the placer deposits are better developed on the Long Beach Peninsula than along the Clatsop Plains. The systematic increase in mineral dissimilarity with longshore distance, and its asymmetry between north and south of the Columbia River mouth, further support this general longshore sediment transport pattern. The greater seaward extent of the south jetty compared with the north jetty has probably also reduced the southward transport of beach sediments to the Clatsop Plains. The combination of this jetty blockage and weaker southward summer longshore currents is probably responsible for the finer median grain sizes of beach sands on the Clatsop Plains compared with the sands of the Long Beach Peninsula.

Longshore grain sorting patterns and their effects on placer development are summarized in Figure 47, in which longshore variations of averaged median grain sizes of the heavy minerals, total heavy mineral concentrations and relative abundances of major heavy minerals on the Long Beach Peninsula are compared, and different zones are defined according to the dominant sorting processes. The median grain sizes of heavy minerals in Figure 20 have been averaged and their overall longshore variations are plotted in Figure 47a, while Figures 22 and 24 are partially replotted in Figures 47b and 47c. Starting from the Columbia River mouth, the following zones have been defined toward the north: G1 is a northward selective sorting zone, G2 is a northward normal sorting zone, G3 is still a northward normal sorting zone but affected by southward selective sorting processes, and G4 is an erosion and tide-winnowing zone.

As sediments are discharged from the Columbia River, they are spread out fanwise around the river mouth. In this original sediment

Figure 47

Comparison of longshore variations of the average median
grain size of the heavy minerals (a), total heavy mineral
concentration (b) and relative abundances of major heavy minerals
(c) on the Long Beach Peninsula. Different zones are classified
according to the dominant sorting process.
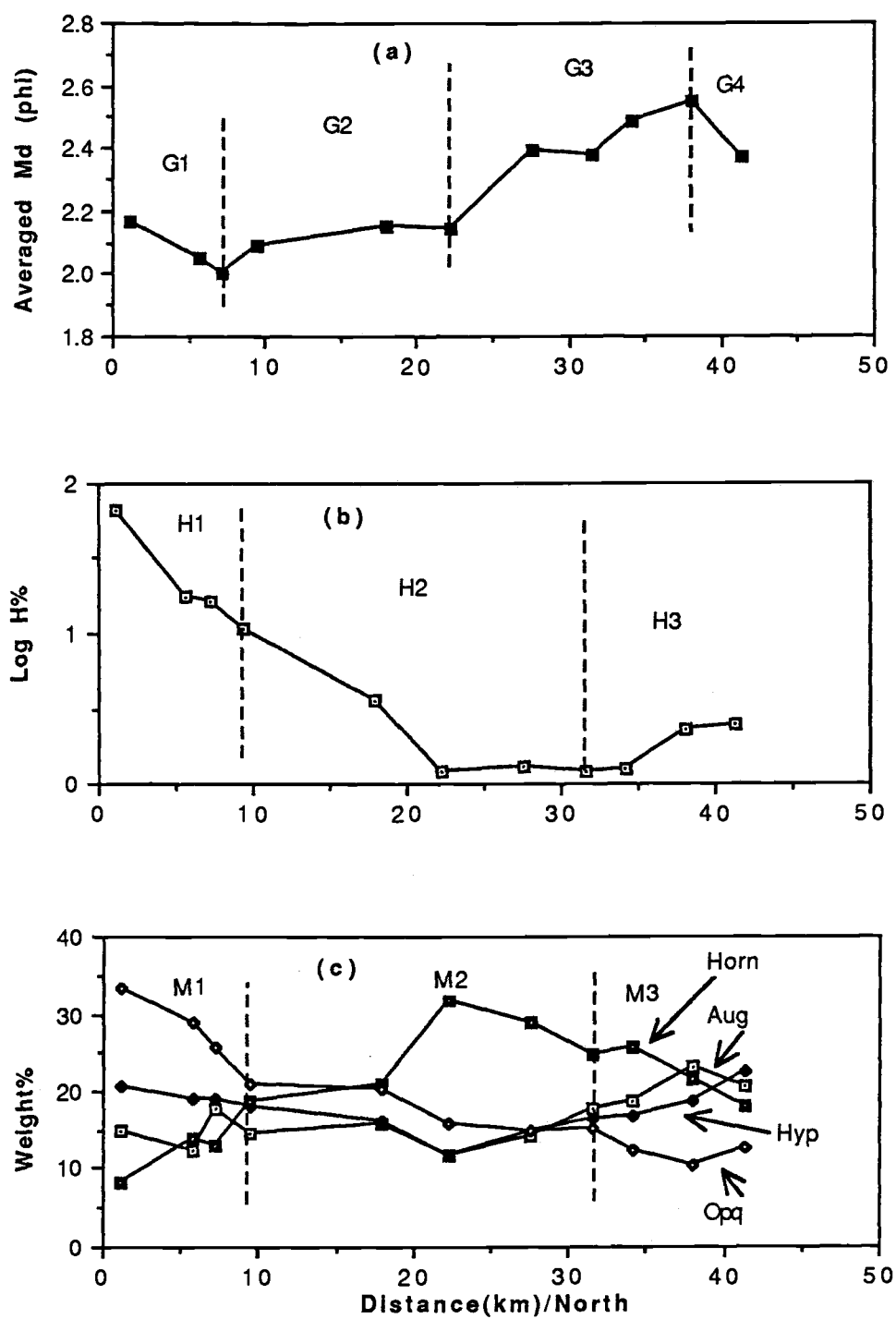
Figure 47

supplied by the river, the more-dense heavy minerals augite, hypersthene and opaques are roughly in settling equivalence, while settling velocities of quartz and hornblende are significantly lower (Figure 27 and Table 10). Thus, as beach sands are transported alongshore, the more slowly-settling lighter minerals are transported rapidly away from the source (the Columbia River) and outdistance the faster-settling heavy minerals. This settling sorting is therefore responsible for the overall separation of the heavy and light minerals as shown in Figure 47b. Shoreline erosioin after jetty construction and seasonal beach erosion during winter storms have selectively transported the coarse-grained linght minerals offshore and alongshore away from the river source, and therefore are also responsible for the initial concentration of the heavy minerls close to the jetties. Further separation of the settling-equivalent heavier minerals, however, is mainly due to selective grain sorting processes. The Columbia River sediment contains more than 10% heavy minerals, and these heavy minerals are generally finer grained than the associated light minerals. The wave shoaling on the delta and sheltering of the jetties tend to reduce the wave conditions immediately north and south of the Columbia River mouth, to cause low to medium flow stresses in this area. According to the results of the flume experiments described in section 7.4.5, these reduced flow stresses, together with high heavy mineral availability and the reverse correlation between mineral grain size and density in the original sediment supply, determine that selective entrainment and differential transport sorting are dominant close to the jetty. During this selective grain sorting, coarser-grained light minerals are selectively entrained and transported away from the source area due to their lower pivoting angles and greater protrusion heights in the flow, while the

finer-grained heavy minerals are left behind close to the river mouth. This has produced the away-from-source coarsening of the grain sizes in zone G1 and the overall high concentration of heavy minerals in zone H1 shown in Figure 47.

Within the heavy minerals, the denser and finer-grained opaques and hypersthene require higher flow stresses for entrainment, and their longshore transport rates are very low. In contrast, less-dense and coarser-grained hornblende requires a lower entrainment stress and its transport rate is higher. Thus, moderate-energy wave swash and longshore currents will selectively entrain the less-dense and coarser-grained hornblende as well as quartz, and transport them northward away from the river mouth, while most of the opaques and hypersthene are left behind (zone M1 in Figure 47c). The grain sizes and density of augite are intermediate between hypersthene and hornblende, and selective sorting processes are not as effective for its separation from the light minerals. Thus, its abundance within the heavy minerals does not show a significant longshore trend in zones M1 and M2. Northward from zone G1, heavy mineral availability is dramatically reduced and flow stresses are also increased on the open beaches. Thus, normal grain sorting and transport processes within the light mineral fraction become more important and replace the selective sorting mode to produce the systematic decrease of grain size in zones G2 and G3.

Stronger northward longshore currents caused by winter storms can transport a small amount of heavy minerals to the end of the Long Beach Peninsula. There, strong tidal currents of the Willapa Bay inlet winnow and transport finer mineral grains offshore to cause the increase in grain size in zone G4. Historical shoreline erosion at the Leadbetter Point due

to tidal channel migration has caused the removal of the light minerals and thus the initial concentration of heavy minerals at the north end of the peninsula. Beach sands that have reached the end of the Long Beach Peninsula are dominantly carried by normal sorting and transport processes as described for zones G2 and G3. Thus, minerals in these sediments are roughly settling-equivalent when they are deposited at the end of the peninsula. This settling equivalence again requires that minerals of higher densities are finer-grained than less-dense minerals. Therefore, southward longshore currents in the summer will selectively entrain and transport coarser-grained light minerals back to the south, while finer-grained heavy minerals are left behind. This southward selective grain sorting in zone G3, combined with the beach erosion in G4, has caused the slight increase in total heavy mineral concentration at the end of the Long Beach Peninsula as shown in zone H3 of Figure 47b. It is probably also responsible for the steeper slope of zone G3, indicating a greater decrease of median grain size. Due to the reduction in concentrations of opaque minerals at the northern end of the peninsula, selective sorting is effective on augite as well as on hypersthene, and causes them to be relatively concentrated in zone M3, while the lighter and coarser-grained hornblende is selectively transported to the south to cause its highest relative abundance at about the mid-point of zone M2 in Figure 47c.

8.3 Controlling Factors in Selective Grain Sorting and Placer Development

The efficiency of the selective grain sorting processes and placer development depends on several factors. The primary controlling factors,

however, are grain sizes and densities of the minerals in the sediment. Analyses of hydraulic ratios under equivalent settling velocities have shown that for various mineral pairs, the selective sorting of the heavy mineral is more effective when its density is greater and its relative grain size is finer (Figures 37 and 38). This density and grain size control is not limited to paired minerals, but is also applicable to the overall mineral separation and placer development. The selective entrainment stresses, differential transport rates and concentration factors for the principal minerals in the original sediment supply, given in Table 10, are plotted in Figure 48 against a dimensionless density-grain size parameter, DS, for the Long Beach Peninsula. This DS ratio is defined as the mineral's density divided by its intermediate diameter D_b. Therefore, a larger DS ratio represents a mineral of higher density and smaller grain size in the original sediment supply. Figure 48 shows that as the density/grain size ratio increases in order from quartz to hornblende, augite, hypersthene and opaques, their selective entrainment stresses also increase. This results in the systematic decrease in longshore transport rates as shown in Figure 48b. This means that higher densities and finer grain sizes of the heavy minerals make it more difficult for them to be entrained, and result in their longshore transport being slower than the light minerals. Thus, mineral concentration factors increase with their DS ratios as shown in Figure 48c, indicating that higher density and finer grain size favor the lagging behind of the heavy minerals in longshore sediment transport to cause them to be concentrated in the placer deposits close to the river mouth.

The present study proves that selective grain-sorting processes leading to placer formation exist in longshore sediment dispersal as well

Figure 48

Mineral selective entrainment stresses and longshore transport rates in the original sediment supply, and their concentration factors in the placer deposits plotted against the dimensionless density-grain size parameter, DS ratio for the Long Beach Peninsula.
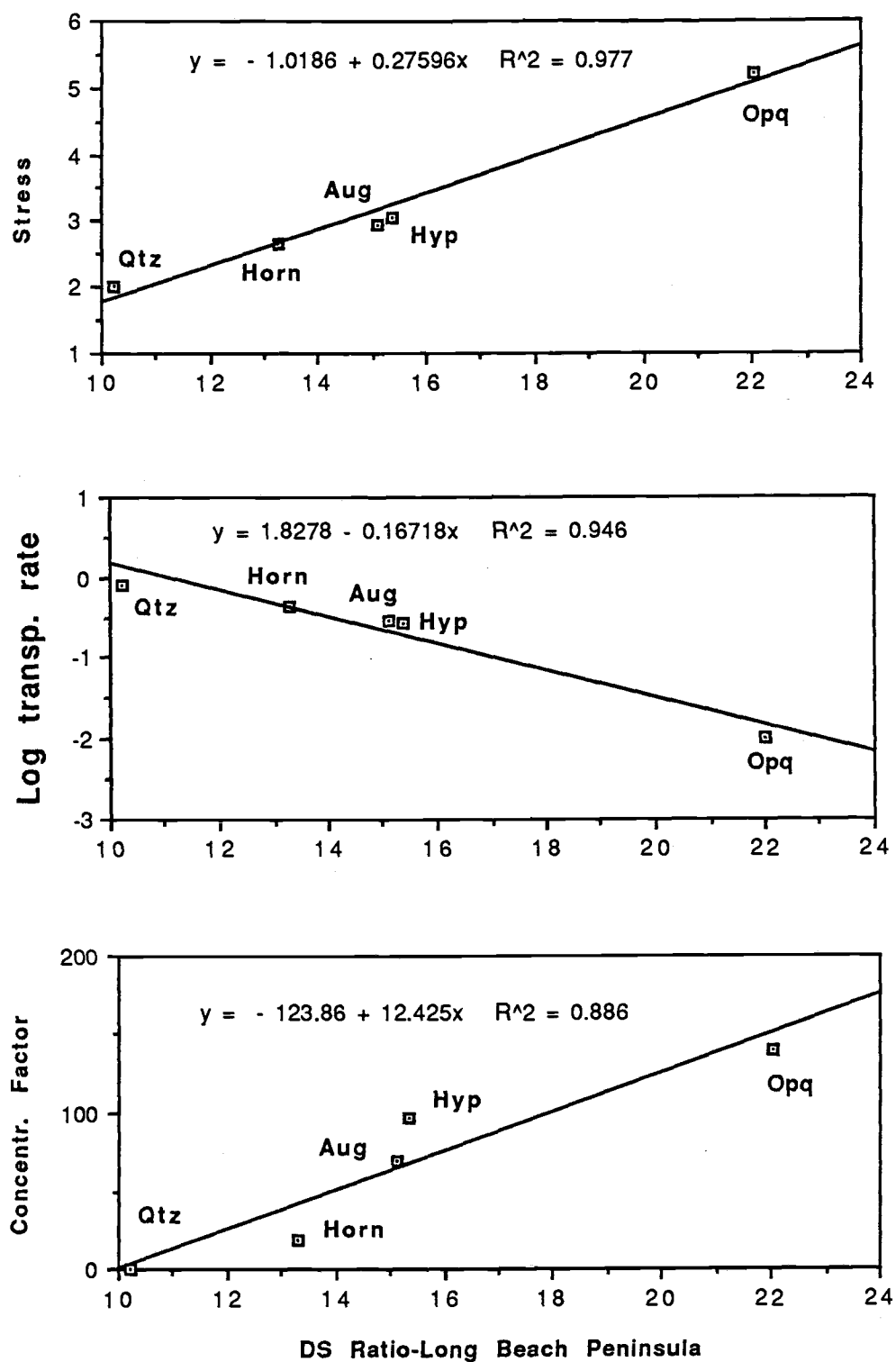
Figure 48

as in cross-shore sediment transport as investigated by Komar and Wang (1984). The general decrease in sediment grain sizes with longshore distance, shown in Figures 17 and 20, indicates that normal grain sorting and sediment transport dominate the major part of the beach. However, the away-from-source coarsening of sediment median grain sizes found close to the Columbia River mouth shows that selective grain sorting and sediment transport are more important immediately north and south of the river mouth. This longshore change from a selective sorting mode to a normal mode is determined by the variations in wave conditions and heavy mineral availability with longshore distance. Flume experiments conducted in this study have shown that the selective grain sorting process is more effective at low to medium flow stresses than at high flow stresses, while for a given flow stress the process is more effective for sands of higher heavy mineral abundances (Figures 45 and 46). Close to the Columbia River mouth, shoalings on the delta and the sheltering of the jetties have caused low wave and current conditions. The waves and currents are apparently strong enough to selectively entrain and transport the coarser-grained light minerals, but generally not strong enough to overcome the higher threshold stresses of the high-density and finer-grained heavy minerals. The high concentration of heavy minerals in the Columbia River sediment supply also provides a wide size range and density difference. All of these factors favor the dominance of selective grain sorting in the area close to the river mouth. As sediments are transported alongshore, heavy minerals become depleted due to this selective grain sorting. The size range and density differences are minimized, and the sorting process in the light-mineral fraction becomes more important. As transport distance increases, jetty protection also

decreases and strong waves and currents on the open beaches are significantly higher than the threshold stresses of all the minerals. Thus, the selective sorting mode is replaced by the normal sorting mode on this part of the beach, in which finer mineral grains outdistance the coarser mineral grains (Figure 20).

The coincidence between the away-from-source coarsening of the median grain sizes and high concentrations of heavy minerals close to the river mouth suggests that although settling sorting is responsible for the general separation of the heavy minerals from the light minerals, selective entrainment and differential transport are the most important sorting processes for the heavy mineral concentration and placer formation in the study area. Absolute abundance of heavy minerals in the original sediment supply is important in that it is the base for further concentration of heavy minerals, but the grain size distributions of both the heavy and the light minerals are more critical. It seems that the settling velocities of the heavy minerals should be greater than that of the light minerals to cause their overall separation during longshore transport. However, this difference should be limited. When the grain sizes of the heavy minerals are too large, sheltering and selective entrainment due to size differences will not be significant and the potential for placer development reduced.

Coastal structures and changing shoreline orientations usually cause beach sheltering and reduced wave conditions. Studies have shown that beach erosion tends to selectively transport light minerals offshore and alongshore away from the source, thereby causing higher concentrations of heavy minerals in the placer deposits. In contrast, accreting beaches will incorporate these eroded light minerals to dilute

the abundance of the heavy minerals (Sunamura and Horikawa, 1971; Frihy and Komar, 1990). Following the jetty construction in the study area, the most striking feature is the rapid beach accretion adjacent to the jetties. However, periodical erosion had occured close to the south jetty on the Clatsop Spit and was also likely on Peacock Beach. These periodical erosions are important in causing the selective removal of light minerals and high concentration of heavy minerals in these areas. Rapid beach accretion caused by jetty construction in the study area probably diluted the absolute concentrations of the heavy minerals in the placer deposits, but is responsible for the significantly larger volumes of the placer deposits. The sheltering of the jetties together with the wave shoaling on the delta also enhances the efficiency of selective sorting processes. Thus, the overall effects of jetty construction are still positive for placer development in this area.

It is believed that rising sea-levels tend to incorporate the heavy minerals and transport them landward (Emery and Noaks, 1968; Komar, 1989). The slower rising rates of relative sea-level in the Pacific Northwest certainly have favored this incorporation and landward migration. The length of time during which the shorelines were occupied is also important in that the longer period of standing sea-level means a higher degree of sediment reworking and a longer continuation of heavy-mineral concentrating processes (Sutherland, 1987). The generally stable sea-level and shorelines after the Holocene transgression imply that modern beaches have been subject to these cross-shore and longshore selective sorting processes for the last few thousand years. This has undoubtly increased the degree of heavy mineral concentration in the placer deposits.

8.4 Summary of Conclusions

Based on the present study, the following conclusions have been reached:

1. Jetty construction has caused sheltering and rapid beach accretion with periodical erosions immediately adjacent to the Columbia River mouth, and therefore is responsible for the large volumes of placer deposits in the study area.

2. The Columbia River is the major sediment source to the study area, and the sediments are then transported both north and south along the adjacent ocean beaches. The high concentration of heavy minerals close to jetties and the slight increase of heavy mineral concentrations at the end of each beach section are caused by beach erosion, and the seasonal shifting of the longshore currents and sediment transport directions.

3. Selective grain sorting is the dominant process within 10 to 15 km from the Columbia River mouth, and has caused the higher concentrations and finer grain sizes of heavy minerals in the placer deposits. Normal grain sorting and sediment transport processes become more important away from this area, and have produced the overall systematic longshore decreases in grain sizes for the major stretches of these beaches. This longshore transformation of dominant sorting modes is caused by longshore variations in the wave conditions and heavy mineral availability.

4. Although settling sorting is probably responsible for the overall separation of the heavy and light minerals, selective entrainment and differential transport are the major sorting mechanisms responsible for the mineral separation and placer development in the study area.

5. These sorting processes selectively entrain and transport the coarser-grained and less dense quartz and feldspars away from the source, while the heavy minerals are left behind and concentrated in the placer deposits. The degree to which a heavy mineral lags behind the light minerals increases with its density and decreases with its relative grain size with respect to the light minerals.

6. Although flume experiments have shown that the selective entrainment and transport model used in this study is generally correct for quartz-density minerals, it needs to be further tested by flume experiments involving both light and heavy minerals.

BIBLIOGRAPHY

Abbott, J.E., and Francis, J.R.D., 1977. Saltation and suspension trajectories of solid grains in a water stream. Phils. Trans. Roy. Soc., London, 284: 225-254.

Bagnold, R.A., 1954. Experiments on a gravity-free dispersion of large solid spheres in Newtonian fluid under shear. Proc. Roy. Soc. London, Series A, 225: 49-63.

Bagnold, R.A., 1956. The flow of cohesionless grains in fluids. Proc. Roy. Soc. London, Series A, 265: 315-319.

Ballard, R.L., 1964. Distribution of beach sediment near the Columbia River. Dept. Oceanography, Univ. Washington, Tech. Rept. No.98, 82 pp.

Barnett, T.P., 1984. The estimation of global sea level change: a problem of uniqueness. Jour. Geophys. Res., 89: 7980-7988.

Bascom, W.N. and McAdam, D., 1947. Beach and Surf conditions on the beaches of the Oregon and Washington coasts between October 9, 1946 and November 18, 1946. Univ. California, Berkeley, Dept. Engineering, Tech. Memo. HE-116-247, April 16, 1947 (Water Resources Center Archives).

Beiersdorf, H., Kudrass, H.R., and von Stackelberg, U., 1980. Placer deposits of ilmenite and zircon on the Zambezi shelf. Geol. Jahrbuch, v.D36, p.5-85.

Bloom, A.L., 1977. Atlas of sea-level curves. Int. Geol. Correl. Progr., Proj. 61. Dept. of Geol. Sci., Cornell University, Ithaca, N. Y.

Bourke, R.H., 1971. Waves. In: Oceanography of the nearshore coastal waters of the Pacific Northwest relating to possible pollution. v.1, Oregon State Univ., Corvallis, Oregon, 615 pp.

Briggs, L.I., 1965. Heavy mineral correlations and provenances. Jour. Sed. Petrology, 35: 939-955.

Byrne, J.V., 1963. Geomorphology of the continental terrace of the Oregon coast. Oregon Dept. of Geology and Mineral Industries, Ore Bin, 12: 128-130.

Callahan, J., 1987. A nontoxic heavy liquid and inexpensive filters for separation of mineral grains. Jour. Sed. Petrology, 57: 765-766.

Clemens, K.E., 1987. Along-coast variations of Oregon beach-sand compositions produced by the mixing of sediments from multiple sources under a transgressing sea: Unpubl. Master's Thesis, Oregon State University, Corvallis, 75p.

Clemens, K.E., and Komar, P.D., 1988. Oregon beach-sand compositions produced by the mixing of sediments under a transgressing sea. Jour. Sed. Petrology, 58: 519-529.

Clifton, H.E., 1969. Beach lamination: nature and origin. Marine Geology, 7: 553-559.

Climatological Data: Oregon, 1985. National Climatic Center, Asheville, N.C., 1985.

Cooper, W.S., 1958. Coastal sand dunes of Oregon and Washington. Geol. Soc. Am. Mem., 72: 169 pp.

Curray, J.R., 1965. Late Quaternary history, continental shelfs of the United States: in The Quaternary of the United States, edited by H.E. Wright and D.G. Frey, Princeton Univ. Press, p. 723-735.

Davies, C.N., 1945. Definitive equations for the fluid resistance of spheres. Proc. Physical Soc., 57: 259-270.

Davies, J.K., 1964. A morphogenic approach to world shorelines. Zeit. fur Geomorph., 8: 127-142.

Day, D.T., and Richards, T.H., 1906. Useful minerals in the black sands of the Pacific slope. U.S. Geological Survey Mineral Resources of the United States, 1905, p. 1175-1258.

Dicken, S.N., 1961. Some recent physical changes of the Oregon coast. Report, Dept. of Geography, Univ. of Oregon, Eugene, OR., 151pp.

Einstein, H.A., 1950. The bed-load function for sediment transportation in open-channel flows. U. S. Dept. Agriculture, Soil Conservation Service, Tech. Bull.,1026, 78pp.

Einstein, H.A., 1964. River sedimentation. In: Chow, V.T., ed., Handbook of Applied Hydrology, New York, McGraw-Hill, Section 17-II.

Emery, K.O., and Noaks, 1968. Economic placer deposits on the continental shelf. UN Committee to Coordinate Joint Prospecting for Mineral Resources in Asian Offshore Areas, Tech. Bull. 1: 95-111.

Emery, K.O., and Stevenson, R.E., 1950. Laminated beach sand. Jour. Sed. Petrology, 20: 220-223.

Fairbridge, R.W., 1960. The changing level of the sea. Scientific American, 202: 70-79.

Fenton, J.D., and Abbott, J.E., 1977. Initial movement of grains on a stream bed: the effect of relative protrution. Proc. Roy. Soc. London, Series A, 352: 523-527.

Folk, R.L., and Ward, W.L., 1957. Measures for describing size of sediments whose size frequency curves are non-normal. Jour. Sed. Petrology, 27: 3-26.

Francis, J.R.D., 1973. Experiments on the motion of solidary grains along the bed of a water-stream. Proc. Roy. Soc., London, A332: 443-471.

Frihy, O.E., and Komar, P.D., 1990. Patterns of beach-sand sorting and shoreline erosion on the Nile delta. Submitted to Jour. Sed. Petrology.

Glasby, G.P., 1986. Near-shore mineral depostis in the SW Pacific. In: Sedimentation and Mineral Deposits in the Southwestern Pacific Ocean, D.S. Cronen (ed.), Academic Press, London.

Glover, S.L., 1942. Washington Iron Ores, A Summary Report, Washington Div. of Mines and Mining, RI No. 2, 1942, 23pp.

Gornitz, V., Lebedeff, S., and Hansen, J., 1982. Global sea level trend in the past century. Science, 215: 1611-1614.

Griggs, A.B., 1945. Chromite bearing sands of the southern part of the coast of Oregon. U. S. Geol. Survey Bull., 945-E: 113-150.

Hand, B.M., 1967. Differentiation of beach and dune sands using settling velocities of light and heavy minerals. Jour. Sed. Petrology, 37: 514-521.

Hicks, S.D., 1972. On the classification and trends of long period sea level series. Shore and Beach, 40: 32-36.

Hidaka, F.T., 1966. Water resources and development. In: Mineral and Water Resources of Washington. Washingtion Division of Mines and Geology Reprint No.9, P. 311-355.

Highsmith, R.M., Jr., 1962. Water; in Atlas of the Pacific Northwest Resources and Development; R.M. Highsmith, Jr., ed.; Corvallis, Ore., Oregon State Univ. Press.

Hodge, E.T., 1934. Geology of beaches adjacent to the mouth of the Columbia River and petrography of their sands, Beach Erostion Investigation, Beach Erosion Board, 34p.

Inman, D.L., Ewing, D.C., and Corliss, J.B., 1966. Coastal sand dunes of Guerro Negro, Baja California, Mexico. Geol. Soc. Am. Bull., 11: 787-802.

Jartiz, W., Ruder, J., and Schlenker, B., 1977. Das Quartar im Kustengebiet von Mocambique und seine Schwermineralfuhrung. Geol. Jahrbuch, B26: 3-93.

Jay, D. and Good, J., 1977. Columbia River estuary sediment and sediment transport. Section 208 of Columbia River Estuary Inventory of Physical, Biological, and Cultural Characteristics. CREST, Astoria, OR.

Kamel, A.M., 1962. Transportation of coastal sediments. Inst. Eng. Res., Tech. Rep., Ser. 185, University of California.

Karlin, R., 1980. Sediment sources and clay mineral distributions off the Oregon coast. Jour. Sed. Petrology, 50: 543-560.

Kelly, J.V., 1947. Columbia River magnetite sands, Clatsop County, Oregon, and Pacific County, Washington, Hammond and McGowan deposits. Report of Investigations 4011, U. S. Bureau of Mines.

Kent, P., 1980. Minerals from the Marine Environment. John Wiley & Sons, New York, 88pp.

Kerr, P. F., 1959. Optical Mineralogy. New York, McGraw-Hill Book Copmp. Inc., 3rd Ed., 442PP.

Kidby, H.A., and Oliver, J.G., 1966. Erosion and accretion along the Clatsop Spit: in Coastal Engineering, American Society of Civil Engineers, 7th Santa Barbara Specialty Conference, Santa Barbara, Calif., 1966, p.647-667.

Komar, P.D., 1976. Beach Processes and Sedimentation. New Jersey, Englewood Cliffs, Prentice-Hall, Inc., 429 pp.

Komar, P.D., Quinn, W., Creech, C., Rea, C.C., and Lizarraga-Arciniega, J.R., 1976. Wave conditions and beach erosion on the Oregon coast. The Ore Bin, 38: 103-112.

Komar, P.D., 1977. Beach profiles obtained with an amphibious DUKW on the Oregon and Washington coasts. The Ore Bin, 39: 169-184.

Komar, P.D., and Cui, B., 1984. The analysis of grain-size measurements by sieving and settling tube techniques. Jour. Sed. Petrology, 54: 630-614.

Komar, P.D., and Wang, C., 1984. Processes of selective grain transport and the formation of placers on beaches. Journal of Geology, 92: 637-655.

Komar, P.D., and Li, Z., 1986. Pivoting analysis of selective entrainment of sediments by shape and size with application to gravel threshold. Sedimentology, 33: 425-436.

Komar, P.D., 1989. Physical proceses of waves and currents and the formation of marine placers. Reviews in Aquatic Sciences, 1: 393-423.

Komar, P.D., Clemens, K.E., Li, Z., and Shih, S-M, 1989. The effects of selective sorting on factor-analysis of heavy mineral assemblenges. Jour. Sed. Petrology, 59: 590-596.

Kudrass, H.R., 1987. Sedimertary models to estimate the heavy-mineral potential of shelf sediments: Marine Minerals. Advances in Research and Resource Assessment, P.G. Teleki et al., (editors), NATO Advanced Study Institutes Series, Series C, Mathematical and Physical Sciences, 588pp.

Kulm, L.D., Heinricks, D.F., Buehrig, R.M., and Cambers, D.M., 1968. Evidence for possible placer accumulations on the southern Oregon continental shelf. Ore Bin, 30: 81-104.

Kulm, L.D., Scheidegger, K.F., Byrne, J.V., and Spigai, J.J., 1968. A preliminary investigation of the heavy mineral suites of the coastal rivers and beaches of Oregon and northern California: Ore Bin, 30: 165-180.

Kulm, L.D., 1988. Potential heavy mineral and metal placers on the southern Oregon continental shelf. Marine Mining, 4: 361-395.

Lewis, D. W., 1984. Practical sedimentology. Hutchinson Ross Pupblishing Company, Stoudsburg, Pennsylvania, 229pp.

Li, Z., 1986. Pivoting angles of gravel with applications in sediment threshold studies. M.S thesis, Oregon State University, Corvallis, OR., 101pp.

Li, Z., and Komar, P.D., 1986. Laboratory measurements of pivoting angles for applications to selective entrainment of gravel in a current. Sedimentology, 33: 413-423.

Lockett, J.B., 1959. Interim considerations of the Columbia river entrance, Proc. American Society of Civil Engineers, Journal of Hydrologics Division, v.85, paper 1902, P. 17-40.

Lockett, J.B., 1962. Phenomena affecting improvement of the Lower Columbia River esturay. Chapter 40 in Proc. of the 8th Annual Conference on Coastal Engineering (J.W. Johnson, ed.).

Lockett, J.B., 1967. Sediment transport and diffusion- Columbia River estuary and entrance: Am. Soc. Civil Eng. Proc., v.93, No. WW4, P. 167-175.

Lowright, R., Williams, E.G., and Dachille, F., 1972. An analysis of factors controlling deviations in hydraulic equivalence in some modern sands. Jour. Sed. Petrology, 42: 635-645.

Luepke, G. and Clifton, H.E., 1983. Heavy-mineral distribution in modern and ancient bay deposits, Willapa Bay, Washington, U. S. A. Sedimentary Geology, 35: 233-247.

Mackie, W., 1923. The principles that regulate the distribution of particles of heavy minerals in sedimentary rocks, as illustrated by the sandstones of the North-East of Scotland. Trans. Edinburgh Geol. Soc., 11: pt.2, 138-164.

Marmer, H.A., 1952. Changes in sea level determined from tide observations. Proc. 2nd Conf. Coastal Engr., p.62-67.

Meland, N., and Norrman, J.O., 1966. Transport velocities of single particles in bed-load motion. Geogr. Ann., 48: Series A,165-182.

Miller, R. L., and Byrne, R.J., 1966. The angle of repose for a single grain on a fixed rough bed. Sedimentology, 6: 303-314.

Miller, M.C., McCave, I.N., and Komar, P.D., 1977. Threshold of sediment motion under unidirectional currents. Sedimentology, 24: 507-527.

Milliman, J.D. and Emery, K.O., 1968. Sea levels during the past 35,000 years. Science, 162: 1121-1123.

McIntyre, D.D., 1959. The hydraulic equivalence and size distributions of some mineral grains from a beach. Jour. Geol., 67: 278-301.

McManus, P.A., 1972. Bottom topography and sediment texture near the Columbia River mouth. In: Pruter, A.T., and Alverson, D.L., (eds.), 1972, The Columbia River Estuary and Adjacent Ocean Waters, Univ. of Washington Press, Seattle, WA., 868 pp.

McMaster, R.C., 1954. Petrography and genesis of the New Jersey beach sands . New Jersey Dept. of Conservation and Economic Development, Geologic Series, Bull., 63, 239pp.

National Marine Consultants, 1961. Wave statistics for three deep-water stations along the Oregon-Washington coast. U.S. Army Corps of Engineers, Portland and Seattle Districts.

Norberg, J.R., 1980. Black sand occurrences in the Columbia River estuary and vicinity: Technical Assistance Report, U.S. Bureau of Mines, Western Field Operations Center, Spokane, Washington, 15pp.

O'Brien, M.P., 1936. Mouth of the Columbia River - beach erosion investigations; summary of observations and results, July 1935 to August 1936: Technical Memo. #20, U.S. Tidal Model Laboratory, Berkeley, California.

O'Brien, M.P., 1951. Wave measurements at the Columbia River Light Vessel, 1933-1936. Trans. Am. Geophysical Union, 32: 875-877.

Oregon Dept. Of Geology and Mineral Industries,1941. Oregon Metal Mines Handbook. Bulletin 14-D.

Oregon Dept. Of Geology and Mineral Industries, 1963. Beach sands attract Bunker Hill Co. Ore Bin, 25: 128-130.

Pardee, J. T., 1928. Platinum and black sands in Washington. U.S. Geological Survey Bulletin 805-A, p. 1-15.

Pardee, J.T., 1934. Beach placers on the Oregon coast. U. S. Geol. Survey Circular 8, 41pp.

Peterson, C.D., Scheidegger, K.F., and Schrader, H.J., 1984. Holocene depositional evolution of a small active-margin estuary of the northwestern United States. Mar. Geology, 59: 51-83.

Peterson, C.D., Komar, P.D., and Scheidegger, K.F., 1986. Distribution, geometry, and origin of heavy mineral deposits on Oregon beaches. Jour. Sed. Petrology, 56: 67-77.

Peterson, C.D., Gleeson, G.W., and Wetzel, N., 1987. Stratigraphic development, mineral sources and preservation of marine placers from Pleistocene terraces in southern Oregon, U.S.A. Sedimentary Geology, 53: 203-229.

Peterson, C.D., and Binney, S.E., 1988. Compositional variations of coastal placers in the Pacific Northwest, U.S.A. Marine Mining, 7: 397-316.

Pettijohn, F.J., and Ridge, J.D., 1932. A textural variation series of beach sands from Cedar Point, Ohio. Jour. Sed. Petrology, 2: 76-88.

Phillips W. R. and Griffen, D. T., 1981. Optical mineralogy - the nonopque minerals. W. H. Freeman and Company, San Francisco, 677pp.

Phipps, J.B. and Smith, J.M., 1978. Coastal accretion and erosion in southwest Washington: State Department of Ecology Pub. no. PV-11, Washington, Olympia, 76 PP.

Plopper, C.S., 1978. Hydraulic sorting and longshore transport of beach sand, Pacific coast of Washington. Syracuse University, Syracuse, N.Y., unpublished Ph.D thesis, 156pp.

Pretorius, D.A., 1976. The nature of the Witwatersrand gold-uranium deposits. In: Handbook of Strata-Bound and Stratiform Ore Deposits, K.H. Wolf (ed.), P.29-32. Amsterdam: Elsevier.

Rankin, D.K., 1983. Holocene geologic history of the Clatsop Plains foredune ridge complex. Portland State University, Portland, OR., MS thesis, 148 pp.

Rao, C.B., 1957. Beach erosion and concentration of heavy mineral sands. Jour. Sed. Petrology, 27: 143-147.

Rittenhouse, G., 1943. The transportation and deposition of heavy minerals. Geol. Soc. Am. Bull., 54: 1725-1780.

Roden, G.I., 1967. On river discharge in to the Northeastern Pacific Ocean and the Bering Sea. Jour. Geophys. Res., 72: 5613-5629.

Rouse, H., ed., 1950. Engineering Hydraulics. New York, John Wiley & Sons, 1039 pp.

Rubey, W. W., 1933. The size distribution of heavy minerals within a water-laid sandstone. Jour. Sed. Petrology, 3: 3-29.

Sallenger, A.H., 1979. Inverse grading and hydraulic equivalence in grain-flow deposits. Jour. Sed. Petrology, 49: 553-562.

Sax, N. I. and Lewis, R. J., 1986. Rapid guide to hazardous chemicals in the workplace. New York, Van Nostrand Reinhold Co., 236pp.

Scheidegger, K.F., Kulm, L.D., and Runge, E.J., 1971. Sediment sources and dispersal patterns of Oregon continental shelf sands, Jour. Sed. Petrology, 47: 1112-1120.

Self, R.P., 1977. Longshore variation in beach sands, Nautla area, Veracruz, Mexico. Jour. Sed. Petrology, 47: 1432-1443.

Shepard, F.P., 1963. Thirty-five thousand years of sea level. In: Essays in marine geology, in honor of K.O. Emery, Univ. Southern Calif. Press, Los Angeles, p. 1-10.

Shepard, F.P., and Curray, J.R., 1967. Carbon-14 determination of sea level changes in stable areas. In: Progress in Oceanography, "The Quaternary History of the Ocean Basins", Pergamon Press, Oxford, 4: 283-291.

Slingerland, R.L., 1977. The effects of entrainment on the hydraulic equivalence relationships of light and heavy minerals in sand. Jour. Sed. Petrology, 47: 753-770.

Slingerland, R.L., 1984. Role of hydraulic sorting in the origin of fluvial placers. Jour. Sed. Petrology, 54: 137-150.

Slingerland, R., and Smith, N.D., 1986. Occurrence and formation of water-laid placers. In Annual Rev. Earth and Planetary Sciences, 14: 113-147.

Stapor Jr., F.W., 1973. Heavy mineral concentrating processes and density/shape/size equilibria in the marine and coastal dune sands of the Apalachicola, Florida Region. Jour. Sed. Petrology, 43: 396-407.

Steidtmann, J.R., 1982. Size-density sorting of sand-size spheres during deposition from bed-load transport and implications concerning

hydraulic equivalence. Sedimentology, 29: 877-883.

Sunamura, T., and Horikawa, K., 1971. Predominant direction of littoral transport along Kujyukuri Beach, Japan. Coastal Engineering In Japan, 14: 107-117.

Sutherland, D.G., 1987. Placer deposits of the nearshore and coastal zones: the role of littoral processes and sea-level changes in their formation. In: Sea Surface Studies, R.J.N. Devoy (ed.), Croom Helm, London, P.569-588.

Terich, T. and Levenseller, T., 1986. The severe erosion of Cape Shoalwater, Washington. Journal of Coastal Res., 2: 465-477.

Thornthwaite, C.W., 1948. An approach toward a rational classification of climate. Geographical Review. v.38, Burlington, Vt.: American Geographical Society, p.55-94.

Thwaites, R.G., 1905. Original journals of the Lewis and Clark Expedition, 1804-1806, v.3, New York, Doad and Head & Co., 460pp.

Trask, C.B., 1976. Mineralogy, texture and longshore transport of beach sand, eastern shore of Lake Ontario. Unpubl. Doctoral Dissertation, Syracuse Univ., 306pp.

Trask, C.B., and Hand, B.M., 1985. Differential transport of fall-equivalent sand grains, Lake Ontario, New York. Jour. Sed. Petrology, 55: 226-234.

Twenhofel, W.H., 1943. Origin of the black sands of the coast of southwest Oregon. Oregon Dept. of Geology and Mineral Industries Bull. 24, 25pp.

Twenhofel, W.H., 1946. Mineralogy and physical composition of the sands of the Oregon coast from Coos Bay to the mouth of the Columbia River. Oregon Dept. of Geology and Minineral Industries Bull. 30, 64pp.

U.S. Department Of Commerce/National Oceanic and Atmospheric Adm., 1981. West Coast of North and South America- Tide Tables 1982. 231pp.

U.S. Geol. Survey Water Data Reports, 1965-1976. (Pub. Annually), Water Resources Data for California, Oregon and Washington.

van Winkle, W., 1914. Quality of the surface waters of Washington: U.S. Geol. Survey Water Supply Paper 339, 105 pp.

Venkatarathnam, K. and McManus, D.A., 1973. Origin and distribution of sands and gravels on the northern continental shelf off Washington. Jour. Sed. Petrology, 43: 799-811.

Wang, C., and Komar, P.D., 1985. The sieving of heavy mineral sands. Jour. Sed. Petrology, 55: 479-482.

Warg, J. B., 1973. An analysis of methods for calculating constant terminal settling velocities of spheres in liquids. Mathematical Geology, 5: 59-72.

Whetten, J.T., Kelley, J.C., and Hanson, L.G., 1969. Characteristics of Columbia River sediment and sediment transport: Jour. Sed. Petrology, 39: 1149-1166.

White, S.M., 1970. Mineralogy and geochemistry of continental shelf sediments off the Washington-Oregon coast. Jour. Sed. Petrology, 40: 38-54.

Woolsey, J.R., Henry, V.J., and Hunt, J.J., 1975. Backshore heavy-mineral concentation on Sapelo Island, Georgia. Jour. Sed. Petrology, 45: 280-284.

Yalin, M.S., and Karahan, E., 1979. Inception of sediment transport. Jour. Hydraul. Div., Am. Soc. Civil Eng., 105: 1433-1443.

Young, E.L., 1966. A critique of methods for comparing heavy mineral suites. Jour. Sed. Perology, 36: 57-65.

Zapfee, C., 1949. A review of iron bearing deposits in Washington, Oregon, and Idaho, Raw Materials Survey Resource Report No. 5, Portland, Oregon, 1949, 89pp.

APPENDICES

Appendix I
Heavy Mineral Separation

It has been documented that traditional heavy mineral separation using tetrabromoethane can cause serious health hazards (Sax and Lewis, 1986). For this reason, nontoxic sodium polytungstate ($3Na_2WO_49WO_3H_2O$) has been recommended and tested for heavy mineral separation (Callahan, 1987). The sodium polytungstate used in this study has a specific gravity of 3.00. Thus it will provide basically the same density separation as that of tetrabromoethane (specific gravity of 2.97). The detailed procedures of heavy mineral separation used in the present study are described below:

1. Pre-washed and dried sand samples are split into subsamples of about 10 milliliters (ml).

2. These small subsamples are then put into 45ml centrifuge tubes and mixed with sodium polytungstate.

3. Each tube is well hand-shaken and then centrifuged at 7000 rpms for five minutes.

4. The heavy fraction at the bottom of the tube is frozen with liquid nitrogen and the unfrozen light fraction in the top part of the tube is poured out and filtered to reclaim the polytungstate.

5. When the heavy fraction melts, it is also poured off and filtered.

6. The filters and beakers are throughly rinsed with distilled water, and the water-tungstate mixture is oven-dried to reclaim the polytungstate.

7. The separated lights and heavies were dried and weighed. The total heavy mineral concentration is then calculated as the weight of the heavies divided by the total weight of the sample.

Appendix II
Major Heavy Mineral Identifications

Due to the greater thickness and variable shapes of heavy mineral grains in grain mounts, criteria of mineral identification given in standard mineralogy textbooks can not be applied exactly. Basic distinguishing features of major heavy minerals used in this study are given in this Appendix.

Augite

pale green to brown, 3rd to 4th order interference color with 45° extinction angle, negative elongation.

Diopside

Colorless, bright 4th order interference color, 45° extinction angle, negative elongation.

Hypersthene

Pleochroic from pale green to red, 1st to 2nd order low interference color, parallel extinction with positive elongation.

Enstatite

Mostly colorless, no pleocroic change, 1st order yellow to blue interference color, parallel extinction, positive elongation.

Hornblende

Green to brown, strong pleocroism from green to dark green or brown to dark brown, 2nd to 3rd order briliant interference color, 12-30° extinction angle with positive elongation.

Actinolite-Tremolite

Mostly colorless mineral with the same properties as hornblende.

Garnet

Very high relief, colorless to pale pink or brown, isotropic mineral with concoidal fractures.

Zircon

Extemely high relief, mostly colorless, typical high-order white interference color, parallel extinction with positive elongation.

Epidote

Pale yellowish green color with slight pleoroism, brilliant 3rd order interference color often masked by strong dispersion, show parallel extinction.

Appendix III

Sieve size (D_{sv}, mm), Longest and Intermediate Diameters (D_a and D_b, mm), Calculated and Measured Settling Velocities (W_s and W_m, cm/s) for Mineral Grains Selected From Sample sn2.

Mineral Name	D_{sv} (mm)	D_a (mm)	D_b (mm)	W_s (cm/s)	W_m (cm/s)
Quartz					
1	0.297	0.441	0.352	5.21	3.72
2	0.297	0.494	0.350	5.17	4.07
3	0.297	0.510	0.352	5.21	4.01
4	0.297	0.475	0.342	5.03	3.85
5	0.250	0.418	0.414	6.31	2.80
6	0.250	0.390	0.306	4.38	2.83
7	0.250	0.378	0.297	4.22	2.92
8	0.250	0.453	0.357	5.30	2.98
9	0.210	0.457	0.244	3.28	2.61
10	0.210	0.318	0.247	3.33	2.66
11	0.210	0.323	0.307	4.40	2.56
12	0.210	0.444	0.226	2.96	3.48
13	0.177	0.333	0.263	3.61	2.14
14	0.177	0.320	0.257	3.51	2.33
15	0.177	0.352	0.231	3.05	2.15
16	0.177	0.333	0.248	3.35	2.33
17	0.177	0.355	0.230	3.03	2.34
18	0.149	0.238	0.201	2.52	2.10
19	0.149	0.316	0.202	2.54	2.13
20	0.149	0.332	0.245	3.29	2.19
21	0.149	0.329	0.208	2.64	2.12
22	0.125	0.249	0.162	1.86	1.61
23	0.125	0.180	0.165	1.91	1.55
24	0.125	0.219	0.185	2.25	1.47
25	0.125	0.295	0.163	1.88	1.72
26	0.105	0.257	0.131	1.36	1.48
27	0.105	0.249	0.158	1.79	1.61

Appendix III (continued)

28	0.105	0.217	0.172	2.03	1.44
29	0.105	0.188	0.138	1.47	1.22
30	0.088	0.228	0.142	1.53	1.28
31	0.088	0.219	0.116	1.13	1.28
32	0.088	0.266	0.123	1.24	1.23
33	0.088	0.271	0.115	1.11	1.28
Hornblende					
1	0.250	0.409	0.384	6.97	3.38
2	0.250	0.455	0.422	7.77	3.35
3	0.250	0.411	0.371	6.69	3.64
4	0.250	0.463	0.335	5.93	4.12
5	0.250	0.361	0.336	5.95	3.59
6	0.210	0.485	0.293	5.03	2.62
7	0.210	0.445	0.283	4.82	3.42
8	0.210	0.514	0.279	4.74	3.56
9	0.210	0.376	0.314	5.48	2.84
10	0.177	0.544	0.244	3.99	2.92
11	0.177	0.507	0.252	4.16	3.16
12	0.177	0.518	0.246	4.04	3.15
13	0.177	0.449	0.286	4.89	2.73
14	0.149	0.384	0.197	3.01	2.14
15	0.149	0.371	0.183	2.72	2.04
16	0.149	0.310	0.191	2.88	2.73
17	0.149	0.388	0.240	3.91	2.48
18	0.149	0.286	0.182	2.70	2.73
19	0.125	0.220	0.178	2.62	1.77
20	0.125	0.250	0.168	2.41	2.22
21	0.125	0.361	0.170	2.45	2.19
22	0.125	0.281	0.172	2.49	1.93
23	0.125	0.307	0.152	2.09	1.89
24	0.105	0.272	0.140	1.86	1.62
25	0.105	0.335	0.140	1.86	1.53
26	0.105	0.321	0.176	2.58	1.45
27	0.105	0.369	0.153	2.11	1.74
28	0.105	0.295	0.149	2.03	1.82

Appendix III (continued)

29	0.088	0.304	0.114	1.37	1.72
30	0.088	0.266	0.118	1.44	1.51
31	0.088	0.213	0.148	2.01	1.40
32	0.088	0.237	0.116	1.40	1.45
Augite					
1	0.250	0.390	0.340	6.43	4.43
2	0.250	0.370	0.290	5.30	4.01
3	0.250	0.423	0.290	5.30	3.74
4	0.250	0.410	0.310	5.76	3.84
5	0.250	0.480	0.330	6.21	4.45
6	0.210	0.561	0.295	5.42	3.21
7	0.210	0.402	0.295	5.42	3.41
8	0.210	0.360	0.277	5.01	4.50
9	0.210	0.371	0.285	5.19	4.69
10	0.210	0.399	0.275	4.97	4.49
11	0.177	0.365	0.225	3.84	3.08
12	0.177	0.321	0.297	5.46	2.69
13	0.177	0.390	0.242	4.22	3.26
14	0.177	0.328	0.212	3.55	3.26
15	0.149	0.391	0.220	3.73	2.89
16	0.149	0.228	0.198	3.24	2.37
17	0.149	0.352	0.183	2.91	2.81
18	0.149	0.353	0.182	2.89	2.61
19	0.125	0.231	0.171	2.65	2.07
20	0.125	0.223	0.171	2.65	2.23
21	0.125	0.259	0.162	2.46	2.16
22	0.125	0.241	0.155	2.31	2.03
23	0.105	0.314	0.144	2.08	1.82
24	0.105	0.266	0.161	2.44	1.78
25	0.105	0.310	0.161	2.44	1.81
26	0.105	0.280	0.157	2.35	1.89
27	0.105	0.285	0.139	1.97	1.85
28	0.088	0.306	0.119	1.57	1.69
29	0.088	0.352	0.143	2.06	1.79
30	0.088	0.251	0.117	1.53	1.66

Appendix III (continued)

31	0.088	0.278	0.144	2.08	1.59
32	0.088	0.219	0.105	1.30	1.63

Hypersthene

1	0.250	0.377	0.347	6.79	5.16
2	0.250	0.447	0.29	5.47	4.96
3	0.250	0.420	0.420	8.46	5.08
4	0.250	0.420	0.330	6.39	4.99
5	0.210	0.418	0.321	6.19	3.77
6	0.210	0.485	0.286	5.38	3.64
7	0.210	0.380	0.323	6.23	3.75
8	0.210	0.376	0.348	6.81	3.52
9	0.210	0.370	0.245	4.43	4.15
10	0.177	0.342	0.285	5.35	3.06
11	0.177	0.331	0.224	3.94	3.02
12	0.177	0.396	0.258	4.73	3.35
13	0.177	0.327	0.253	4.61	3.34
14	0.149	0.232	0.181	2.96	2.88
15	0.149	0.224	0.216	3.76	2.38
16	0.149	0.269	0.200	3.39	2.64
17	0.149	0.325	0.190	3.17	2.50
18	0.149	0.295	o.156	2.41	2.39
19	0.125	0.263	0.163	2.56	2.23
20	0.125	0.320	0.160	2.50	2.64
21	0.125	0.216	0.165	2.61	2.28
22	0.125	0.329	0.152	2.32	2.72
23	0.125	0.251	0.159	2.47	2.28
24	0.105	0.217	0.135	1.96	1.91
25	0.105	0.247	0.135	1.96	2.15
26	0.105	0.190	0.141	2.08	2.11
27	0.105	0.245	0.125	1.75	2.19
28	0.105	0.266	0.141	2.08	2.05
29	0.088	0.270	0.149	2.26	1.79
30	0.088	0.249	0.139	2.04	1.67
31	0.088	0.229	0.149	2.26	1.77
32	0.088	0.247	0.135	1.96	1.86

Appendix III (continued)

33	0.088	0.241	0.124	1.73	1.56

Opaques

1	0.250	0.345	0.287	7.35	5.08
2	0.250	0.312	0.267	6.74	3.68
3	0.250	0.367	0.321	8.39	3.67
4	0.250	0.331	0.292	7.50	4.10
5	0.210	0.360	0.320	8.36	3.79
6	0.210	0.344	0.277	7.05	3.86
7	0.210	0.408	0.315	8.21	3.89
8	0.210	0.327	0.304	7.87	3.76
9	0.177	0.270	0.250	6.22	4.22
10	0.177	0.284	0.219	5.27	3.18
11	0.177	0.289	0.206	4.87	3.07
12	0.177	0.342	0.279	7.11	3.68
13	0.149	0.323	0.191	4.42	2.41
14	0.149	0.304	0.173	3.87	2.52
15	0.149	0.259	0.192	4.45	2.16
16	0.149	0.199	0.181	4.11	1.90
17	0.125	0.221	0.173	3.87	2.98
18	0.125	0.194	0.152	3.25	2.64
19	0.125	0.238	0.148	3.13	2.16
20	0.125	0.179	0.167	3.69	2.42
21	0.125	0.234	0.206	4.87	2.44
22	0.105	0.194	0.150	3.19	2.24
23	0.105	0.222	0.152	3.25	2.14
24	0.105	0.196	0.140	2.90	2.31
25	0.105	0.178	0.137	2.81	2.06
26	0.105	0.168	0.144	3.01	2.27
27	0.088	0.187	0.118	2.27	1.84
28	0.088	0.183	0.134	2.72	1.87
29	0.088	0.171	0.137	2.81	2.40
30	0.088	0.152	0.129	2.58	1.78

Appendix IV
Longshore Changes of Median Intermediate Diameters (mm), Settling Velocities (cm/s) and Threshold Stresses (Dynes/cm^2) of the Individual Minerals for the Summer Samples.

sample number	Distance (km)	Qtz	Horn	Aug	Hyp	Opq
Median Intermediate Diameters						
south						
ss1	0.6	0.288	0.208	0.191	0.179	0.163
ss2	5.1	0.224	0.218	0.207	0.209	0.205
ss3	8.6	0.241	0.208	0.188	0.184	0.183
ss4	15	0.242	0.191	0.178	0.177	0.174
ss5	20.4	0.236	0.185	0.176	0.163	0.183
ss6	25.7	0.235	0.185	0.189	0.160	0.172
ss7	27.5	0.226	0.187	0.187	0.163	0.171
north						
sn1	1.2	0.261	0.237	0.222	0.227	0.201
sn2	5.7	0.288	0.255	0.235	0.242	0.234
sn3	7.2	0.310	0.262	0.246	0.250	0.240
sn4	9.4	0.285	0.252	0.233	0.230	0.226
sn5	17.9	0.300	0.240	0.214	0.214	0.232
sn6	22.2	0.294	0.244	0.203	0.214	0.252
sn7	27.6	0.292	0.202	0.181	0.185	0.195
sn8	31.6	0.234	0.204	0.184	0.185	0.194
sn9	34.2	0.227	0.190	0.180	0.170	0.174
sn10	38.0	0.213	0.178	0.174	0.164	0.166
sn11	41.3	0.232	0.205	0.194	0.195	0.183
Settling Velocities						
south						
ss1	0.6	2.25	2.38	2.55	2.51	2.38
ss2	5.1	2.22	2.47	2.76	2.87	2.89
ss3	8.6	2.37	2.38	2.51	2.57	2.63
ss4	15	2.38	2.22	2.38	2.48	2.52
ss5	20.4	2.33	2.17	2.35	2.30	2.63

Appdendix IV (continued)

sample number	Distance (km)	Qtz	Horn	Aug	Hyp	Opq
ss6	25.7	2.32	2.17	2.52	2.27	2.49
ss7	27.5	2.24	2.18	2.50	2.30	2.48
north						
sn1	1.2	2.55	2.63	2.95	3.08	2.84
sn2	5.7	2.77	2.78	3.11	3.25	3.22
sn3	7.2	2.95	2.84	3.25	3.34	3.28
sn4	9.4	2.75	2.76	3.09	3.12	3.13
sn5	17.9	2.87	2.66	2.85	2.93	3.19
sn6	22.2	2.82	2.69	2.71	2.93	3.41
sn7	27.6	2.58	2.32	2.42	2.58	2.77
sn8	31.6	2.31	2.34	2.46	2.58	2.76
sn9	34.2	2.25	2.21	2.40	2.39	2.52
sn10	38.0	2.12	2.10	2.32	2.32	2.42
sn11	41.3	2.29	2.35	2.59	2.70	2.63

Threshold Stresses

sample number	Distance (km)	Qtz	Horn	Aug	Hyp	Opq
south						
ss1	0.6	1.88	2.48	2.78	2.96	4.69
ss2	5.1	1.88	2.45	2.71	2.82	4.30
ss3	8.6	1.90	2.27	2.33	2.40	3.64
ss4	15	1.91	2.16	2.26	2.35	3.54
ss5	20.4	1.88	2.12	2.25	2.24	3.64
ss6	25.7	1.88	2.12	2.34	2.22	3.51
ss7	27.5	1.84	2.13	2.33	2.24	3.50
north						
sn1	1.2	2.01	2.66	2.96	3.06	4.85
sn2	5.7	1.97	2.61	2.91	3.01	4.61
sn3	7.2	1.95	2.60	2.88	2.98	4.58
sn4	9.4	2.09	2.53	2.64	2.73	4.10
sn5	17.9	2.16	2.46	2.51	2.62	4.17
sn6	22.2	2.13	2.48	2.44	2.62	4.37

Appdendix IV (continued)

sample number	Distance (km)	Qtz	Horn	Aug	Hyp	Opq
sn7	27.6	2.12	2.23	2.28	2.41	3.77
sn8	31.6	1.87	2.24	2.31	2.41	3.76
sn9	34.2	1.84	2.15	2.28	2.30	3.54
sn10	38.0	1.78	2.07	2.23	2.25	3.44
sn11	41.3	1.86	2.25	2.38	2.48	3.64

Qtz: quartz, Horn: hornblende, Aug: augite, Hyp: hypersthene, Opq: opques.

Appendix V

Einstein's Bed-Load Function

Einstein's bed-load approach (Einstein, 1950, 1964) includes selective entrainment effects and a correction factor for smaller grains hiding among large grains. Thus it best simulates the differential transport process in placer development. Bed load is defined as bed particles which move mainly by rolling, sliding, or jumping , while bed-load function gives the rates at which different grain sizes of the bed material are transported under a given flow in a channel. A modified version of this approach is used in this study and its major steps are described below:

Step 1: For a given flow stress τ_0 and bed-slope S, shear velocity u_* and flow depth R_b can be calculated as:

$$u_* = \sqrt{\tau_0/\rho}$$

$$R_b = u_*^2/Sg$$

where ρ is the fluid density and g is the gravity acceleration. u_* and R_b should be in feet.

Step 2: If kinematic viscosity of the water v is taken to be 1×10^{-5} ft^2/s, the thickness of the laminar sublayer can be obtained from:

$$\delta = 11.6v/ u_*.$$

Step 3: The roughness of the bed is defined as $K_s = D_{65}$ in feet (D_{65} is the grain size of which 65% of the bed material is finer), and the correction factor x for the transition from smooth to rough boundaries is obtained from Figure 49.
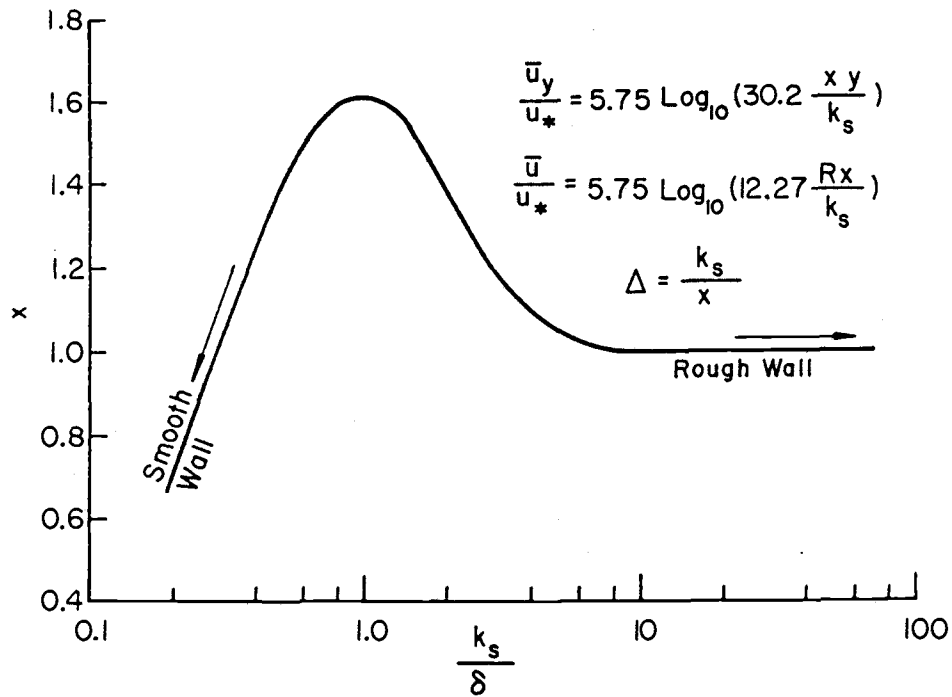
$$\frac{\overline{u}_y}{u_*} = 5.75 \, Log_{10} \left(30.2 \, \frac{x \, y}{k_s} \right)$$

$$\frac{\overline{u}}{u_*} = 5.75 \, Log_{10} \left(12.27 \, \frac{Rx}{k_s} \right)$$

$$\Delta = \frac{k_s}{x}$$

Figure 49

The correction factor x as a function of k_s/δ, where k_s is the bed roughness and δ the thickness of the laminar sublayer (From Einstein, 1950).

Step 4: The value of the apparent roughness $\Delta = K_s/x$ is calculated in feet.

Step 5: The characteristic grain size X then is calculated according to:

$$X = 0.77\,\Delta \qquad \text{for } \Delta/\delta > 1.80$$

$$X = 1.39\,\delta \qquad \text{for } \Delta/\delta < 1.80.$$

Step 6: For a given grain size D in feet, ratio D/X can be calculated. This ratio is then used to obtain the hiding factor ξ from Figure 50.

Step 7: For a given rtio of K_s/δ, Figure 50 is also used to obtain the pressure correction factor Y.

Step 8: The intensity of shear on particles is calculated as:

$$\psi = (\rho_s - 1)\, D/R_b S$$

and intensity of shear for individual grain size is calculated from:

$$\psi_* = \xi Y (\beta/\beta_x)^2\, \psi$$

where $\beta = 1.025$ and $\beta_x = \log_{10}(10.6 X/\Delta)$.

Step 9: For this calculated ψ_* value, the intensity of transport for individual grain size, Φ_* can be read from Figure 51.

Step 10: The selective transport rate for a given grain size D then is calculated as:

$$i_B q_B = 5.17\, \Phi_*\, i_b g^{3/2}\, D^{3/2}\, (\rho_s - 1)^{1/2}$$

in which i_b is the fraction of bed material in the given grain size and is assumed to be 1 in the present study so that $i_B q_B$ should be the selective transport rate when all the entrained grains have the diameter of D.

Step 11: The $i_B q_B$ calculated from step 10 is in lb/ft/s. It is converted to g/cm/s by multiplying it with 14.86.
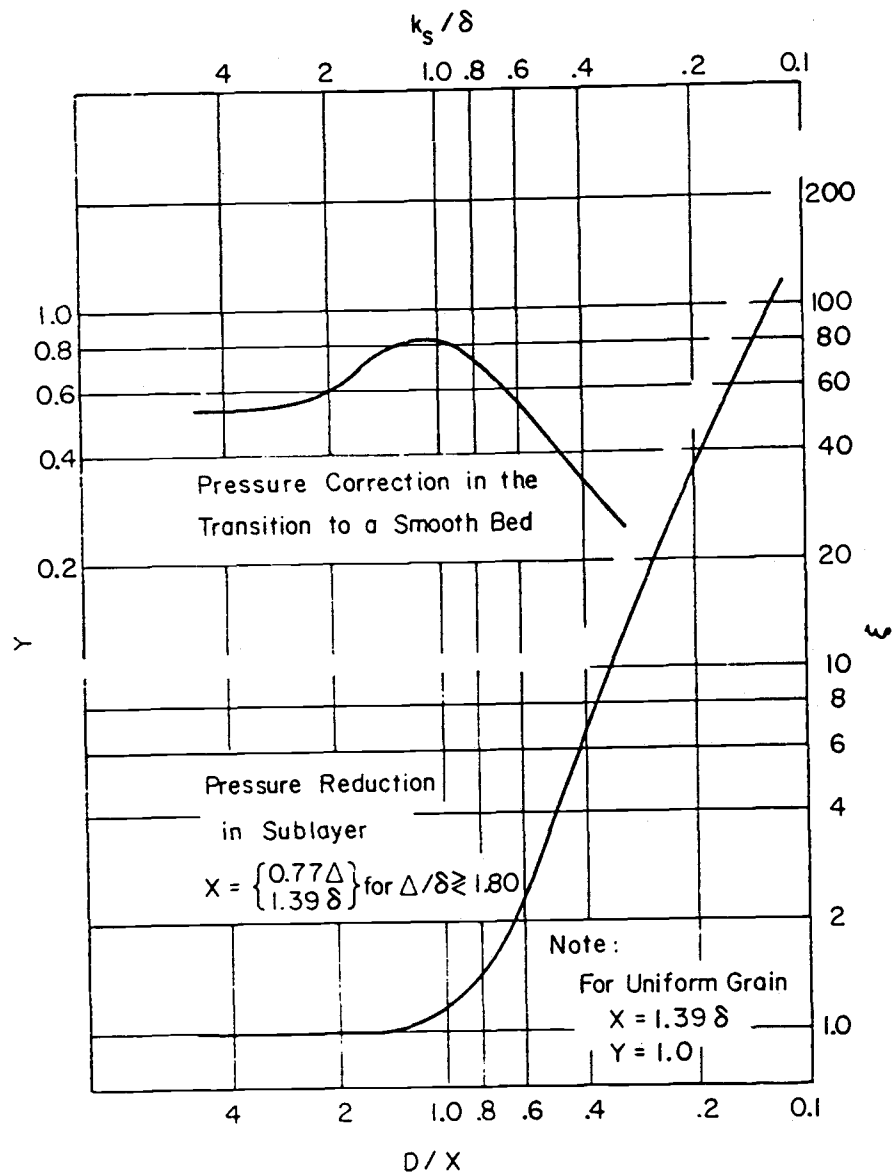
Figure 50
Hiding factor ξ versus grain size ratio D/X (bottom), and
pressure correction factor Y as a function of k_s/δ (top) (From
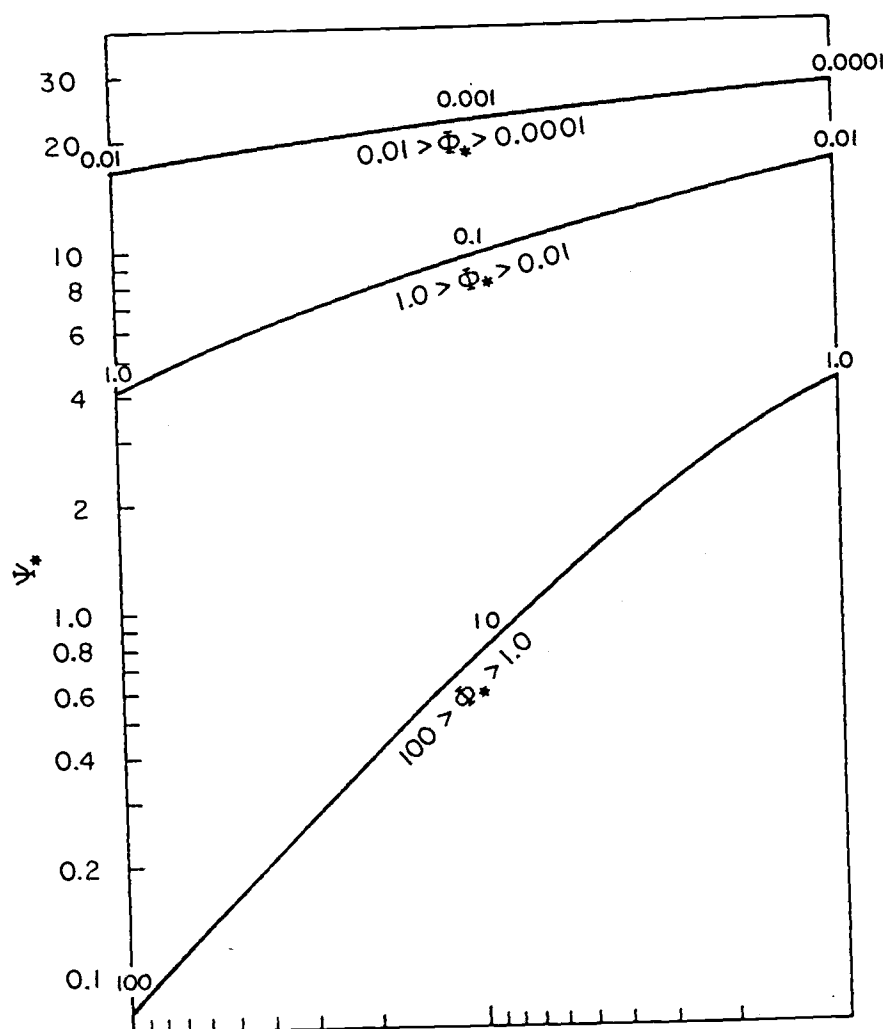Einstein, 1950).

Figure 51
Diagram used to obtain bedload transport intensity Φ_* from
the shear intensity for individual grain size ψ_* (from Einstein,
1950).